UNIVERSITY OF Southampton

University of Southampton Research Repository
ePrints Soton

Copyright © and Moral Rights for this thesis are retained by the author and/or other copyright owners. A copy can be downloaded for personal non-commercial research or study, without prior permission or charge. This thesis cannot be reproduced or quoted extensively from without first obtaining permission in writing from the copyright holder/s. The content must not be changed in any way or sold commercially in any format or medium without the formal permission of the copyright holders.

When referring to this work, full bibliographic details including the author, title, awarding institution and date of the thesis must be given e.g.

AUTHOR (year of submission) "Full thesis title", University of Southampton, name of the University School or Department, PhD Thesis, pagination

http://eprints.soton.ac.uk

UNIVERSITY OF SOUTHAMPTON

# LIGHT-INDUCED STRUCTURAL TRANSITION AND REFLECTIVITY OF A SILICA-GALLIUM INTERFACE

By Vassilios Albanis

A Thesis Submitted for the Degree of
Doctor of Philosophy

FACULTY OF SCIENCE
DEPARTMENT OF PHYSICS AND ASTRONOMY

AUGUST 2003

UNIVERSITY OF SOUTHAMPTON

ABSTRACT

FACULTY OF SCIENCE
DEPARTMENT OF PHYSICS AND ASTRONOMY

Doctor of Philosophy

# LIGHT-INDUCED STRUCTURAL TRANSITION AND REFLECTIVITY OF A SILICA-GALLIUM INTERFACE

By Vassilios Albanis

A broadband optical reflectometer with built-in thermal sample control was developed to study the linear properties of planar silica-gallium interfaces in the continuous range from 450 nm to 1650 nm with increasing and decreasing temperature in the range 12 $^0$C to 36 $^0$C, across the solid to melt phase transition.

An optical setup using an Argon Ion laser capable of operating at different wavelengths (488, 496, 501, 514 nm), with computer aided data acquisition system was developed to study the light-induced reflectivity change in single beam and pump-probe configurations at silica-gallium interfaces, close to the melting temperature of gallium. It allowed for single beam, and transient measurements with a resolution of up to 20 ns, with excitation levels up to 3 kW/cm$^2$.

An all-fibre pump-probe setup using diode lasers at 1.3 μm (signal) and 1.55 μm (control) was developed to study cross-wavelength all-optical switching at a silica-gallium interface. It allowed for intensity modulation measurements with 100 ns resolution and wide range of control powers up to 90 mW.

Continuous linear reflectivity measurements in the wavelength range from 450 nm to 1650 nm were performed for a range of temperatures across the melting transition of gallium at a silica interface prepared by Ultrafast Pulsed Laser Deposition, and a silica-gallium contact interface. A considerable broadband reflectivity increase on melting was seen, across the whole spectral range examined. Strong pre-melting behaviour was observed at the Ultrafast Pulsed Laser Deposited (UPLD) silica-gallium interface attributed to the presence of a transitional layer formed by energetic gallium atoms penetrating into the silica substrate during deposition. The results on reflectivity were compared with values derived from the anisotropic model of gallium optical properties based on published data for gallium single crystals.

Cross-wavelength all-optical signal switching between 1.3 μm and 1.55 μm was achieved for the first time at a silica-gallium interface prepared at the tip of an optical fibre. Cross-wavelength modulation of up to 40% and μs/ns switching times at only a few tens of mW of control laser power were observed.

The light-induced low-reflectivity state at a silica-gallium interface was studied in detail for the first time with cw and pulsed laser excitation. The low-reflectivity state was reversible and occurred within a very narrow temperature interval of 0.4 $^0$C below melting, requiring light intensity of 7 kW/cm$^2$ at cw excitation.

A light-induced reflectivity increase at a silica-gallium interface previously reported in the infrared part of the spectrum was studied at the blue-green spectral range using cw excitation for the first time. A 15% increase of reflectivity at 514 nm for 3 kW/cm$^2$ was seen, with hysteresis behaviour around the melting point of $T_m = 29.8$ $^0$C.

Transient pump-probe reflectivity measurements revealed the dynamics of a silica-gallium interface reflectivity change in the visible part of the spectrum for the first time. Reflectivity rise times of a few μs were observed and the accumulative nature of the reflectivity change with pump energy was seen. Recovery times of 1.2 μs just below melting were recorded for pump pulse duration of 0.4 μs. Thermal and non-thermal mechanisms of the reflectivity change have been identified and related to the properties of the interface.

Dedicated to my parents for all their help and support
all these years of study and hard work

**Contents** **page**

# Acknowledgments

I would like to thank my supervisor, Professor N. I. Zheludev, for his careful guidance and continuing support throughout my studies. I'd also like to thank the people with whom I worked so closely all these past years in the Laser Physics group, P. J. Bennett, S. Dhanjal, P. Petropoulos, K. F. MacDonald, V. A. Fedotov, G. Stevens, my colleagues at the Optoelectronics Research Centre, and in particular Dr. P. G. R. Smith. I acknowledge the University of Southampton for a postgraduate studentship. I would also like to thank my friends and especially my girlfriend for having to put up with me throughout the writing of this thesis. But most importantly I would like to thank my parents for their help at the first stages of my studies and their support and encouragement throughout these years of hard work.

# Chapter 1

# Introduction

## 1.1 Introduction

Recent scientific research has been concentrating on optical switching mechanisms and devices to bridge the gap between the electronic and optical circuits that the present telecommunication technology is based on. The research has been directed towards elemental materials or compound structures that can exhibit a large nonlinearity with a fast response to broadband optical excitation of low power.

A number of different materials have been investigated for any signs of a nonlinearity that could be of use in optical switching. Organic materials have been observed to show large cubic optical nonlinearities, fast response times, and a structural diversity that can only be impeded by synthesization methods [1]. However, unlike inorganic materials they tend to have poor physico-chemical stability and low mechanical strength, and often low laser damage threshold. The optical nonlinear character in organic materials arises from electron delocalisation along the molecular chains, allowing for electron motion across long distances on the chain. Various other much slower optical nonlinearities have been observed in liquid crystals. Extensive research in the nonlinear optical properties of semiconductors has shown that large cubic optical nonlinearities can be generated in semiconductors by inducing resonant near-bandgap excitation [2], [3], [4]. Excitonic nonlinearities in direct bandgap semiconductors are an attractive way of obtaining fast nonlinearities and ultrafast all-optical switching in this regime has been demonstrated. This however can be affected by high linear absorption that can prove problematic in many practical applications, and moreover engaging near-bandgap nonlinearities often

requires low temperature making integration difficult. Nevertheless, remarkable progress using multi-quantum well structures has been achieved, and Q-switched mode locked multi-quantum well elements are now available commercially. An alternative way of generating a nonlinear optical response in a semiconductor is to use optical excitation in the transparency region, below one half of the bandgap. The value of the nonlinear response is smaller but is still sufficient for nonlinear switching applications [5].

The progress in searching for materials that show strong and fast optical nonlinearity has to be considered with respect to practical optoelectronic devices. The ideal characteristics of an all-optical data-processing device have been outlined by H. M. Gibbs in [2], as: "the device should be small, i.e. of characteristic dimension of a micrometer ... the holding power should be less than 1 mW and the switching energy should be less that 1 fJ" Gibbs said that the device " ...should be fast (< 1 ps), so that high-speed operations can be accomplished", but admitted that "response times as slow as 1 ms are acceptable for some parallel-processing applications". Gibbs required that the device "should be operable at room temperature" and "it should be integrable to permit a large number of interconnections". Summarising this set of requirements Gibbs concluded, "clearly, none of the demonstrated devices is a good approximation to the ideal device". The present nonlinear optical switching devices are still somewhat away from Gibbs's requirement, and research into new concepts of obtaining fast and large optical nonlinearities is still extensive.

Recently metals have attracted attention, and several elemental metallic materials have been considered for applications in which light-matter interaction is required, due to the inherent high cubic nonlinear character. For example, the cubic optical nonlinearity of gold [6], nickel [7] and indium [8] has been observed to reach high values. However, the light penetration depth in metals and the effective nonlinear interaction length is of the order of a few nanometers making their nonlinear response very weak to be used in any practical applications.

A novel concept of generating an optical nonlinearity in a material has been proposed, that relies on the interaction between optical wavelengths and the crystalline lattice of a material [9]. Light can be used to stimulate a structural phase transition, into a new phase

of considerably different optical properties from the original phase, thereby manifesting an optical nonlinearity. If the initial phase is recovered, when the optical excitation is withdrawn, then this nonlinearity is reversible and can be potentially a useful process.

However, in most cases the structural phase transition of a material is a first order transition. When a critical temperature is reached, there is a sudden change in the crystalline structure. If this process is reversed then a hysteresis is seen, as for example in the case of bulk melting where the melting temperature can be noticeably higher than the solidification temperature. If such a phase transition is stimulated by light in a bulk material, the original phase will not be recovered when the excitation is withdrawn. The nonlinearity associated with the transition will not be reversible and so would not be suitable for controlling light with light in applications such as data processing.

The sharp phase transitions of bulk materials are characterized by the precise coexistence of different phases. However this becomes a dynamic coexistence of structural forms if the material is placed in a restrictive geometry. Confinement can alter the process of a phase transition in some systems. When a confined solid is brought to the verge of, what otherwise would be, a first order structural phase transition in the bulk, it can become significantly more sensitive to external stimulation, offering an enhanced nonlinearity. Moreover the transition could become continuous and reversible. Confinement, therefore, provides a means of achieving a reversible optical nonlinearity.

The simplest form of confinement is the formation of an interface with another material. Thus, this novel concept of generating a strong optical nonlinearity via a light-induced structural phase transition is a combination of two ideas, confinement and bringing the material to the verge of a structural phase transition [9].

First results of generating a strong optical nonlinearity in metals close to their structural phase transition have been reported for indium [8]. Recent results have suggested that gallium when confined at an interface with silica is a structure that exhibits a fast, fully reversible nonlinear behaviour close to the melting transition of gallium. This behaviour has been attributed to a light-assisted surface metallization [10], [11]. The material has a complicated phase diagram with a number of stable and metastable phases, and an easily

accessible structural phase transition, see Chapter 2. Its stable crystalline phase is considered a molecular metal [12], comprising of metallic and covalent bonding.

Such surface-assisted light-induced metallization of a silica-gallium interface has been observed in the visible [13] and the near-infrared parts of the spectrum [11]. Using the nonlinearity of a silica-gallium interface a practical optical switch [14], cross-wavelength all-optical switching [15] have been demonstrated, along with Q-switching of a fibre laser at different wavelengths [16], [17].

In this thesis, the aim is to investigate nonlinear phenomena by studying the light-induced reflectivity change of gallium confined at a silica interface, and examine the bandwidth of the broadband optical properties of the interface. Results are presented, from measurements in the visible and infrared parts of the spectrum, suggesting that the nonlinear optical behaviour of the interface extends from 400 nm to at least 1800 nm, exhibiting therefore a huge bandwidth and covering all the telecommunication bands used currently. This makes the silica-gallium interface a very useful structure offering potential for true integrated applications.

## 1.2 Thesis Plan

This thesis consists of 5 chapters.

**Chapter 1** is an introduction to the subject covered in this thesis, and a brief outline of the thesis chapters.

**Chapter 2** is a literature review of the properties of gallium. The polymorphic character of gallium is examined. The crystallographic structure of the stable gallium phase and the main structural modifications and metastable phases are discussed. The melting transition of gallium crystals is presented with respect to premelting and surface phenomena and the properties of the liquid phase of gallium are reviewed.

**Chapter 3** is an investigation of all-optical switching at a silica-gallium interface. The strong nonlinear behaviour of a silica-gallium interface is used to demonstrate cross-wavelength modulation between signals at 1.3 μm and 1.55 μm. The nonlinear optical

behaviour of gallium confined at an interface with silica is associated with a light-induced structural phase transition. A theory explaining the mechanism behind the optical response is discussed. An additional light-induced effect at a silica-gallium interface was discovered and is presented and examined. The reflectivity of a silica-gallium interface was reduced in a reversible manner when the interface was excited by a few milliwatts of laser power. The effect was observed to take place at temperatures just below the melting temperature of gallium. It is argued that this behaviour can be associated with some form of light-induced structuring at the silica-gallium interface and some potential mechanisms are discussed.

**Chapter 4** is an investigation of the broadband optical properties of gallium at an interface with silica across the melting transition. The optical properties of vacuum and silica-gallium interfaces are examined for the solid and liquid phases of gallium, using previously published data. The linear reflectivity of a silica-gallium interface is estimated using Fresnel formulae and existing data for the solid and liquid phases of gallium. The reflectivity of a contact interface between silica and gallium in which gallium has low affinity to silica, and an interface prepared by the Ultrafast Pulsed Laser Deposition process is measured, across the melting transition of gallium as a function of wavelength. A considerable increase in interface reflectivity across the whole spectral range examined was observed. The measured reflectivity values are compared with calculated values and some conclusions are made. The light-induced reflectivity change of the Ultrafast Pulsed Laser Deposited silica-gallium interface is examined in the blue-green spectral region. A considerable increase was seen, at temperatures just below the melting temperature of gallium under cw excitation. In addition, the transient dynamics of the light-induced reflectivity change is examined, for the first time, using pulsed excitation. Two types of reflectivity response, depending on the properties of the interface are documented. The mechanisms behind these two behaviours are identified as a light-induced non-thermal, and a predominantly thermal one.

**Chapter 5** is a summary of the topics covered in this thesis and the results presented.

## References


[1] J. Zyss, *Molecular Nonlinear Optics: Materials, Physics, and Devices*, Edited by J. Zyss, Academic Press 1994

[2] H. M .Gibbs, *Optical Bistability: Controlling Light with Light*, Academic Press, 1985

[3] A. Miller, D. Duncan, *Optical Nonlinearities in Narrow Gap Semiconductors in Optical Properties of Narrow-Gap Low-Dimensional Structures*, Plenum New York, 1987

[4] J. R. Hill, G. Parry, A. Miller, Optics Communications, page 151, vol. 43, 1982

[5] A. Villeneuve, C. C. Yang, P. G. J. Wigley, G. I. Stegeman, J. S. Aitchinson, C. N. Ironside, Applied Physics Letters, page 147, vol. 61, no. 2, 1992

[6] N. I. Zheludev, P. J. Bennett, H. Loh, S. V. Popov, I. R. Shatwell, Yu. P. Svirko, V. E. Gusev, V. F. Kamalov, E. V. Slobodchikov, Optics Letters, page 1368, vol. 20, 1995

[7] P. J. Bennett, A. Malinowski, B. D. Rainford, I. R. Shatwell, Yu. P. Svirko, N. I. Zheludev, Optics Communications, page 148, vol. 147, 1998

[8] S. Dhanjal, S. V. Popov, I. R. Shatwell, Yu. P. Svirko, N. I. Zheludev, V. E. Gusev, Optics Letters, page 1879, vol. 22, 1997

[9] N. I. Zheludev, *Nonlinear Optics at the Nano-Scale*, Contemporary Physics, page 365, vol. 43, no. 5, 2002

[10] V. Albanis, S. Dhanjal, V. A. Fedotov, K. F. MacDonald, N. I. Zheludev, P. Petropoulos, D. J. Richardson, V. I. Emely'anov Physical Review B., page 165207, vol. 63, 2001

[11] K. F. MacDonald, V. A. Fedotov, R. W. Eason, N. I. Zheludev, A. V. Rode, B. Luther-Davies,V. I. Eme'yanov, J. Opt. Soc. Am., page 331, vol 18. 2001.

[12] X. G. Gong, G. L. Chiarotti, M. Parrinello, E. Tosatti, Physical Review B., page 14277, vol. 43, no. 17, 1991

[13] V. Albanis, V. A. Fedotov, N. I. Zheludev, Optics Communications, page 271, vol. 214, 2002

[14] P. J. Bennett, S. Dhanjal, P. Petropoulos, D. J. Richardson, N. I. Zheludev, V. I. Emel'yanov, Applied Physics Letters, page 1787, vol. 73, no. 13, 1998

[15] V. Albanis, S. Dhanjal, N. I. Zheludev, P. Petropoulos, D. J. Richardson, Optics Express, page 157, vol. 5, no. 8, 1999

[16] P. Petropoulos, H. L. Offerhaus, D. J. Richardson, S, Dhanjal, N. I. Zheludev, Applied Physics Letters, page 3619, vol. 74, no. 24, 1999

[17] N. J. C. Libatique, J. D. Tafoya, S. H. Feng, D. J. Mirell, R. J. Kain, Advanced Solid State Lasers, page 417, vol. 34, Optical Society of America, Washington DC, 2000

## Additional References, Bibliography

K. H. Bennemann, *Nonlinear Optics in Metals*, in The International Series of Monographs on Physics, vol. 98,Edited by K.H. Bennemann, Clarendon Press, Oxford, 1998

R. W. Boyd, *Nonlinear Optics*, 2nd Edition, Academic Press, 2000

C. C. Davies, *Lasers and Electro-Optics: Fundamentals and Engineering*, Cambridge University Press, 1996

V. G. Dmitriev, G. G. Gurzadyan, D. N. Nikogosyan, *Handbook of Nonlinear Crystals*, Springer Series in Optical Sciences, vol. 64, Springer-Verlag, 1991

E. Garmire, A. Kost, *Nonlinear Optics in Semiconductors I*, Volume Editors E. Garmire, A. Kost, Semiconductors and Semimetals, vol. 58, Academic Press 1999

H. S. Nalwa, *Nonlinear Optical Materials*, in Handbook of Advanced Electronic and Photonic Materials, vol. 9, Edited by H. S. Nalwa, Academic Press, 2001

E. G. Sauter, *Nonlinear Optics*, Wiley, New York, 1996

Y. Shen, *The Principles of Nonlinear Optics*, Wiley, 1984

J. H. Simmons, K. S. Potter, *Optical Materials*, Academic Press, 2000

G. I. Stegeman, E. M. Wright, *All-Optical Waveguide Switching*, Opt. Quantum electronics, page 92, vol. 22, 1990

A. Yariv, *Optical Electronics in Modern Communications*, 5th Edition, Oxford University Press, 1997

# Chapter 2

# A Review of the Properties of Polymorphic Gallium

## 2.1 Synopsis

In this chapter a literature review of the properties of gallium is presented. The polymorphic character of the material is discussed and the properties of the stable crystalline form and the main structural modifications are presented.

The melting transition of gallium crystals and the properties of the liquid phase are examined.

## 2.2 History of research on gallium

Gallium was discovered in 1875 by Paul-Emile Lecoq de Boisbaudran who observed its spectral lines, while examining materials separated from zinc-blende. It was the first element to be isolated after the publication of the periodic table of elements by Mendeleyev in 1869. Mendeleyev had anticipated its discovery a few years earlier, as an element called "eka-aluminium" which was predicted to exist between aluminium and indium in the periodic table. Gallium was firstly obtained as a free metal by electrolysis of a solution of hydroxide in KOH, but it can be found in nature, though not occurring free, and is usually extracted as a by-product from zinc-blende, iron pyrites, bauxite and germanite, and can be supplied in ultra high purity (99.9999%).

Gallium was initially described as a tetragonal crystal structure. On a later publication the crystal structure of the material was stated as orthorhombic with two of the lattice

dimensions almost identical [1 and references therein]. Further measurements of the structural properties and determination of the lattice parameters were produced in [2], [3].

The optical properties of gallium, in its stable crystalline and liquid phases have been investigated by different researchers. The existing values of the optical properties can differ though, as they were obtained for samples of different types (single crystal, polycrystalline, thin gallium fims) or samples that had been treated in different ways (polishing, chemical treatment) [4].

The optical properties of thin polycrystalline samples were examined in [5] in the visible and near infrared regions of the spectrum. The optical properties at the ultra-violet range were examined in [6], [7]. The optical properties of the different crystallographic directions of the orthorhombic α-gallium crystal were examined in [8], [9], [10], [11]. Nevertheless, these researchers have used different treatment procedures for their samples.

The first investigation of the optical properties across the melting transition of gallium was reported in [12]. The optical constants of the liquid phase of the material were examined in [13], [14]. The electronic properties of gallium across the melting transition were examined in [15], and extensive changes were observed.

## 2.3 General properties and use

On appearance, a free gallium surface has a silvery-blue colour, due to a slow superficial oxidisation occurring when in air, during which a protective film grows at the surface. The metal when solid exhibits a conchoidal fracture similar to that of glass. Gallium exhibits a very low, for a metal, melting point of about 30 $^0$C. Along with mercury, caesium and rubidium is one of the metals that can be found liquid at room temperature. Its low melting point in addition with its high boiling point of 2204 $^0$C, makes it the metal with the longest useful liquid range of all the known elements. In the other end of its temperature range it has a strong tendency to supercool, and it can remain a liquid at temperatures as low as 0 $^0$C.

Chemically it is similar to aluminium, and reacts slowly with HCl along with other mineral acids, to give the gallium ion, $Ga^{3+}$. It can be attacked by halogens, and reacts

with sodium and potassium hydroxide solutions to give a gallate and hydrogen gas. In terms of toxicity, no known reactions are known to occur, and its toxicity is considered to be of low order. In terms of electronic configuration, gallium is a broadband sp metal with an $s^2p^1$ outer valence shell configuration, and electronic configuration $[Ar]3d^{10}4s^24p^1$.

The first significant use of gallium was in the spectroscopic analysis of uranium oxide. Moreover, due to its thermal properties gallium has long been considered as a heat exchange medium in nuclear reactors (although it has a high neutron cross-section) and in high temperature engines. It has also been used as a liquid sealant in high vacuum systems.

The application of gallium that has received the most attention is the production of semiconducting compounds. For many years the elemental semiconductors, silicon and germanium dominated this technology. However, in 1952, German researchers reported the achievement of semiconducting properties in compounds between elements of the III and V groups. Of these, the most important are the compounds of gallium with antimony, arsenic, and phosphorous. Nowadays gallium arsenide (GaAs) is a commonly encountered semiconductor compound, used in the production of several electronic parts, and even more importantly in the production of lasers. Furthermore, magnesium gallate doped with divalent impurities is finding use in commercial ultraviolet-activated powder phosphors.

Gallium is a group III element, which when adding nitrogen atoms to its structure can become a semiconducting material that, if paired with the appropriate substrate materials, can become a transistor for advanced applications. Gallium-nitride promises improvements in a wide range of applications, from simple light bulbs that could, potentially have a lifetime of up to ten years, to a blue laser that will quadruple the storage capacity of the currently used compact discs.

The material when confined at an interface with silica exhibits strong nonlinear optical properties that have been used to demonstrate practical optoelectronic applications, such as all-optical switching [16], cross-wavelength all-optical switching [17] and q-switching of fibre lasers at different wavelengths [18], [19]. The nonlinear optical properties of gallium are examined in chapters 3 and 4.

Apart from these high technology fields gallium has found use in the medical sciences. An isotope of gallium, gallium-72, has been used, with promising results in the study of bone cancer, as the cancerous portion of the bone absorbs a compound of this isotope.

## 2.4 Structure and metastable phases of gallium

Gallium shows a high degree of polymorphism, possessing a complicated phase diagram with the main and metastable phases competing for the ground state of the material [20].

Up to now between four to nine phases have been identified [21] native at different conditions of temperature and pressure, with different structural and physical properties. The phase diagram in figure 2.1 below shows the stability regions of the main phases and the metastable phases as a function of pressure and temperature.

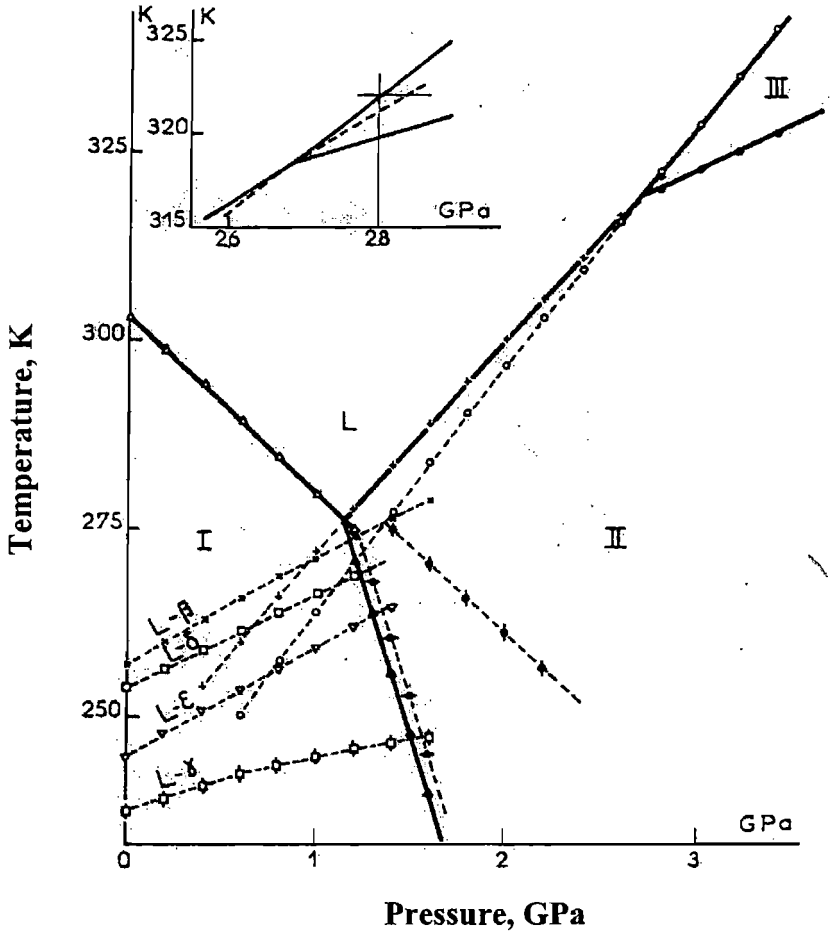


**FIGURE 2.1:** Temperature as a function of pressure diagram for gallium, showing the main modifications of the material and the equilibrium phase boundaries. The inset shows the triple point between liquid and the two modifications Ga(II) and Ga(III). Taken from [29].

## 2.5 The α-gallium phase

The stable structural phase at normal conditions of pressure and temperature is the so-called α-gallium phase. Single crystals of α-gallium can be grown from the melt in a characteristic from, shown in figure 2.2 [4], illustrating the three crystallographic axes [100]a, [010]b and [001]c. Here, four types of low-index facets can be seen: (100), (010), (111) and (112). The (010) and (111) faces form large facets that cover most of the surface of single crystals whereas the (100) and (112) form much smaller facets. The [001] direction does not naturally form a facet on the single crystal grown from the melt.

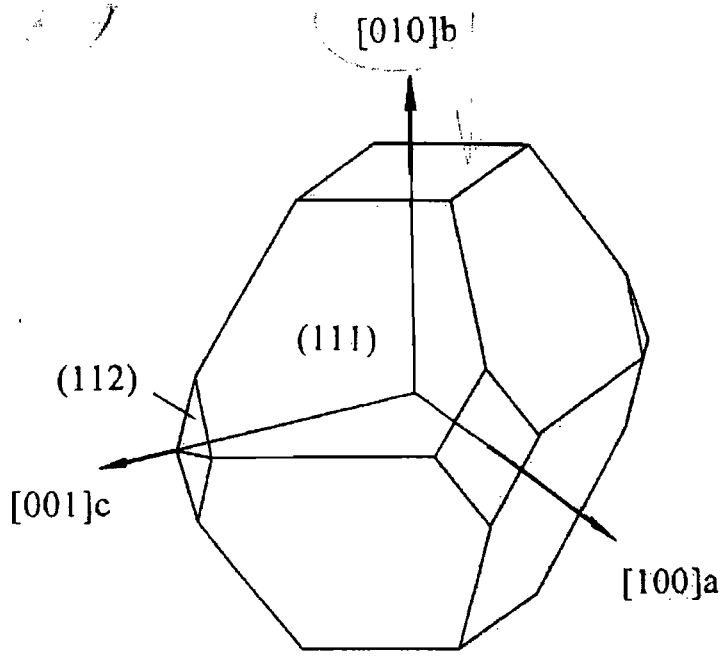


**FIGURE 2.2:** The characteristic form of a α-gallium crystal grown from the melt, taken from [4]. The three main crystallographic directions [100], [010] and [001] can be seen.

This phase is characterised by an orthorhombic symmetry of the Cmca space group, with a unit cell containing eight gallium atoms [22]. Each atom is coordinated by one nearest neighbour at 2.44 Å, and six more in a shell with distances between 2.71 Å and 2.79 Å. These six atoms are located in a plane that is about 1.9 Å thick [23]. The structure is loosely packed with directional bonding [15] and can be generally visualised as a stacking of highly disordered hexagonal closely packed layers [1].

The dimensions of the lattice parameters of the unit cell are (Cmca space group notation): [001] (a axis) 4.519 Å, [010] (b axis) 7.658 Å and [001] (c axis) 4.526 Å. The morphology of these planes, in relation to the crystallographic orientations is shown below in figure 2.3, taken from [22]. Note that in a number of publications the α-gallium phase is described as an Abma space group. For an in-depth investigation on the properties of space groups see the International Tables for X-Ray Crystallography.

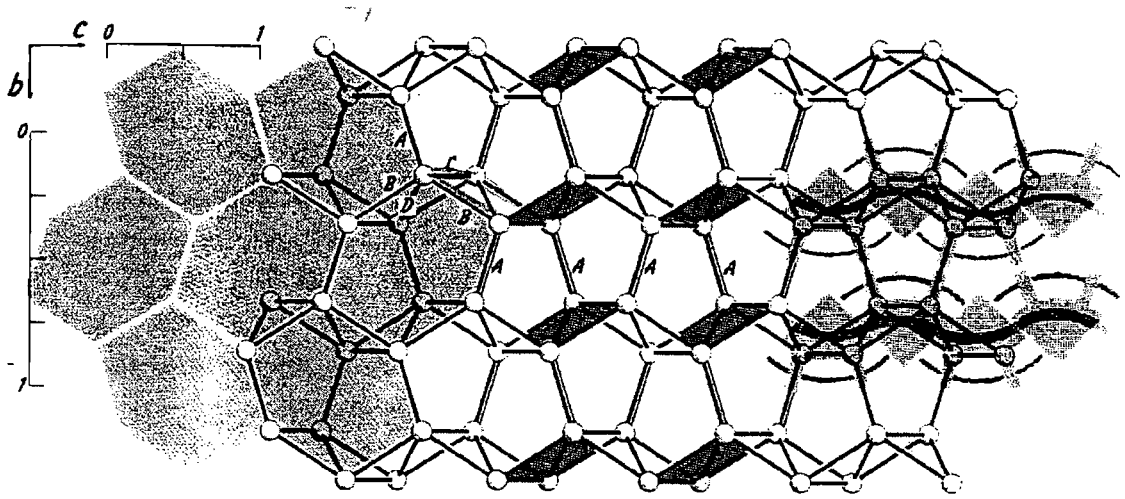


**FIGURE 2.3:** The crystal structure of α-gallium showing the distribution of the gallium atoms in the hexagonal unit cells. Here b is the [010] direction, c is the [001] direction, whereas the [100] a direction (not shown here) is directed perpendicular to the plane of the page. From [22].

An interesting feature of the α-gallium phase is the nearest-neighbour distance between the atom pairs that is short for a normal metallic bond. This detail has long been considered as a signature of a covalent character in a material. This possibility of the covalent character of gallium was theoretically predicted by [24], based on band structure and pseudopotential calculations, prompted by the short-distanced bond between the two closest gallium atoms, which was considered to form a molecule-like structure.

The covalent character of the α-gallium structure was further discussed in [25], in terms of the atomic and electronic properties of the material. An indication of covalency was found in the electron density of the α-phase, which shows a well-structured character with a deep and pronounced gap situated exactly at the Fermi level, see figure 2.10. These features observed around the Fermi level, were suggested to arise from the overlap of the electronic wave functions created due to their interaction along the buckled planes, perpendicular to the direction of covalent bonds.

The electronic properties of the α-gallium phase have also been examined in terms of the band structure of the material in [23]. Figure 2.4, below, shows the band structure of α-

gallium as a function of energy and wavevector, for some high symmetry directions in the Brillouin zone of α-gallium. In the inset, the Brillouin zone is shown with the high symmetry points labelled. The horizontal line in the energy axis corresponds to the Fermi energy of the α-gallium structure, which represents the transition from occupied states to unoccupied states in the band structure of the material.

In the band structure of gallium a number of energy states occupy the different parts of the Brillouin zone, with a complicated pattern above and below the Fermi energy level. Some states can be seen to overlap and occupy the same energy levels around the Fermi level. More interestingly, regions of the Brillouin zone can be seen in which energy bands run approximately parallel and symmetrical about the Fermi level. This indicates that the bands will be partly empty and partly filled a typical property of semimetals, like gallium. Such bands are considered to occur in most polyvalent materials, and their existence has been reported for aluminium, an isoelectronic material to gallium.

These types of bands, running roughly parallel to each other, play a specific role in governing the optical properties of a material, by contributing to a narrow peak in the optical absorption spectrum [26]. The presence of such bands allows for well defined interband transitions, which involve the absorption of a photon by an electron occupying an energy state below the Fermi level, inducing this way a transition to a state above the Fermi level. The difference between the two energy states will be equal to the photon energy absorbed. These transitions are more effective if the energy separation between the two states remains roughly constant across a large region of wavevector values. In that case there are a greater number of energy states that can be coupled to the energy of the photon.

In gallium, such bands have been observed in the energy band structure and have been associated directly with the covalent character of the material [25]. In figure 2.4 these transitions are indicated by arrows, and represent the finite amount of energy needed to remove an electron from the bonding state, between the two gallium atoms forming the gallium dimer, to the antibonding state.

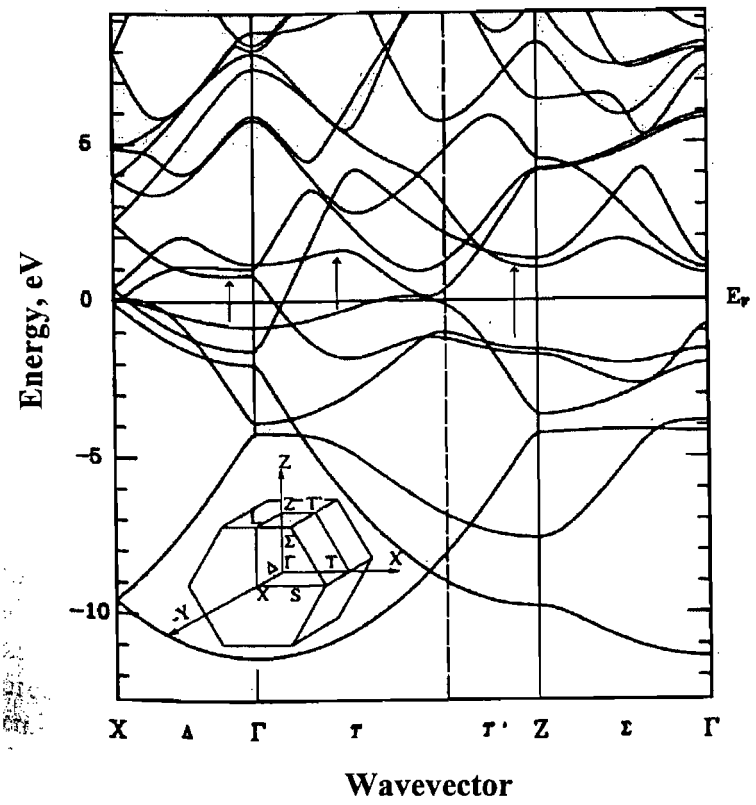


**FIGURE 2.4:** Band structure of α-gallium along some high symmetry points in the Brillouin zone, as taken from [20].

The energy band structure, shown in figure 2.4, has been associated with the absorption properties of the material. Indeed, figure 2.5 below, shows the real part of the optical conductivity of gallium, $\sigma_1 = \varepsilon_2\omega/4\pi$, where $\varepsilon_2$ is the imaginary part of the complex dielectric constants of gallium (see Chapter 4) and ω is the frequency in relation to energy as discussed in [25]. The optical conductivity of an electronic system, describes the absorptive response to an electromagnetic field as a function of the frequency of the field. It is convenient to use the optical conductivity to represent the absorption, because the power absorbed for a given amplitude of an electromagnetic field is simply a factor of the optical conductivity and the square of the field amplitude, $\sigma_1(\omega)E^2$, with no additional frequency dependent factor. As the frequency tends to zero the optical conductivity becomes the same as the electrical conductivity.

In the case of α-gallium, the shape of the optical conductivity is shown in figure 2.5 below. There, an absorption band can be seen, spanning from approximately 0.8 eV to 4

eV, with a peak in the optical conductivity at about 2.3 eV. The absorption band is directly related to the electronic properties of the material, and more specifically to the presence of parallel energy bands, illustrated in figure 2.4, which allow the absorption of photons with photon energy between 0.8 eV to 4 eV to successfully couple their energies and induce an electron transition from an occupied state below the Fermi energy to an unoccupied one above the Fermi energy. This transition represents the bonding-antibonding transition within the gallium dimer that initiates an optically induced phase transition, see Chapter 4. In this transition the strongest band, at approximately 2.3 eV, gives rise to the peak in the shape of the optical conductivity as shown in figure 2.5, below.

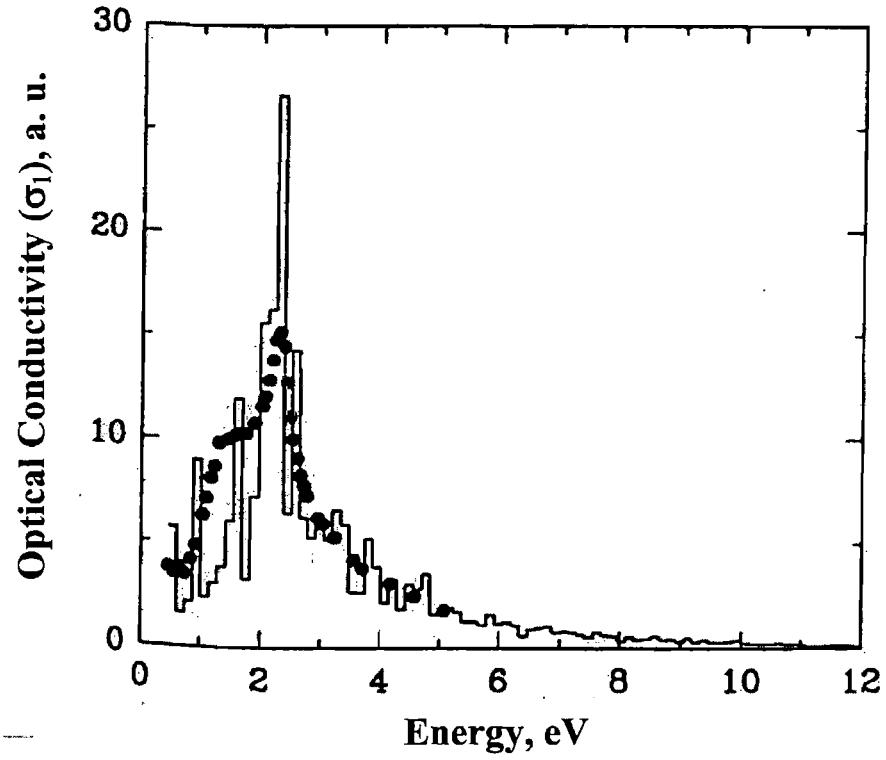


**FIGURE 2.5:** The real part of the optical conductivity of α-gallium, showing the absorption band and the peak at 2.3 eV, taken from [25].

With respect to the covalent character, the α-gallium phase can be described as a "molecular metal" [25], with the Ga-Ga dimers ($Ga_2$) forming the central molecular unit and corresponding to the short atom distance. The structure consists of strongly buckled planes, orthogonal to the [010] direction, with each gallium atom weakly bound to its six nearest neighbours in the layer, and strongly bound (with the short interatomic distance) to one atom in a plane either above it or below it.

The different planes are connected though the dimers, which are orientated roughly along the [010] direction, see figure 2.3 above.

## 2.6 The Ga(II) phase

Two modifications of the stable form of gallium are Ga(II) and Ga(III) which exist at higher pressures. The Ga(II) phase exhibits a body centred cubic structure. The extensive range of pressure over which Ga(II) is stable, is a result of the body centred cubic structure that this phase possesses [27].

In the literature, it can be found possessing six atoms per unit cell [25], or twelve atoms per unit cell [28], [29]. The density of this phase, as calculated by X-ray data for a cell containing twelve atoms was found to be 6.59 $gcm^{-3}$ [29]. Figure 2.6, below, shows the structure of Ga(II) taken from [23].

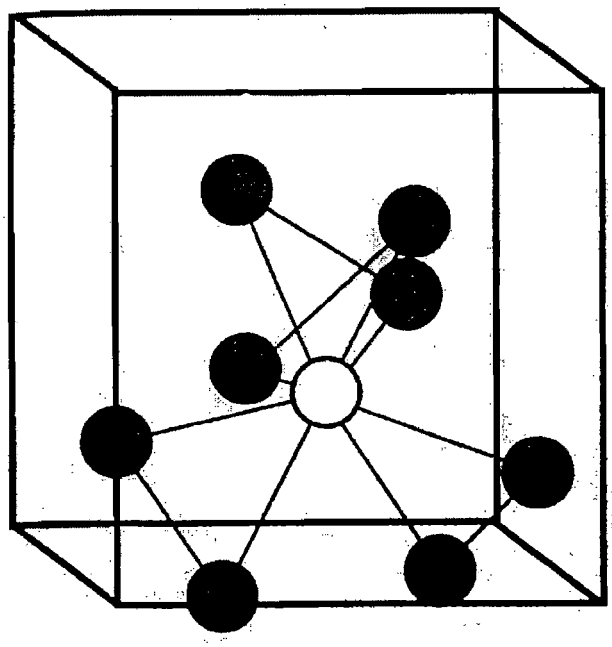

**FIGURE 2.6:** The body-centred cubic structure of Ga(II), one of the main modifications of the solid crystalline α-gallium, showing the nearest neighbour distribution. Taken from [23].

## 2.7 The Ga(III) phase

Ga(III) has a face centred tetragonal structure, similar to that of indium. In [29] the density of Ga(III) phase is estimated to be 6.57 $gcm^{-3}$. This phase can be produced in a metastable manner by either compressing or cooling the liquid gallium phase. The similarity between the Ga(III) structure and that of indium can be attributed to the tendency that the Group III elements have to acquire the structure of the elements situated below them in the periodic table, as the pressure increases [29], [30]. Figure 2.7 below, shows the structure of Ga(III). Ga(III) has been found to be mechanically unstable and it is transformed into a face centred cubic structure [20].

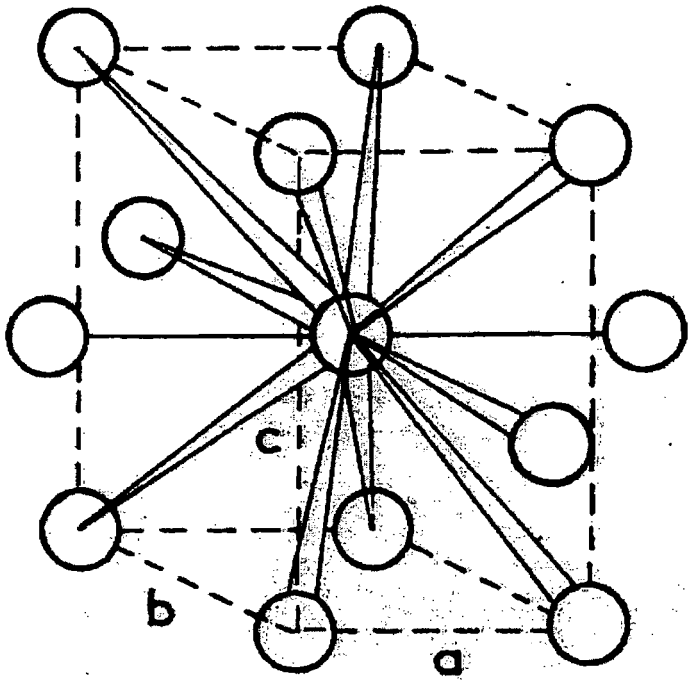


**FIGURE 2.7:** The body centred structure of Ga(III) showing the arrangement of the atoms in the unit cell. Taken from [20].

## 2.8 The β-gallium phase

Another modification of gallium is the β-gallium phase. It can readily form on supercooling of liquid gallium, and it also takes part in the transition from α-gallium to liquid gallium [28]. This modification of gallium has been observed to be metastable at all temperatures and pressures. It has also been experimentally shown that β-gallium can be produced in the crystal transition from amorphous gallium, as obtained by vapour deposition on a cold substrate, when this is reheated up to the melting temperature of gallium [31], [27].

This phase is characterised by a monoclinic crystal structure, see figure 2.8 below, with two atoms in the unit cell, and a melting point of about -16.9 $^{0}$C at atmospheric pressure. The density of this phase is about 7% higher than that of the α-phase, which can explain the affinity with which liquid can easily supercool into the β-phase [23]. Furthermore β-gallium exhibits a radial distribution of the nearest neighbours similar to that of the liquid [32].

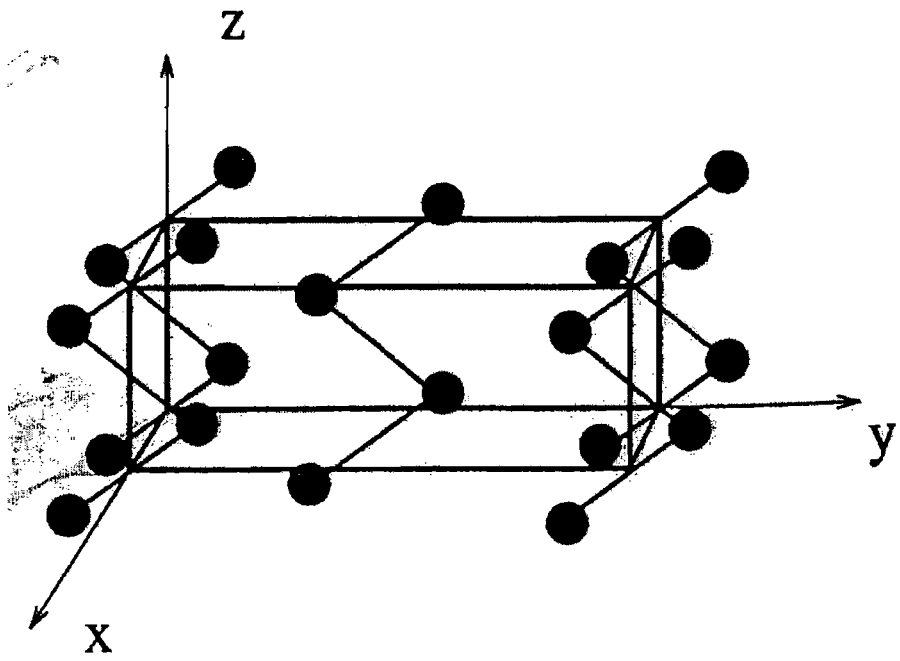


**FIGURE 2.8:** The atomic arrangement of the monoclinic cell of β-gallium, from [20].

## 2.9 Relation between the main phases of gallium

As it was seen in the sections above, the main phases of gallium (α-gallium, β-gallium, Ga(II) and Ga(III)) exhibit structural similarities and differences. In a similar manner, these phases exhibit similarities and differences in their electronic properties. Figure 2.9 below taken from [23], shows the energy of an atom within the crystal cell in relation to the volume of the unit cell for the main modifications of the gallium structure. The three modifications, β-gallium, Ga(II) and Ga(III), show a very similar behaviour in terms of energy per unit-cell volume, whereas the α-gallium phase is shifted from the rest three phases and illustrates the different electronic properties that this phase possesses. Also shown is the fcc phase of gallium, whose energy vs volume relation seems to coincide with that of the Ga(III), which would be expected since the Ga(III) transforms to the fcc phase at higher pressures.

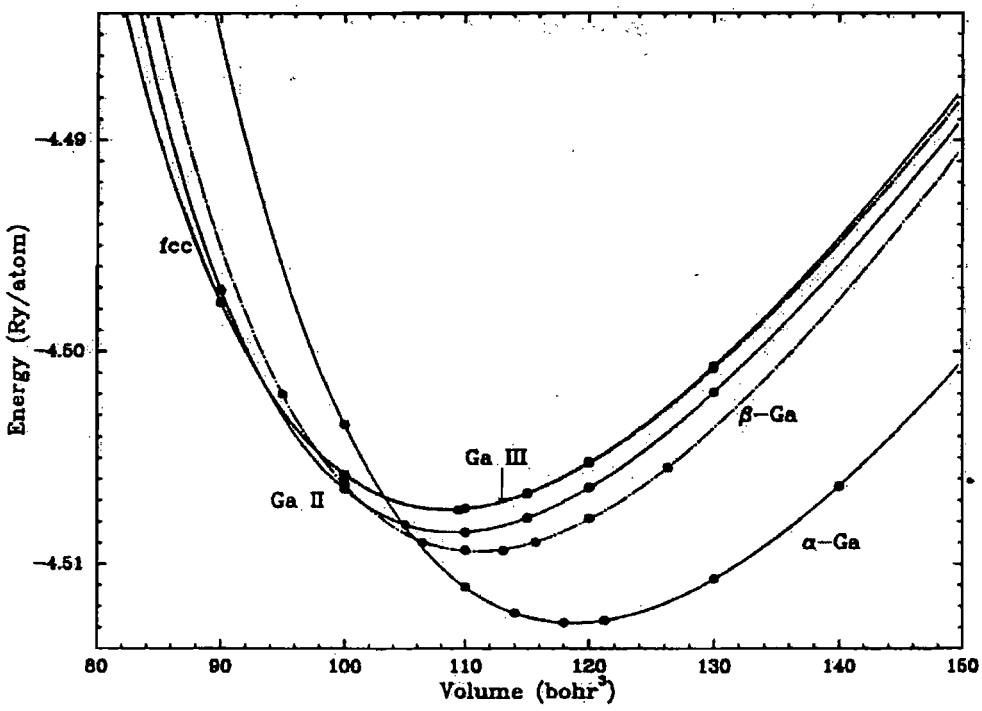


**FIGURE 2.9:** Energy as a function of unit-cell volume diagram for the stable phase and the main modifications of gallium. Taken from [23].

A more direct approach in examining the electronic properties of the main phases of gallium can be made through the density of states (DOS), which represent the number of

unoccupied electronic states as a function of energy. The DOS diagram for the α-phase and the rest of the main gallium modifications is shown in figure 2.10 below, as taken from [23]. From figure 2.10, some similarities and a clear difference in the DOS of the main gallium phases can be seen. Indeed, as a general trend all the phases exhibit free electron behaviour in their DOS, manifested by the increase of the DOS with increasing energy.

In the case of α-gallium, the DOS spectrum shows the typical features of free electron behaviour similar to that of the other phases, exhibited by the increasing DOS with increasing energy. More importantly it shows a structured character with a deep and pronounced pseudogap at the Fermi level. The latter was discussed in [24], where it was suggested to be a manifestation of the covalent character of this gallium phase. This feature of α-gallium reflects the energy band structure, shown in figure 2.4, where bands of overlapping energy states exist close to the Fermi level. In a typical semiconductor, with an energy band gap present on the band structure, the DOS spectrum would consist of the valence and conduction bands separated by a gap representing the band gap at the Fermi level. In α-gallium however, the band structure of the material does not show a continuous band gap, but rather a number of overlapping states at the Fermi level. In this case the gap at the Fermi level is replaced by a pseudogap and the DOS do not go to zero, representing the nearly empty bonding states and nearly filled antibonding states of the gallium dimer.

This distinct feature in the DOS of α-gallium is not present in the rest of the main modifications. Indeed, in β-gallium at the Fermi level there is a considerably less pronounced drop of the DOS, possibly a remnant of the α-gallium pseudogap, whereas Ga(II) and Ga(III) show an even less structured DOS with a clearer free electron behaviour, indicating that the loss of the covalent properties exhibited by α-gallium and the transition to gallium phases that exhibit metallic characteristics. Indeed, the covalent character of the α-phase disappears across the transition α-Ga β-Ga Ga(II) Ga(III) liquid gallium (not shown here) [28], with the latter exhibiting a free electron character.

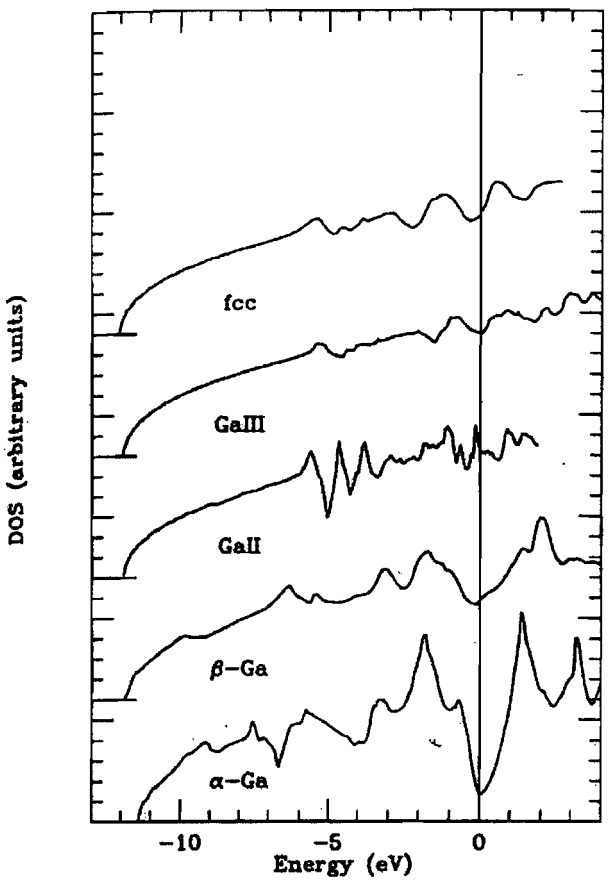


**FIGURE 2.10:** The density of states for the different phases of gallium. The covalent character of the α-phase is clearly illustrated by the well structured feature at the Fermi energy. Taken from [23].

## 2.10 More metastable phases

In addition to the main modifications of gallium, more phases have been reported in atmospheric pressure, which are mainly distinguished by their melting points and are known as γ, δ and ε with melting points, respectively: -19.4 $^0$C, -28.6 $^0$C and -35.6 $^0$C. The structure of the γ and δ phases is shown in figures 2.11, 2.12 taken from [33]. The γ phase is an orthorhombic crystalline structure with forty atoms in the unit cell, whereas the δ phase is a rhombohedral structure with its unit cell containing six atoms.

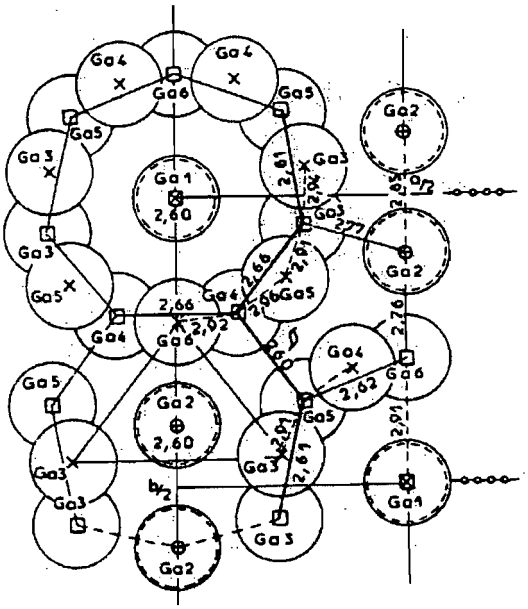


**FIGURE 2.11:** Atomic arrangement of the structure of γ-gallium, taken from [33].

Moreover, in [21] the existence of two more metastable phases has been reported. The ζ-gallium phase appears through the transformation of the γ-phase below -70 $^0$C. Another metastable phase can be obtained known as η-phase, below -130 $^0$C, and at the expense of the ζ phase

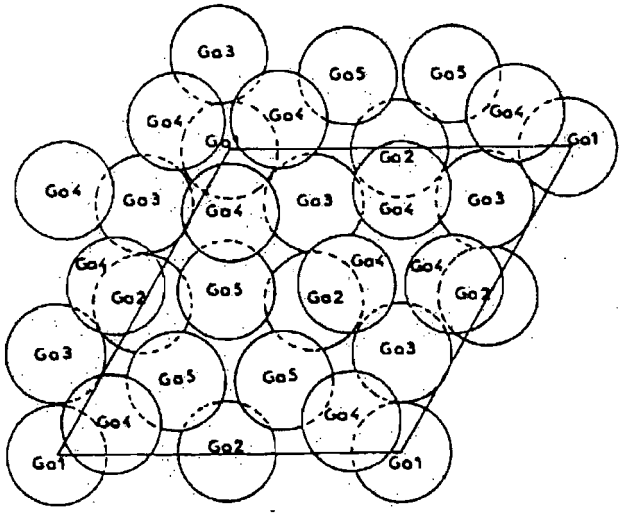


**FIGURE 2.12:** The structure of the δ phase of gallium, taken from [33].

Apart from these main modifications a non-crystalline state of amorphous gallium, which exhibits metallic properties [34] has also been reported. This metastable phase can be produced when gallium is deposited by condensation onto substrates, which are cooled down to liquid helium temperatures.

## 2.11 Conclusions

In the above sections the general properties of the material were reviewed. The polymorphic character of gallium was examined, and the properties of the various known phases were presented. The stable crystalline form of gallium, the α-gallium phase was identified, which has a partial covalent character. The main modifications of gallium were identified as the β-gallium phase, Ga(II) and Ga(III) and their properties were presented. A number of other gallium phases were discussed.

## 2.12 Phase transitions and melting in general

In this section the general features of phase transitions and associated phenomena such as premelting are examined as a guide for further study. The melting transition of gallium is then discussed.

In a phase transition a system is transformed from one state into another, with different initial and final properties. The transition occurs because the involved systems, going into a state of thermodynamic equilibrium, will tend to minimize their free energy. The best known examples of such a procedure are the melting of ice into water at its melting temperature, the evaporation of water, the superconducting to normal transition, the ferromagnetic transition at the Curie point. During a phase transition changes in the specific heat, latent heat, elastic constants, electrical properties, thermal conductivity and density take place, as well as volume and compressibility changes. Phase transitions can be divided into two main types, first-order transitions and higher order transitions (such as second-order). The difference in the properties of these two cases of transitions can be investigated using thermodynamic arguments in a macroscopic analysis. The distinction between the aforementioned cases was mainly made by Ehrenfest whereby if the n-th derivative of the Gibbs function is discontinuous and all other lower derivatives are not, the transition is of the n-th order [35]. If we consider a finite system of uniform

constituents then such a system can be described in terms of its thermodynamical properties. Namely, by defining the thermodynamic potential as a function of pressure and temperature, such as:

$$\mu = \mu (P, T) \qquad (2.1)$$

If such a system has two phases there will exist a point in which the specific Gibbs functions for the two phases will be equal, with the Gibbs function for each phase is:

$$G = \mu N \qquad (2.2)$$

Where $\mu$ is the already defined thermodynamic potential, and N is the number of molecules. At the equilibrium point of the two phases during the phase transition, from the above is easy to see that the thermodynamic potentials will be equal. By differentiating we get the first derivatives (see [35] for the full derivation via the Clausius-Clapeyron equation)

$$\partial\mu/\partial T \text{ and } \partial\mu/\partial P \qquad (2.3)$$

According to the Ehrenfest classification mentioned above, a first-order transition of a system can be defined as a transition for which the first derivatives, (2.3), have different values for the two phases of the system. Therefore the derivatives in (2.3) will be discontinuous at the point of the phase transition, and there will be a discontinuous change in the volume and in the internal energy. In this case, there is total separation of the two phases, initial and final, involved in the process. Transitions of a higher order, such as second-order phase transitions, can be defined using the same Ehrenfest classification, for which the second derivatives of the thermodynamic potential will be discontinuous but the internal energy will be continuous. The crystal to liquid melting transition shows features of both a first order and a higher order transition, with premelting effects that take place close to the crystal melting temperature [36]. The loss of long-range order in the crystalline system makes melting an order-disorder transition.

## 2.13 Surface Phenomena and Premelting effects

The existence of a free surface on a crystal modifies its properties through the way that the material interacts with its environment. Crystal surfaces exhibit properties that are structure sensitive and vary considerably according to the configuration of the surface at the atomic scale. The atomic and electronic properties of a crystal surface can differ significantly from those of the bulk. At the surface, atoms are not necessarily arranged in the same way as the atoms of the bulk, a property of the surface called reconstruction. Furthermore relaxation effects tend to alter the lattice distances at the top few atomic layers of the surface.

Moreover, a free surface, for any kind of crystal, constitutes a reservoir of an unwanted amount of energy. The atoms situated in the topmost layers of such a free surface are missing their nearest neighbours that gives rise to a charge redistribution. In such a case the crystal reduces the excess amount of energy by means of reconstruction processes taking place at the surface [4]. Furthermore the local stress is increased as compared to that of the bulk, due to the expansion of the outer lattice planes. This results in the easy generation of dislocation defects at the surface, since the energy of a dislocation will be much less in the surface than in the bulk crystal [37].

The surface is thus seen as a favoured site for the generation of dislocations. When the crystal is below its thermodynamic melting point, any defects (dislocations) that are created near the surface will be drawn closer to it. As the crystal moves closer to its melting temperature these defects will act as a liquid layer and initiate melting (premelting effects). However if such a layer was thick enough it would act to eliminate the effect of the surface and would suppress the possibility of a surface-initiated melting. In such a case the crystal would melt from the inside. In general melting of a solid can usually commence at its surface. However the presence of impurities, oxides, etc at a crystal surface, affects the melting transition by promoting or suppressing such a surface-initiated melting transition.

At the surfaces of most of the crystals, at temperatures well below their thermodynamic melting point, a microscopically thin liquid-like films appears [38], [39]. This

phenomenon of the appearance of this thin liquid-like phase of the material on the surface is a wetting phenomenon, or transition, which leads to interesting phenomena taking place, such as surface-initiated melting, roughening and freezing [38]. The basis for such self-wetting phenomena is that the emerging surface has a lower total free energy, so as to balance the energies of the thin film and the interface [20], [40].

The thickness of this layer is dependent on the temperature of the crystal T, and in most cases it grows critically as it approaches the melting temperature, $T_m$, [4], [38], [39] extending infinitely into the bulk at the melting point. This case is identified as surface-initiated melting. However, in other cases the thickness assumes a finite value at the melting temperature indicating the case of a blocked or incomplete melting. Finally, in some cases no such liquid film can appear at melting, and the surface maintains its crystal form throughout the melting transition [38].

In the case of surface melting, and when the thickness of this layer extends only a few monolayers inside the bulk, the atoms are still subjected to the influence of bulk forces [4]. For this reason this layer is usually referred to as a quasi-liquid layer because it is not the true liquid phase of the material, since the bulk solid under the layer induces a short crystalline order [39], [4]. The properties of it are intermediate between those of the solid and the liquid. Moreover such a layer is in thermal equilibrium with the underlying solid, and infinitesimally close to the bulk melting temperature the layer penetrates deeply into the bulk. At that point the solid, liquid and vapour phases of the material coexist [4].

The presence and growth of such a layer is highly dependent on the surface geometry and orientation of a material. Namely, materials whose crystal faces show an open packing character can exhibit premelting effects. In contrast with close-packed faces that will not melt until the melting point has been reached [41]. Furthermore, the crystal orientation at the surface may increase or decrease the appearance of the number of such layers [41], [4].

The thickness of such a layer has been predicted to diverge logarithmically or according to a power-law dependence, with respect to the proximity of the crystal temperature to its melting point, $(T_m - T)$. These two regimes apply depending on whether the forces, between such a layer and the bulk, are of short or long-range order respectively [41].

Namely, by calculating the free energy of such a surface layer, by means of mean-field theory [4 and references therein], the thickness of the layer, $l$, is given by equation (2.4) for short-range order, and equation (2.5) for long-range order.

$$l = \frac{\xi}{2}\ln\left[\frac{2\Delta\gamma T_m}{(T_m - T)L_m\xi}\right] \tag{2.4}$$

$$l = \left[\frac{2WT_m}{(T_m - T)L_m}\right]^{1/3} \tag{2.5}$$

Figure 2.13, below, shows the growth of such a layer as determined by the two equations mentioned above. The increase in thickness follows a logarithmic growth for temperatures $T_m - T > 0.5$ K defined by equation 2.4, and a power-law growth for temperatures $T_m - T < 0.2$ K defined by equation 2.5.

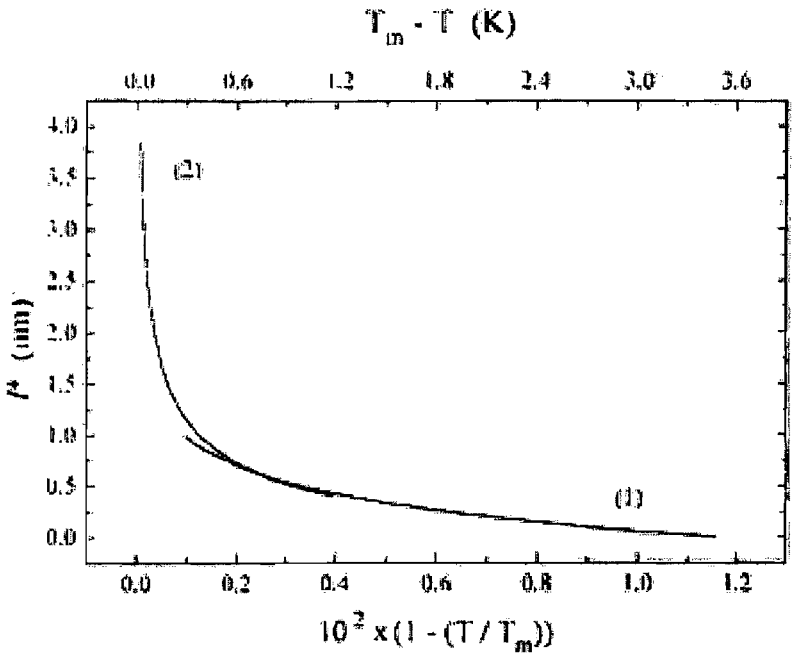


**FIGURE 2.13**: Layer thickness, *l*, plotted as a function of sample temperature. Taken from [4] for illustrative purposes only.

In both cases $L_m$, $\Delta\gamma$, and $\xi$, are the latent heat of melting per unit volume, the free energy of the solid-vapour interface, and the correlation length of the order parameter, and W is the Hamaker constant of the material. Studies have suggested that in gallium the Hamaker constant has a negative value, a typical case when in a material the liquid phase is denser than the solid phase. A similar case has been observed with Bi and Ge, two materials showing a full metallic character on melting compared with their covalent solid phases [42], [38]. The physical meaning of a negative Hamaker constant is non-melting or in another case incomplete melting [38]. Incomplete melting has been observed in the case of some facets of an $\alpha$-gallium crystal grown from the melt.

## 2.14 The melting transition of gallium

The melting of gallium was investigated by [43], using the differential thermal analysis method. This technique involves heating the material, at a controlled rate, up to its melting

temperature and comparing the emission or absorption of heat with respect to a control material. This type of measurement technique has proved a precision technique for studying phase transitions. The results showed for gallium single crystals, with slow heating rates, that melting didn't occur at a well-specified melting point, as was expected. The transition extended over a range of temperatures, having three distinct stages that required different amounts of energy. The melting stages observed were attributed to the process of collapse of different portions of the crystalline structure well below the melting temperature. Moreover this type of multi-stage melting has also been considered as an indication of surface effects taking place. This behaviour was only observed in single crystal samples, and not in polycrystalline ones. Rapid recrystallisation of the samples altered the transition. The melting transition of gallium crystals was also investigated in [44] using the same differential thermal analysis method. In this case, melting of single crystals of gallium was observed to take place in four stages compared with the three observed by [43]. Finally the optical properties of gallium across the melting transition were investigated by [12]. Results showed that extensive changes take place in the structural and optical properties of the material on melting. The changes in the optical properties of gallium across melting as a function of wavelength are examined in detail in Chapter 4.

In another publication the existence of a thin liquid-like surface layer was observed, that when thick enough can make the melting of the gallium crystal incomplete [45]. When a certain finite thickness is reached then melting proceeds as a typical first-order transition. This corroborates the observations discussed earlier on the surface phenomena during the melting transition.

## 2.15 Melting of various gallium surfaces

Different gallium surfaces exhibit various melting behaviours. Indeed, in a typical α-gallium crystal, as shown in figure 2.2, a number of low index facets can be observed namely (010), (111), and (112) [4]. Another facet that can be found on a gallium crystal is the (100) that doesn't form naturally in the crystal but has to be prepared. Research has shown that the (100) and (010) surfaces exhibit a remarkable stability up to the melting point [46], [20], [4]. Further research has shown that the (112) surface of gallium readily exhibits precursory effects well below the melting temperature. The (112) surface is

formed in a typical single crystal of gallium, and has the lowest packing density of dimers, with 2.5 dimers/nm$^2$ [47]. Moreover the free energy of this surface is the highest, compared with different crystallographic directions [4]. This facet is a very good candidate when it comes to the disordering of the surface atoms and the formation and growth of a quasi-liquid layer. Indeed, this surface has been observed to be covered by a quasi-liquid layer that grows in thickness with increasing temperatures [4].

The growth of this layer begins with a logarithmic character, see Equation (2.4), and switches to a power-law dependence, see Equation (2.5), for temperatures very close to the melting point. Similar results were observed in a (110) Pb surface [39].

The (010) surface exhibits a negative Hamaker constant value and shows extensive thermal stability up to the melting point. This indicates that there are no surface induced effects, such as surface melting. This face is the main stable surface in a gallium crystal having the highest packing density of about 9.8 dimers/nm$^2$, and can appear spontaneously at the crystal. In [20], [23] it has been reported that the (010) surface is covered by a few monolayers of Ga(III), see figure 2.14. This is due to surface reconstruction, in an effort by the $\alpha$-gallium crystal to remove the unsaturated surface dangling bonds.

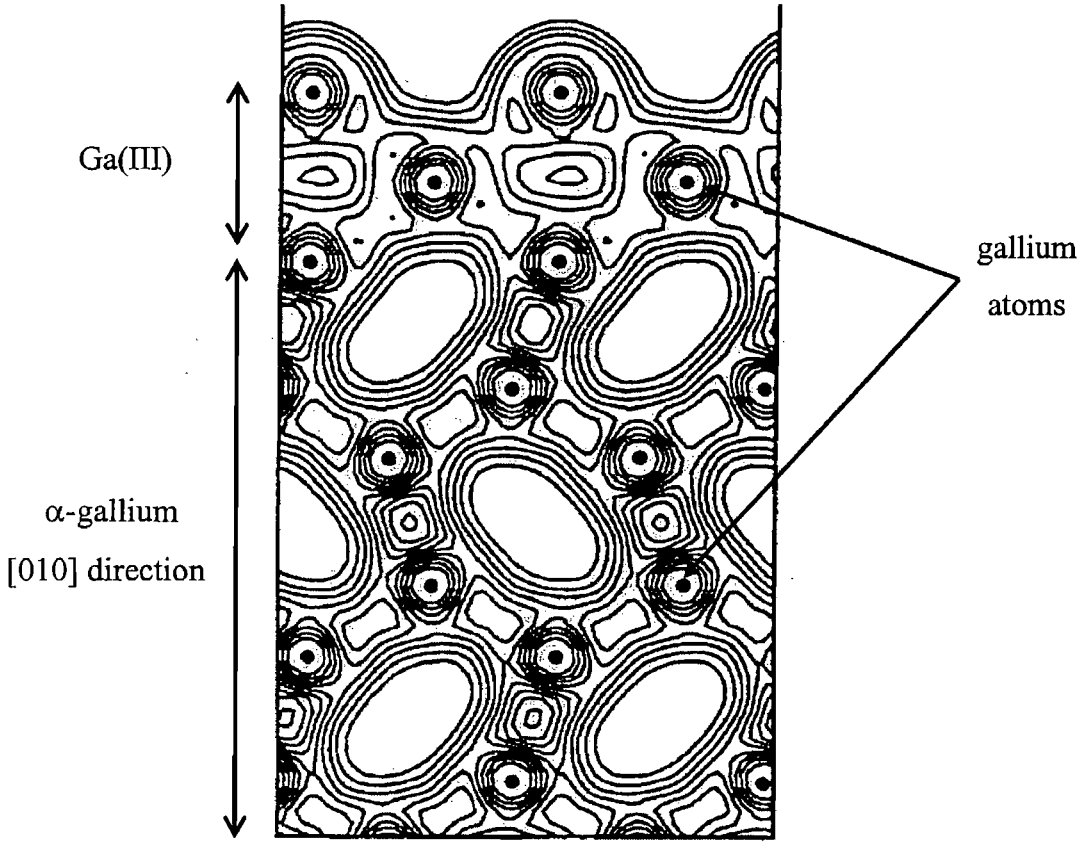


**FIGURE 2.14:** Charge density in the self-wetting arrangement of Ga(III) grown on the (010) surface of α-gallium. Taken from [20].

In this case of self-wetting of the gallium surface by Ga(III), shown in figure 2.14, the total surface energy of the layer is much less than that of a free gallium surface, making it energetically favourable [20]. Furthermore, Ga(III) is known to melt, at about 100K higher than α-gallium. This case has been observed in gallium (010) surfaces, covered by the Ga(III) layers of finite thickness, where at $T_m$ the crystal seems to melt from the inside [20], [23], [46].

Another free surface of a α-gallium crystal that has been investigated for its melting properties is the (100) surface. This facet does not appear naturally in the α-gallium crystal, grown from the melt, but has to be prepared by cutting the crystal [20]. This face has the next lowest dimer packing density, after the (112) surface, with 5.8 dimers/nm$^2$ [4]. This surface, like the (010) face, shows no precursory effects as the crystal temperature is increased up to the melting point, suggesting a self-wetting effect similar to the (010) surface, since these two facets have similar packing densities [20].

## 2.16 Liquid gallium

In general, metals exhibit a decrease in their coordination number, with the mean interatomic distance increasing on melting. This increase accounts for the typical decrease in the density of liquid metals [47]. Gallium, however, on melting moves from a low-symmetry crystalline phase to a loose close packing liquid phase and is one of the few known substances, along with Sb, Bi, and water, which show a contraction in volume in liquid. On melting the majority of the covalent bonds of the gallium structure break resulting in tighter packing of the atoms, which in turn explains the difference in the density of the two states. Namely the liquid exhibits a density of about 3.2% higher than that of the crystalline phase [30], in contrast to most other metals that, on average, show a 2 to 6% increase in volume on melting [15]. This contraction on melting has the further result of lowering the binding energy of gallium [15].

The collapse of the majority of the gallium covalent bonds has a clear effect on the covalent character and is reflected on the DOS diagram of the liquid phase. On melting, these covalent features are all completely lost and the liquid phase of gallium exhibits an almost free electron behaviour. This change in the electronic properties in the transition from the α-phase to the liquid indicates the change in the local atomic order on melting, and therefore reflects the short-range order loss [30]. Figure 2.15, below shows the density of states for the stable solid phase (α-gallium), one of its modifications (β-gallium) and the liquid state, as taken from [48]. The loss of the covalent character in the liquid phase can be seen, with the vast majority of the structuring found in the α-gallium DOS, missing in liquid gallium. However, some structuring in the case of the liquid DOS is still present, for the reasons discussed in the next paragraph. Also some limited similarity between the density of states of the β-gallium phase and liquid gallium can be seen. Both show increasing density of states with increasing energy. Also, compared with α-gallium, both have lost the pseudogap at the Fermi level. The difference between these two phases is that the β-gallium phase retains more features in its DOS spectrum, which reflect a greater number of residual properties of the α-gallium phase, in contrast with liquid gallium, which shows much less features on its DOS.

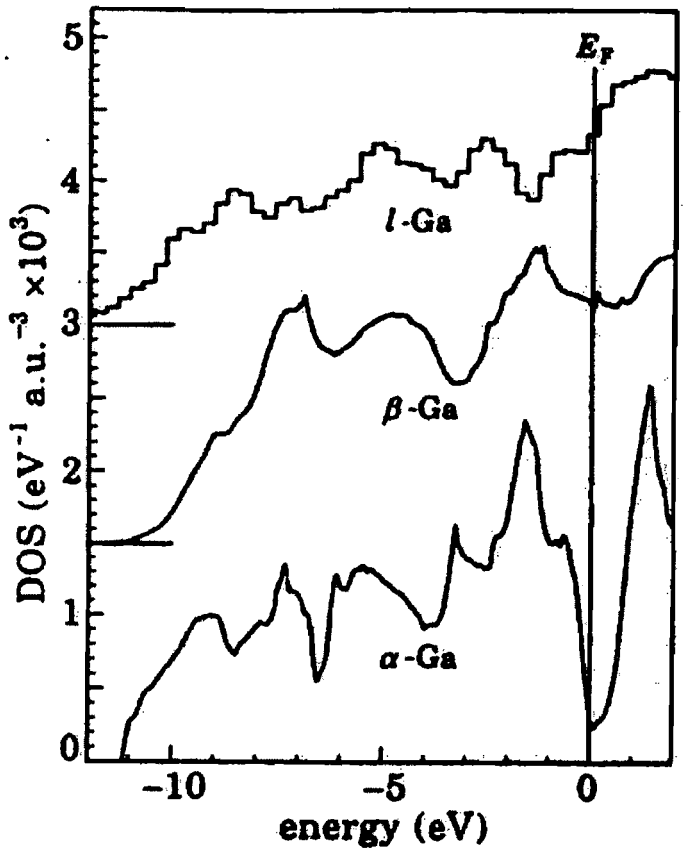


**FIGURE 2.15:** The density of states for α, β, and liquid gallium, taken from [48].

Moreover, research has shown an asymmetry in the structure factor of liquid gallium [49]. Such a feature could indicate the existence in the liquid phase of a covalent character, similar but not as extensive as that of the crystalline phase [47]. More specifically the investigation of the structure factor of liquid gallium has revealed a similarity to liquid Si and Ge. These group-IV elements show partially covalent characteristics. No such feature has been seen in Al, In, and Tl, isoelectronic metals to gallium, but which show no covalent character in their stable crystalline phases [30]. Such findings suggest a covalent character in the liquid phase of gallium, similar to that of its stable crystalline phase. This covalent character is manifested with the existence of a certain amount of very short-lived $Ga_2$ dimers [48], representing the remnants of the covalent bonds in the α-phase [30]. The concentration of these short-lived molecules depends on the temperature, increasing with lower liquid temperatures (closer to the solid temperatures).

Another interesting feature of the liquid state of gallium is surface layering. Theory predicts the existence of packed atomic layers in the surface of liquid metals [50], in contrast with the surface of non-metallic elements which show no such layering [49Regan 1]. The interface of a liquid with its vapour is the subject of continuous disturbances, which are active on the molecular level. The disturbances are in the form of random fluctuations at the surface of the liquid, which produce capillary waves [51]. The surface tension of the liquid surface influences the appearance of these capillary waves, with the metals having high surface tension, such as gallium, exhibiting smaller fluctuations [49].

X-ray reflectivity measurements have confirmed the theoretical predictions of layering on a liquid metal surface, showing that the upper-most atoms close to the surface of the liquid are stratified in packed atomic layers, parallel to the surface, in liquid Hg and liquid gallium [49]. Results showed that liquid gallium exhibits a surface-induced layering with spacing similar to the atomic dimensions of crystalline gallium, extending a few atomic layers into the bulk of the liquid. The interlayer spacing was found to be about 10% less than the near neighbour distance in the bulk of the liquid.

Further experiments have shown the existence of an oxide layer in the surface of liquid gallium [52]. The presence of the oxide layer has been proposed to be a direct result of the limited existence of gallium ions at the outmost surface of the liquid. These ions are produced by the unsaturated dimers mentioned above, similar to those present at the surface of crystalline gallium. The ions react with the oxygen ions present at the surface creating the oxide layer, consisting of alternating layers of gallium and oxygen ions. These layers create an oscillatory profile, which account for the atomic layering observed in the X-ray experiments.

Finally, liquid gallium shows interesting features when in contact with a hard wall. In general when a liquid is in contact with a solid wall there seems to be a layering of the atoms closest to the solid wall-liquid boundary. In liquid gallium this has been observed in the case of contact with the (111) surface of a diamond [53]. Figure 2.16, shows this arrangement at the interface with a hard wall, here liquid gallium is shown to preferentially wet the interface with a diamond (111) surface.

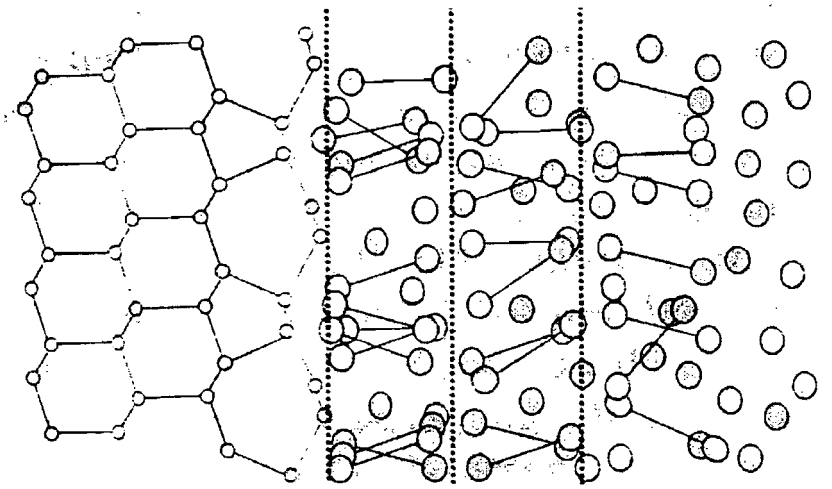

**FIGURE 2.16:** The preferential orientation of the gallium dimers when the liquid is in contact with a hard wall. This figure shows planes of dimers in an increasingly disordered fashion moving away from the wall. Taken from [53].

In this preferential arrangement, the liquid assumes an α-gallium like structure, extending for a few layers into the bulk liquid. This layering is a result of liquid gallium trying to imitate the morphology of the diamond structure, and to minimize the energy of the interface. When solidified this arrangement is sustained, as it is energetically favourable for the material.

Another case of preferential arrangement has been reported, with the gallium dimers being in parallel with the underlying structure. Rows of gallium (and indium) atoms were observed, in the so-called parallel dimer model, on the (001) surface of silicon [54].

## 2.18 Summary of Chapter 2

In this chapter a literature review of the properties of gallium was presented. The material possesses a complicated polymorphic character with a number of stable and metastable phases existing at different conditions of pressure and temperature. The main phases of gallium were identified and their properties were discussed.

The stable crystalline phase is the α-gallium phase, which has a partial covalent character. Its crystalline structure comprises metallic and molecular bonding in which some bonds form dimers and the rest are metallic. The other main structural modifications are the β-gallium phase, Ga(II) and Ga(III). A number of more metastable phases also exits.

The melting transition of gallium was presented, and the melting of different surfaces present on a gallium crystal was discussed. On melting gallium loses its covalent character and it becomes a free electron metal. The liquid phase of gallium exhibits a weak covalent character with the existence of very short-lived gallium dimers, imitating the crystalline phase of the material.

The covalent bonding gives rise to a very broad absorption band that offers unique opportunities for light-matter interaction by stimulating structural transitions with light. The substantial difference in the electronic properties between the various gallium phases, make it a potentially interesting and unique material for inducing nonlinear phenomena through light-induced structural transitions.

## References


[1] J. Donohue, The Structures of the Elements, page 236, John Wiley & Sons, New York, 1974

[2] J. C. Slater, G. F. Koster, J. H. Wood, Physical Review, page 1307. vol. 126, no. 4, 1962

[3] C. S. Barrett, F. J. Spooner, Nature, page 1382, vol. 207, 1965

[4] R. Trittibach, Ch. Grutter, J. H. Bilgram, Physical Review B., page 2529, vol. 50, no. 4, 1994

[5] I. Yu. Rapp, I. N. Shklyarevskii, R. G. Yarovaya, Soviet Physics: Solid State, page 1780, vol. 10, no. 7, 1969

[6] J. Bor. C. Bartholomew, Proceedings of the Physical Society, page 115, vol. 90, 1967

[7] G. Jezequel, J. C. Lemonnier, J. Thomas, Journal of Physics F: Metal Physics, page 1613, vol. 7, no. 8, 1977

[8] I. Yu. Rapp, R. G. Yarovaya, L. A. Bondarenko, Fiz. Metal. Metalloved, page 728, vol. 32, no. 4, 1971

[9] A. P. Lenham, Proceedings of the Physical Society, page 933, vol. 82, 1963

[10] A. P. Lenham, D. M. Treherne, Journal of the Optical Society of America, page 752, vol. 56, no. 6, 1966

[11] R. Kofman P. Cheyssac J. Richard, Physical Review B., page 5216, vol. 16, no. 12, 1977

[12 R. Kofman, P. Cheyssac, R. Garrigos, Journal of Physics F: Metal Physics, page 2345, vol. 9, no. 12, 1979

[13] L. G. Schulz, Journal of the Optical Society of America, page 64, vol. 47, no. 1, 1957

[14] R. Sh. Teshev, A. A. Shebzukhov, Optics and Spectroscopy (USSR), page 693, vol. 65, no. 5, 1989

[15] S. R. Barman, D. D. Sarma, Physical Review B., page 4007, vol. 51, no. 7, 1995

[16] P. J. Bennett, S. Dhanjal, P. Petropoulos, D. J. Richardson, N. I. Zheludev, V. I. Emel'yanov, Applied Physics Letters, page 1787, vol. 73, no. 13, 1998

[17] V. Albanis, S. Dhanjal, N. I. Zheludev, P. Petropoulos, D. J. Richardson, Optics Express, page 157, vol. 5, no. 8, 1999

[18] P. Petropoulos, H. L. Offerhaus, D. J. Richardson, S, Dhanjal, N. I. Zheludev, Applied Physics Letters, page 3619, vol. 74, no. 24, 1999

[19] N. J. C. Libatique, J. D. Tafoya, S. H. Feng, D. J. Mirell, R. J. Kain, Advanced Solid State Lasers, page 417, vol. 34, Optical Society of America, Washington DC, 2000

[20] M. Bernasconi, G. L. Chiaroti, E. Tosatti, Physical Review B., page 9999, vol. 52, no. 14, 1995

[21] R. D. Heyding, W. Keeney, Journal of Physical Chemistry of Solids, page 133, vol. 34, 1973

[22] H. G. von Schnering, R. Nesper, Acta Chemica Scandinavica, page 870, vol. 45, 1991

[23] M. Bernasconi, G. L. Chiarotti, E. Tosatti, Physical Review B., page 9988, vol. 52, no. 14, 1995

[24] V. Heine, Journal of Physics C., page 222, vol. 1, no. 2, 1968

[25] X. G. Gong, G. L. Chiarotti, M. Parrinello, E. Tosatti, Physical Review B., page 14277, vol. 43, no. 17, 1991

[26] F. Abeles, Optical Properties of Solids, Edited by F. Abeles, North-Holland Publishing Company, 1972

[27] L. Bosio, C. G. Windsor, Physical Review Letters, page 1652, vol. 35, no. 24, 1975

[28] F. J. Bermejo, R. Fernandez-Perea, M. Alvarez, B. Roessli, H. E. Fischer, J. Bossy, Physical Review B., page 3358, vol. 56, no. 3, 1997

[29] L. Bosio, Journal of Chemical Physics, page 1221, vol. 68, no. 3, 1978

[30] J. Hafner, W. Jank, Physical Review B., page 11530, vol. 42, no. 18, 1990

[31] S. F. Tsay, Physical Review B., page 103, vol. 50, no. 1, 1994

[32] P. Ascarelli, Physical Review, page 36, vol. 143, no.1, 1996

[33] A. Defrain, Journal de Chimie Physique, page 851, vol. 74, no. 7-8, 1977

[34] O. Hunderi, R. Ryberg, Journal of Physics F: Metal Physics, page 2096, vol. 4, 1974

[35] C. J. Adkins, Equilibrium Thermodynamics, Third Edition, Cambridge University Press, 1983

[36] H. Wenzl, G. Mair, Zeischriff fur Physik B., page 95, vol. 21, 1975

[37] J. K. Kristensen, R. M. J. Cotterill, Philosophical Magazine, page 437, vol. 36, no. 2, 1977

[38] A. Dal Corso, E. Tosatti, Physical Review B., page 9742, vol. 47, no. 15, 1993

[39] B. Pluis, D. Frenkel, J. F. van der Veen, Surface Science, page 282, vol. 239, 1990

[40] M. Bernasconi, G. L. Chiarotti, E. Tosatti, Physical Review Letters, page 3295, vol. 70, no. 21, 1993

[41] B. Pluis, A. W. Denier van der Gon, J. W. M. Frenken, J. F. van der Veen, Physical Review Letters, page 2678, vol. 59, no. 23, 1987

[42] X. J. Chen, A. C. Levi, E. Tosatti, Surface Science, page 641, vol. 251-252, 1991

[43] J. Jach, F. Sebba, Transactions of the Faraday Society, page 226, vol. 50, 1954

[44] O. A. Boedtker, R. C. La Force, W. B. Kendall, F. S. Ravitz, Transactions of the Faraday Society, page 665, vol. 61, 1965

[45] G. Fritsch, E. Luscher, Philosophical Magazine, page 21, vol. 48. no. 1, 1983

[46] O. Zuger, U. Durig, Physical Review B., page 7319, vol. 46, no. 11, 1992

[47] C. Grutter, R. Trittibach, J. H. Bilgram, Helvetica Acta, page 215, vol. 67, no. 2, 1994

[48] X. G. Gong, G. L. Chiarotti, M. Parrinello, E. Tosatti, Europhysics Letters, page 469, vol. 21, no. 4, 1993

[49] M. J. Regan, E. H. Kawamoto, S. Lee, N. Maskil, M. Deutsch, O. M. Magnussen, B. M. Ocko, L. E. Berman, Physical Review Letters, page 2498, vol. 75, no. 13, 1995

[50] G. Makov, A. A. Kornyshev, Journal of Chemical Physics, page 1963, vol. 104, no. 4, 1996

[51] V. Kolevzon, G, Gerbeth, Journal of Physics D: Applied Physics, page 2071, vol. 29, 1996

[52] M. J. Regan, H. Tostmann, P. S. Pershan, O. M. Magnussen, E. DiMasi, B. M. Ocko, M. Deutsch, Physical Review B., page 10786, vol, 55, no. 16, 1997

[53] W. Huisman, J. F. Peters, M. J. Zwaneburg. S. A. de Vries, T. E. Derry, D. Abernathy, J. F. van der Veen, Nature, page 379, vol. 370, no. 27, 1997

[54] H. G. von Schnering, R. Nesper, Acta Chemica Scandinavica, page 870, vol. 45, 1991 M. M. R. Evans, J. Nogami, Physical Review B., page 7644, vol. 59, no. 11, 1999

# Chapter 3

# All-Optical Switching at a Silica-Gallium interface

## 3.1 Synopsis

A silica-gallium interface prepared at the tip of an optical fibre, exhibits a strong nonlinear behaviour, associated with a light-induced structural phase transition. This transition involves the stable crystalline phase, α-gallium, converting into a more metallic phase of higher reflectivity. The nonlinear character exhibits broadband spectral response. Using the nonlinearity of the interface cross-wavelength modulation between signals at 1.3μm and 1.55μm was achieved.

An additional effect was also observed. The reflectivity of a silica-gallium interface, formed on an optical flat or at the tip of a cleaved optical fibre, can be reduced in a reversible fashion when the interface is excited by a few milliwatts of laser power. This phenomenon has been observed to occur at interface temperatures just below gallium's melting point. The effect can be attributed to some form of light-induced structuring at the interface of gallium with silica.

## 3.2 Introduction

Nowadays, the quest for materials that can be useful in photonic and optoelectronic applications, such as all-optical switching, optical processing etc, has concentrated on materials that can exhibit a large optical nonlinearity in a reversible manner with low excitation power. Recent research has shown that gallium belongs to this group of materials. When confined at a glass interface it is a very intriguing structure and potentially useful for optoelectronic applications due to its enhanced nonlinear optical properties.

Indeed, the reflectivity of a silica-gallium interface has been reported to be modified by as much as 30% by just a few milliwatts of incident light intensity [1]. Moreover, a change of several degrees can be induced on the polarisation state of the light reflected of a silica-gallium interface [2], when the material is kept close to its melting temperature, $T_m = 29.8\ ^0C$. The gallium nonlinearity was attributed to a light-induced, reversible and fast structural phase transition. The transition involves the stable structural phase of gallium converting into a new more metallic phase of considerably higher reflectivity. During this transition, gallium's electronic and optical properties undergo changes (see Chapter 2) that make the interface properties sensitive to broadband optical excitation, spanning from 480 nm to 1800 nm [3]. The gallium nonlinearity was used to demonstrate q-switching of fibre lasers at different wavelengths [4], [5].

In another application, the silica-gallium interface nonlinearity was used to demonstrate an all-optical fiberised switch, in which the light intensity of pump beam was used to modulate the light intensity of a probe beam [1]. However, this all-optical switch was demonstrated using a frequency degenerate optical nonlinearity, where the pump and probe wavelengths were both at 1.55 μm. As already mentioned above, on the verge of the structural phase transition, the gallium nonlinearity has been observed to be extremely broadband. This offers unique opportunities for light-by-light control between wavelengths in the 480 – 1800 nm band. Therefore, it was decided to investigate cross-wavelength all-optical switching at a silica-gallium interface. In this chapter, all-optical switching between signals at 1.3 μm and 1.55 μm is demonstrated. The results indicate

that the silica-gallium interface is able to perform sub-microsecond switching. Modulation of the reflected intensity by as much as 45% was observed.

During the investigation of the cross-wavelength all-optical switch, another optical behaviour was also observed. This behaviour is an additional light-induced effect, which takes place within a narrow temperature interval, typically less than 1°C, just below $T_m$. In this region the typical reversible light-induced reflectivity increase, encountered in the experiments above, is replaced by an abrupt reversible, light-induced decrease in reflectivity (see section 3.6).

The results, presented herein, from both investigations offer a unique opportunity for extremely useful optoelectronic and photonic applications. Namely, the all-optical switch is compatible with lasers of different wavelengths, and is fully customisable with existing fibre optics technology. Moreover, switching between signals of different wavelengths is extremely useful for applications such as optical routing, and optical data processing in the field of integrated optics. At the same time, the additional effect of interface reflectivity suppression can be used for power limiting applications in all-optical data processing systems.

## 3.3 Cross-Wavelength All-optical Switching at a Silica-Gallium Interface

The work presented in this section was undertaken in collaboration with S. Dhanjal and P. Petropoulos, under the supervision of Professors D. J. Richardson and N. I. Zheludev.

In this experiment the switching properties of the silica-gallium interface, were investigated close to the melting temperature of gallium, $T_m$, using a pump-probe setup. The reflectivity of the interface was examined using pump pulses of different intensities, for various interface temperatures up to the melting point of gallium.

The silica-gallium interface (mirror) was formed at the tip of standard, single mode, telecommunications silica fibre that was cleaved and immersed into a small bead of gallium of 5N purity. The gallium bead was initially maintained in the molten phase and was forced to solidify as soon as the fibre tip was satisfactorily immersed. Thermal control of the silica-gallium interface was provided by the miniature thermoelectric heat pump

(Peltier element) and a fast digital temperature controller, with nominal precision of 0.01 $^0$C. The temperature of the gallium bead was monitored constantly by a thermistor situated on the ceramic plate of the peltier element.

In the pump-probe experiment, the pump was an amplified, directly modulated, distributed feedback diode laser, operating at the wavelength of $\lambda_C$ = 1.550 μm, with 1 MHz available bandwidth. The probe was a cw diode laser, operating at the wavelength of $\lambda_S$ = 1.3 μm. The pump and probe were coupled on and off the silica-gallium interface using a wavelength division multiplexer (WDM). The peak power of the pump pulses could be varied between 0 and 90 mW, while the power of the continuous wave probe beam was 60 μW at the gallium mirror.

On reflection, the pump wavelength was filtered out using about 10 m of erbium doped fibre (EDF), which transmits the probe but absorbs the pump. The interface reflectivity was monitored by detecting the probe beam at the switch output with a 125 MHz InGaAs detector. The outline of the optical setup used in this experiment is shown in figure 3.1

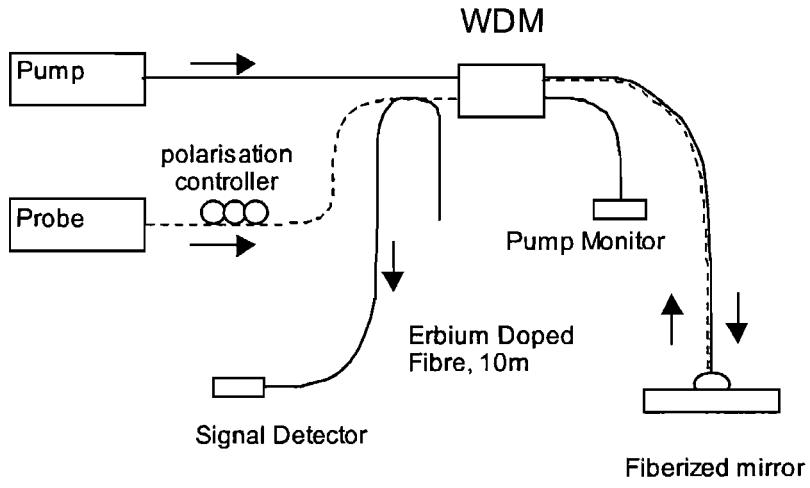


**FIGURE 3.1:** the experimental setup used to demonstrate all-optical switching at a silica-gallium interface.

The silica-gallium interface is anisotropic, as was shown in Chapter 2, due to the preferential orientation of gallium at the interface. See Chapter 4, for a calculation of the

silica-gallium interface reflectivity according to the specific crystallographic direction present at the interface. In this experiment, to ensure that the initial reflectivity levels corresponded to the α-gallium reflectivity, the light from the probe laser was linearly polarized, and was adjusted using a polarization controller to obtain the minimum value of silica-gallium reflectivity. In addition, the polarisation of the probe was adjusted to give maximum reflectivity change.

In the experiment, the intensity modulation of the pump beam induces a change in the reflectivity of the silica-gallium interface, causing a modulation of the probe intensity, corresponding to the cross-talk between the two channels. Here, the probe reflectivity was altered using pump pulses of 100 ns duration, at 10 kHz repetition rate. Figure 3.2, below, shows the response of the silica-gallium interface for pump pulses of 83 mW peak power, 100 ns, as a function of sample temperature.

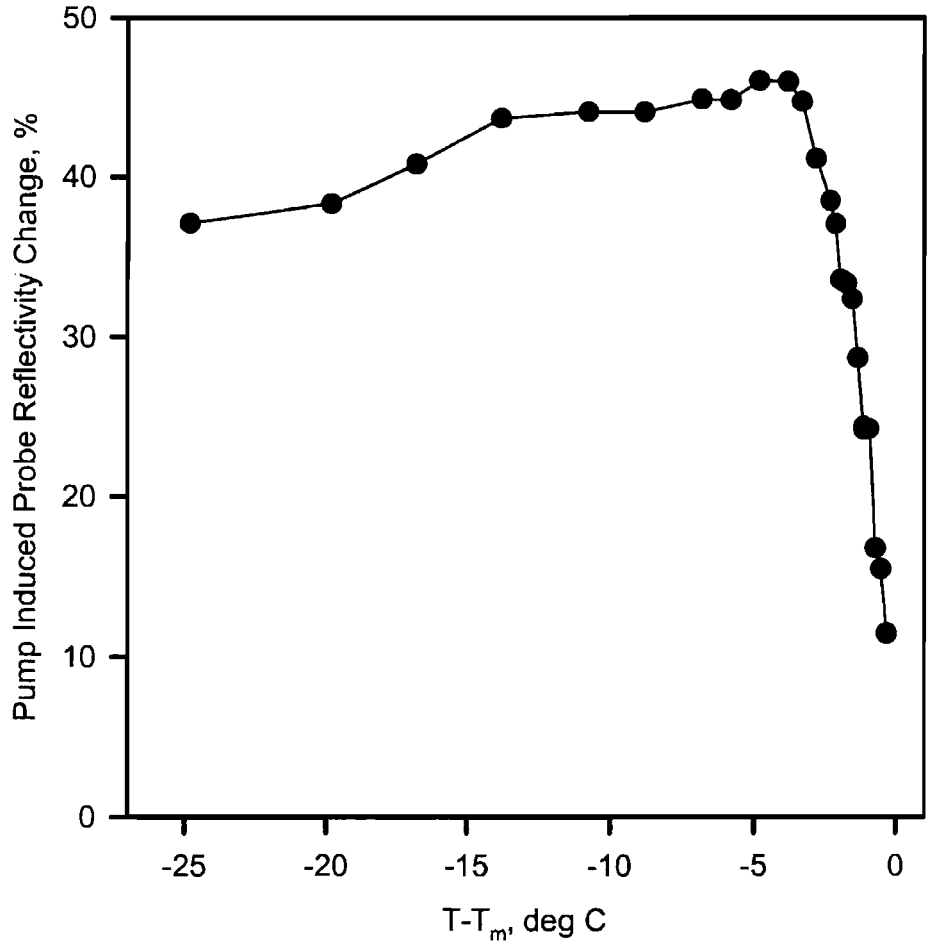


**FIGURE 3.2:** The change in the intensity of the reflected probe intensity by the 83 mW peak power, 100 ns pump pulses, for increasing temperature.

The results show that as the temperature of the interface, T, is increased towards the melting point, $T_m$, the induced nonlinear response rises steadily up, and reaches a level of about 45%. The maximum pump-induced probe reflectivity change occurs about 4 $^0$C below the melting point, and it then falls rapidly. The induced probe change becomes undetectable above the melting temperature.

The modification of the behaviour of the probe reflectivity was observed to be fully reversible. The results show that the reflectivity recovery time depends on the gallium temperature and increases with the temperature approaching the melting point of bulk gallium, see figure 3.3.

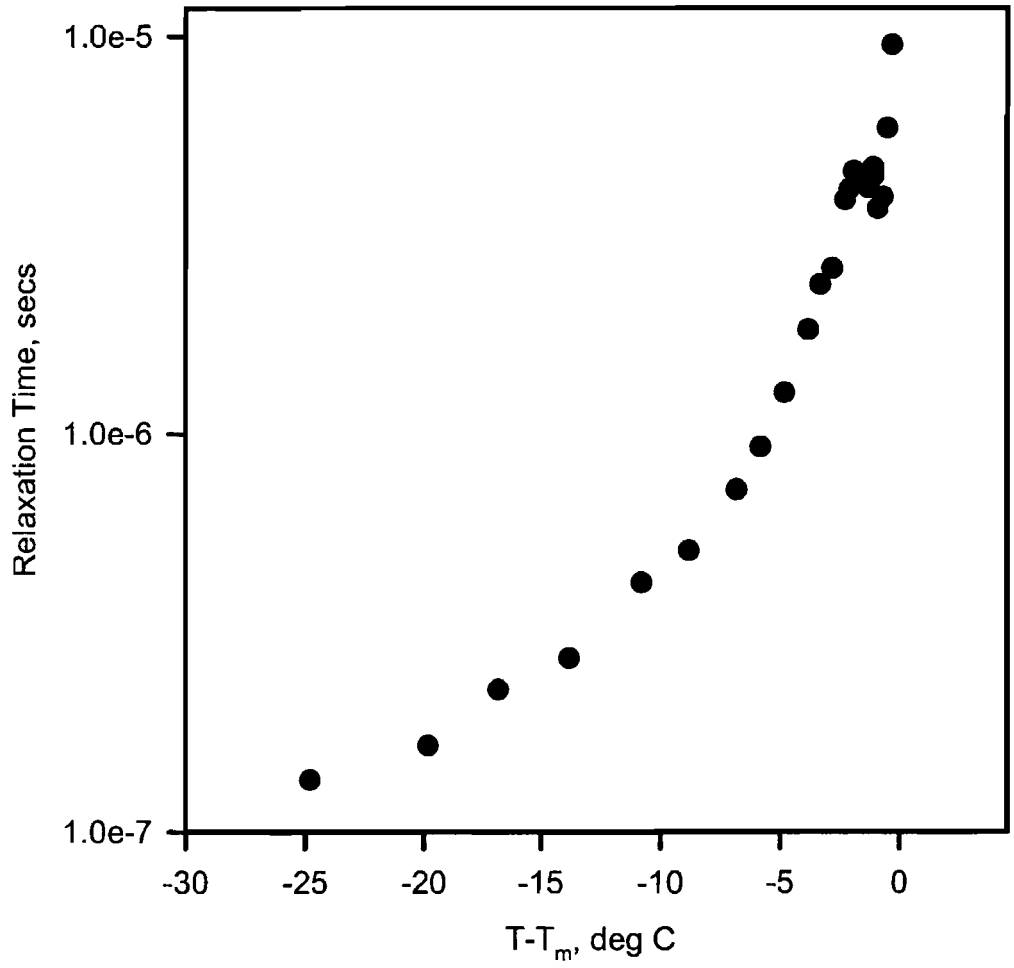


**FIGURE 3.3**: The relaxation time of the reflected probe intensity shown as a function of $T - T_m$.

Figure 3.4, below, shows the dynamic response of the interface reflectivity when the silica-gallium interface is excited by a pump pulse of 100 ns duration. The dashed box in figure 3.4 below represents the duration of the pump pulse in relation to the transient response of the interface reflectivity, and is shown as an illustration only.

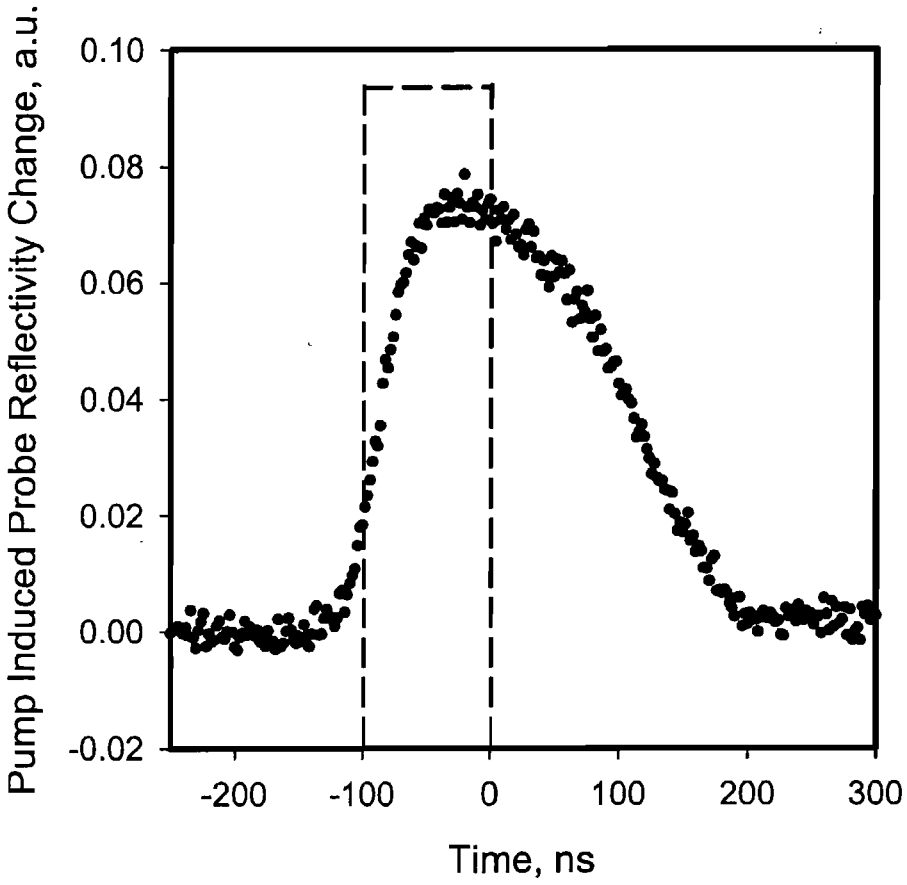


**FIGURE 3.4**: The modulation of the probe intensity when excited by the pump pulse. Here the dashed box represents the duration of a 100 ns pulse and is presented as an illustration only.

In figure 3.5, the dependence of the induced change with pump power is plotted, for a number of temperatures. The results indicate that a change of up to 45% was observed in the reflected probe intensity induced by the pump beam for power of only a few tens of mW.

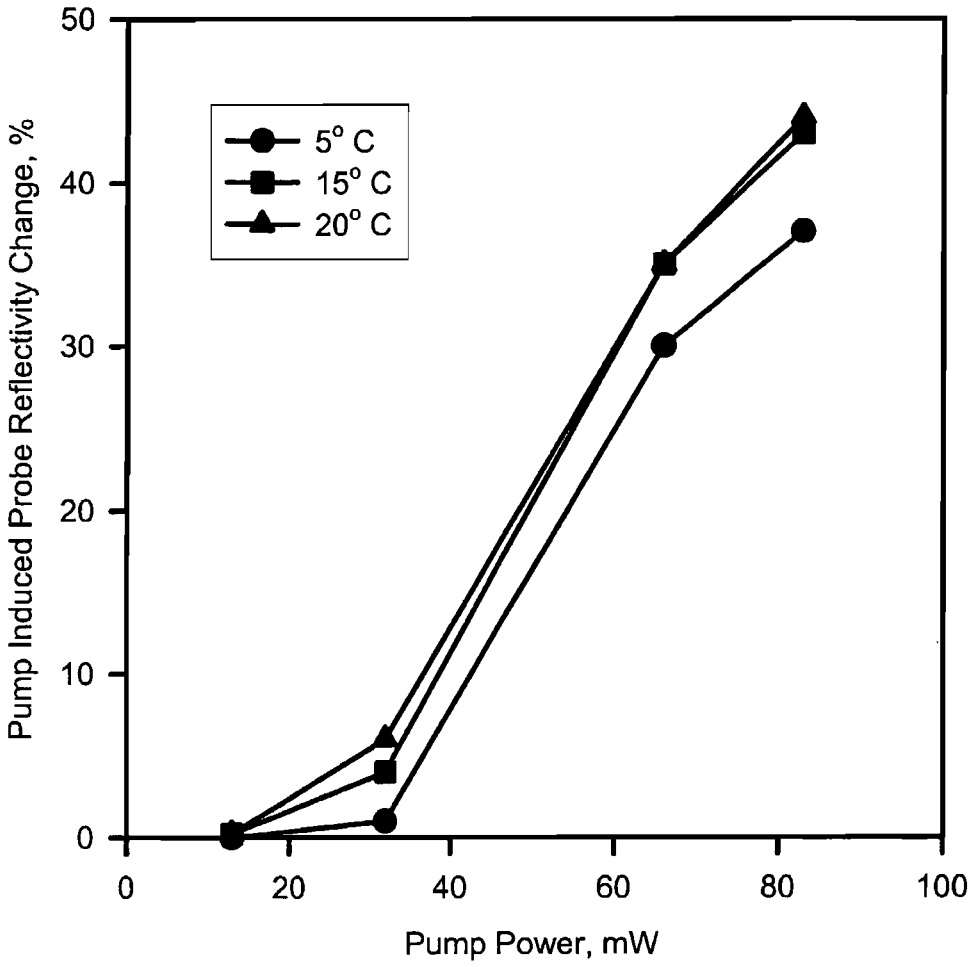


**FIGURE 3.5**: The pump induced probe reflectivity change as a function of various pump powers.

## 3.4 Conclusion

In conclusion, a mirror formed at the gallium-silica interface allows for sub-microsecond cross-wavelength switching with a percentage change in the modulation of the reflected light intensity of up to 45%. The gallium nonlinearity allows optical switching between pump and probe wavelengths at 1.55 μm and 1.3 μm.

## 3.5 Discussion

The gallium nonlinearity is associated with a light-induced, surface-assisted, structural phase transition which takes place at the interface of gallium with silica, and involves the common form of gallium (α-gallium) being transformed into a new more metallic phase, of higher reflectivity. When the light excitation is increased the density of the new phase increases and therefore reflectivity increases. When the excitation is withdrawn, the reflectivity returns to its original α-gallium state. The mechanism behind the effect, involves a fast, light-induced, transition to a new metastable phase, which becomes stable in the presence of light.

This transition is made possible by the unique crystalline structure of α-gallium, comprising metallic and molecular bonding, in which some of the bonds form Ga-Ga dimer units and the rest are metallic [6], [7], for a complete overview of the α-gallium properties see Chapter 2 and all the references therein. The presence of the covalent bonds results in a broad optical absorption band from 0.8 to 4 eV [7]. The pump wavelength used in the experiments, $\lambda = 1.55$ μm, falls into this band.

The exact nature of the light-induced phase is not known, but it is most likely to be one of the material's existing metastable phases, such as β-gallium, Ga(II) and Ga(III), see Chapter 2. These phases exhibit metallic characteristics, similar to those of the liquid state and are involved in the continuous transition from the solid crystalline α-phase to the liquid (α-gallium β-gallium Ga(II) Ga(III) liquid) [8].

The transition is assisted by the presence of the silica interface, which transforms the first order structural phase transition into a continuous phase transition [9]. Furthermore, α-gallium exhibits precursory effects at the surface and self-wetting behaviour at normal conditions [10]. A thin layer of liquid gallium will cover the surface of an α-gallium crystal without any optical excitation, see Chapter 2. The presence of such a layer will affect the balance of the interface forces, making the interface susceptable to premelting phenomena. Under increasing optical stimulation the thickness of such a covering layer will increase, and therefore the interface reflectivity will increase. As the thickness of this

layer depends on the temperature of the interface, the light-induced effect will increase with increasing temperature as the melting point is approached.

During the light-induced transition, optical excitation is highly localized and stimulates a bonding-antibonding transition in α-gallium. The covalent bonding of the crystalline structure becomes unstable initiating a phase transition from α-gallium to a metastable phase with essentially free electron characteristics, assisted by the presence of the interface. The thickness of the new phase increases with increasing optical excitation, increasing the interface reflectivity. The effect saturates and rolls-off as the thickness reaches the optical skin depth of gallium, about 25nm. When the excitation is withdrawn, the metastable layer re-crystallizes back to the α-gallium phase. The crystallization front moves towards the silica-gallium interface.

## 3.6 The Light-Induced Low Reflectivity State in a Planar Gallium Interface

In this section an additional light-induced effect observed at a silica-gallium interface is examined. Some of the measurements reported herein, were assisted by V. A. Fedotov, a postgraduate student working under the supervision of Prof. Zheludev.

In this experiment the light-induced reflectivity suppression (also referred to as reflectivity decrease) of a planar gallium-interface (mirror) was investigated, by measuring the dependence of the interface reflectivity with incident light intensity, for a range of temperatures starting well below the melting temperature of gallium ($T_m$ = 29.8 $^0$C) and reaching a few degrees above $T_m$.

A thin gallium film, of 1 – 2μm thickness, was prepared by direct deposition of high purity gallium on the ceramic surface of a miniature Thermoelectric Heat Pump (Peltier element), by Ultrafast Pulsed Laser Deposition (UPLD), under vacuum (~2 x $10^{-6}$ Torr), using a q-switched, mode-locked Nd:YAG laser at 1064nm with 60ps pulse duration. The substrate temperature during deposition was about –100 $^0$C, to ensure gallium will be deposited in the correct crystalline form. After deposition the gallium-deposited ceramic surface of the Peltier element, was covered with a silica glass. The gallium mirror was

formed when the two surfaces were fused together by heating the gallium film just above its melting temperature. The Peltier element was then used to provide the thermal control of the silica-gallium interface with a nominal precision of 0.02 $^0$C. The measurement of temperature was done using a thermistor placed at the ceramic plate of the Peltier element as shown in figure 3.7 below.

The planar silica-gallium interface was manufactured at the facilities of the Laser Physics Centre, The Australian National University, Canberra Australia, by A. V. Rode and B. Luther-Davies. The samples were prepared during the visit to the Australian National University by Professor N. I. Zheludev, as part of a collaboration project sponsored by the Royal Society and the Australian Academy of Sciences. The properties of such an interface are covered in Chapter 4.

A cw argon ion laser (Spectra Physics, Model 2060-10S) operating at a wavelength of 514nm, with beam direction stabilization, was used to measure the reflectivity of the planar silica-gallium interface. The light from the laser was focused onto the gallium film, through the glass substrate, at normal incidence to a spot of 12μm diameter. Measurements were taken using both linearly and circularly polarized light. In the second case, the circularly polarised light ensures that any problems due to the anisotropic character of the silica-gallium interface [11] are avoided. The setup used in this part of the experiment is shown below in figure 3.7, whereas the sample is shown in figure 3.6.

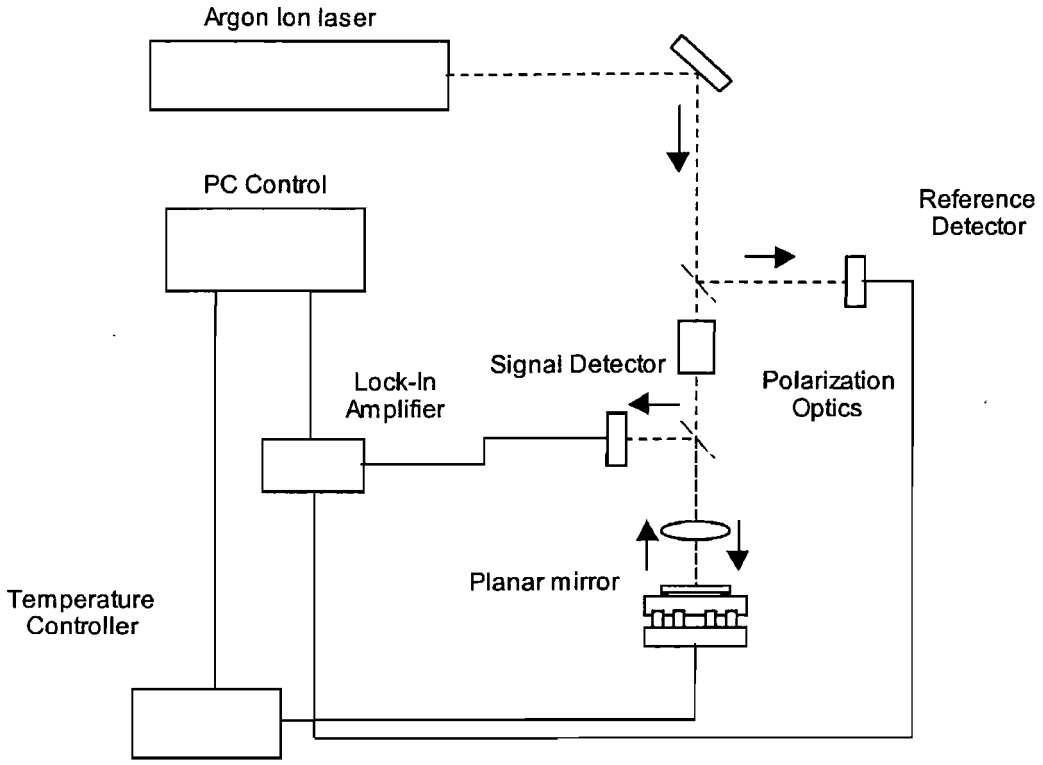


**FIGURE 3.6:** The experimental setup used to investigate the reflectivity suppression in the planar gallium mirror.

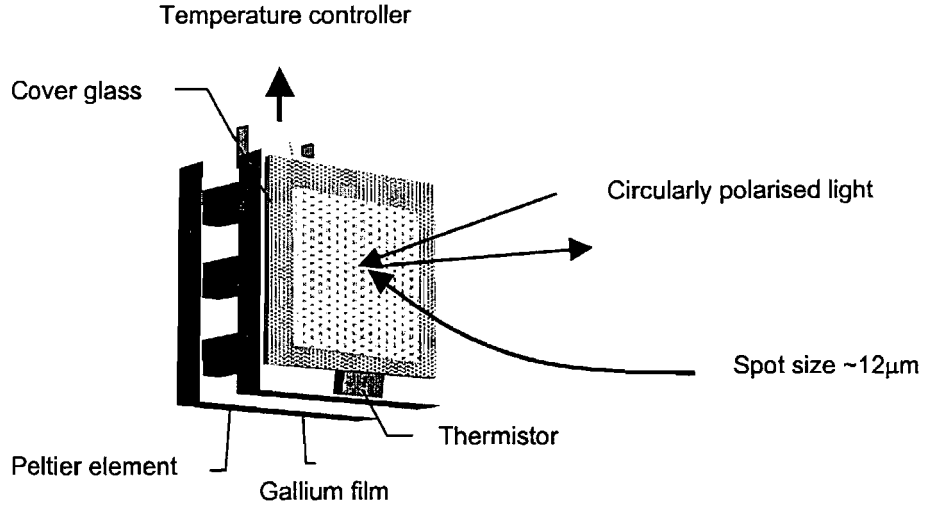


**FIGURE 3.7:** Detail of the planar mirror, showing the Peltier element, silica-gallium interface and the incident light.

The typical temperature dependence of the silica-gallium interface reflectivity, under conditions in which the reflectivity suppression effect has been observed to take place, is shown in figure 3.8. The starting point of the reflectivity-temperature curve, far below the melting point of gallium, corresponds to the reflectivity level of the interface between α-gallium, the stable crystalline form of gallium at normal pressure, and silica.

The interface reflectivity can be seen to increase with light intensity and sample temperature, the typical nonlinear behaviour of the planar silica-gallium interface (see introduction). Then, within a narrow temperature interval just below $T_m$, the interface reflectivity decreases rapidly for increasing sample temperature.

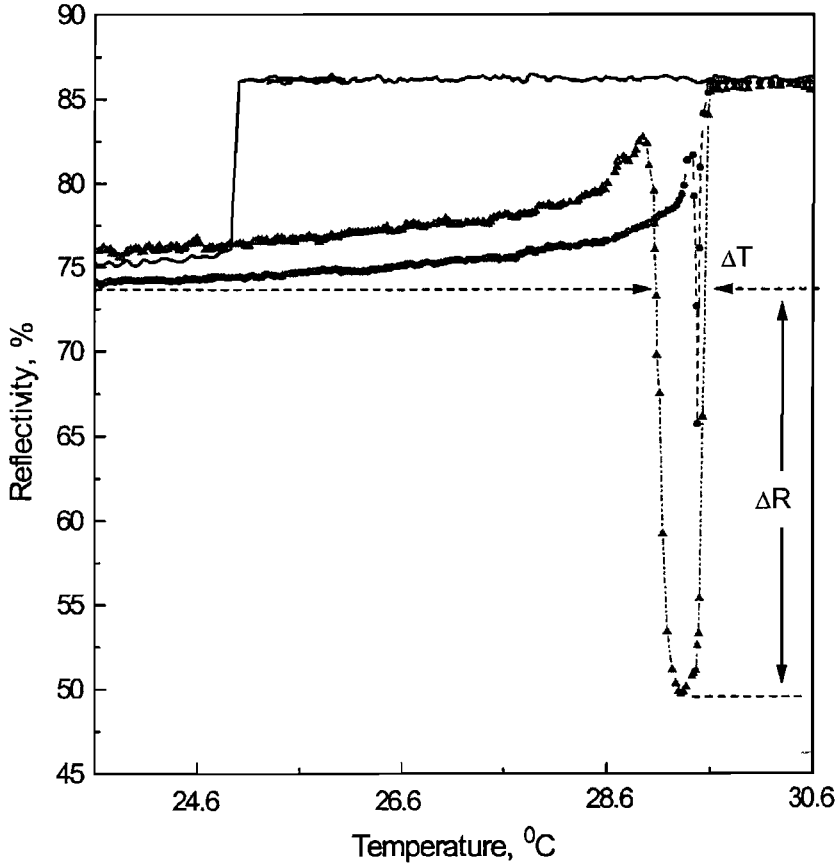


**FIGURE 3.8:** Dependence of interface reflectivity for two incident intensities. shows reflectivity at 1KW/cm$^2$, shows the effect at 7KW/cm$^2$ both for increasing temperature, whereas the solid line represents reflectivity with decreasing temperature.

Figure 3.8, above, shows a typical reflectivity drop of 25% (in absolute units) at a pump power of 8mW, (7kW/cm$^2$). When the interface reaches gallium's melting point, reflectivity jumps up to ~87%, indicating that the gallium film, at the interface, is now in the liquid phase. The temperature width, within which the reflectivity suppression is observed, increases from about $10^{-2}$ °C at 500W/cm$^2$ to about 0.4 °C at 7kW/cm$^2$.

Figure 3.9, below, shows the dependence of the temperature width (ΔT), and reflectivity drop (ΔR) with intensity. The reflectivity drop exhibits threshold behaviour and develops for light intensities exceeding about 500W/cm$^2$. The low reflectivity state was studied with modulated light, of 200Hz frequency, and was found to be reproducible from pulse to pulse across the temperature and intensity range.

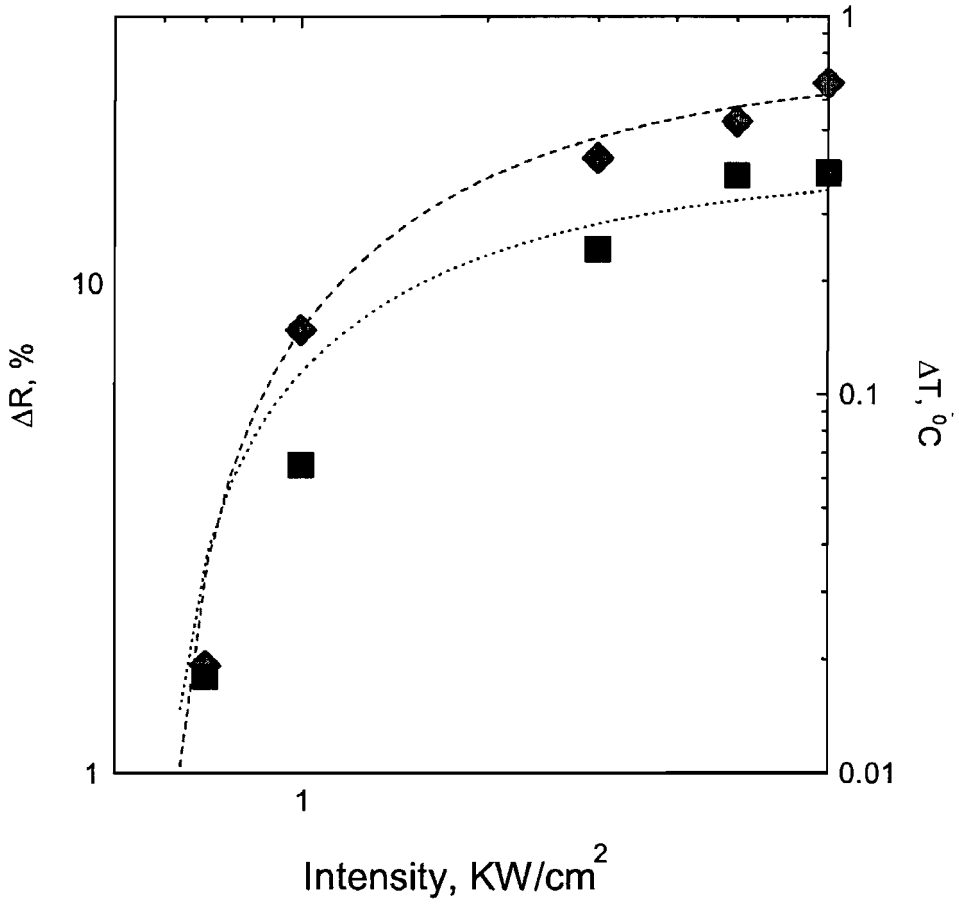


**FIGURE 3.9:** The light-induced reflectivity suppression as observed in the planar gallium mirror. ΔT ( ) is the temperature width of the envelope in which the low-reflectivity state develops, whereas ΔR (♦) is a measure of the reflectivity decrease from figure 3.3.

## 3.7 Conclusion

A light-induced reflectivity decrease was observed in a planar silica-gallium interface. It is reversible and reproducible, and requires low excitation power. It occurs within a narrow temperature interval, below the melting point of gallium. The low reflectivity state exhibits a threshold behaviour with incident light intensity, and shows an increase of the reflectivity drop ($\Delta R$) and the temperature envelope ($\Delta T$) with increasing incident light intensity. A reflectivity drop of 25% was observed with 8mW of light excitation. The width of the temperature envelope increased from $10^{-2}$ $^0$C at 0.5kW/cm$^{-2}$ to 0.4 $^0$C at 7kW/cm$^{-2}$. Saturation is exhibited for higher intensities.

The state of low reflectivity was observed for most of the planar silica-gallium interfaces, prepared with the technique described above. However, it was impossible to observe it in samples where a thin gallium film was deposited directly on both the ceramic surface of the Peltier element and the silica flat. This indicates that the interface conditions, between silica and gallium, are important for the observation of the effect.

## 3.8 The Light-Induced Reflectivity Suppression in a Fiberised Gallium Interface

Fibrerized silica-gallium interfaces have been examined previously by [1] for their nonlinear behaviour. Evidence of the existence of such reflectivity decrease was mentioned therein but no further investigation was performed. Moreover, the effect was also mentioned in [12]. The results presented herein were originally obtained by S. Dhanjal and P. Petropoulos, under the supervision of Professors D. J. Richardson and N. I. Zheludev. At that time, the identity of the effect was unknown and the results remained unpublished.

In this experiment, the light-induced reflectivity decrease in a fiberized silica-gallium interface was examined by looking at the transient response of reflectivity at different interface temperatures, up to the melting temperature of gallium, $T_m$, using a pump-probe technique.

The interface was prepared by immersing the tip of a freshly cleaved, single mode, optical fibre into a small bead of gallium that was kept above its melting temperature, similar to section 3.3. The interface temperature was controlled by a miniature Peltier element, similar to the one used in the planar mirrors, with a nominal accuracy of 0.01 $^{0}$C.

The all-fibre optical setup used to examine the low reflectivity state in a fibrerised silica-gallium mirror is shown in figure 3.10, whereas figure 3.11 shows the sample.

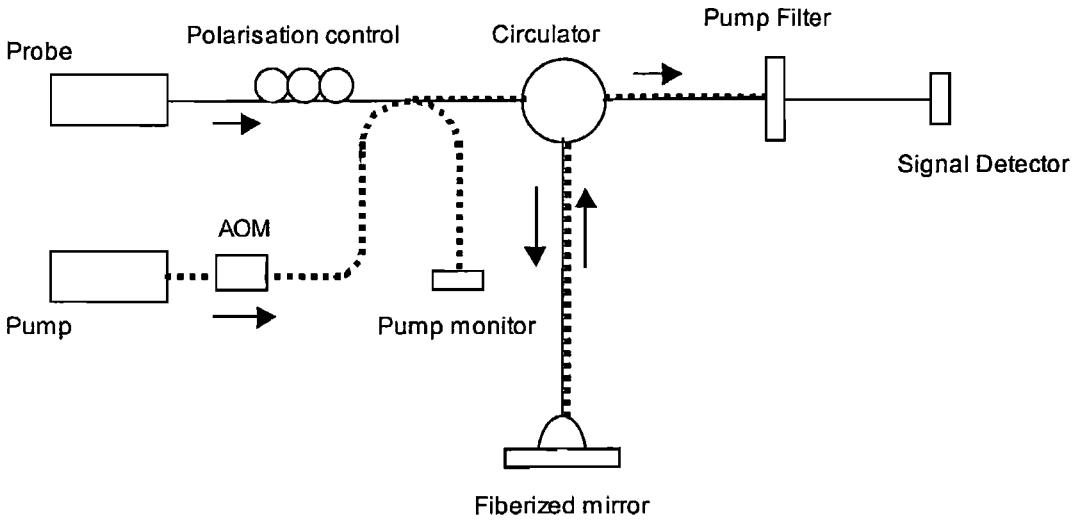


**FIGURE 3.10:** Schematic of the pump-probe experiment used to investigate the light-induced reflectivity decrease in a fiberised silica-gallium interface.

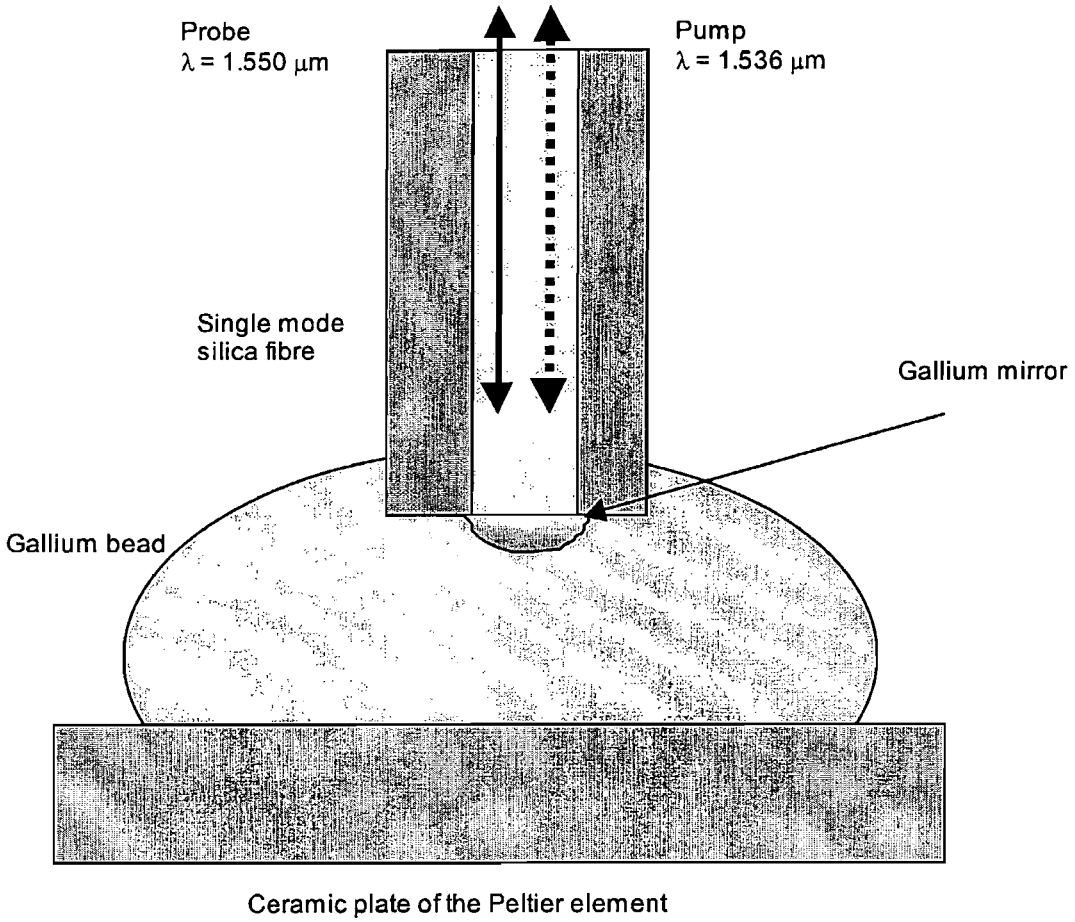


**FIGURE 3.11:** Detail of the silica-gallium interface, showing the silica fibre immersed in the gallium bead.

An amplified external-cavity diode laser, acting as the pump laser, stimulated the interface. The peak power of the pump pulses at the silica-gallium interface ranged from 0 to 8mW, at a wavelength of 1.536 μm. The pump was modulated at a frequency of 500Hz. At the same time the interface reflectivity was monitored by a 60 μW cw distributed feedback diode laser at a wavelength of 1.550 μm (probe). The two wavelengths were combined using a fibre coupler, used also to monitor the pump pulses. An optical circulator coupled the pump and probe signals to the silica-gallium mirror. On reflection from the interface, the pump was removed using a filter. Figures 3.12 to 3.14, below, show the reflectivity of the fiberised silica-gallium interface at the probe wavelength (1.550 μm),

modulated by the pump (1.536 μm). In all the inserted frames, , the upper trace shows the reflected probe, the lower trace is the pump signal, the amplitudes of the two traces are in arbitrary units and not in scale, 2ms/div time base. The frames shown here were originally recorded by S. Dhanjal and P. Petropoulos and are presented here as an illustration of the dynamic properties of the light induced low reflectivity state, in a fiberised silica-gallium interface.

In figure 3.12, frames 1 and 2 taken at temperatures of 15.0 °C and 23.0 °C respectively, show the previously reported regime of the reversible light-induced reflectivity increase at a silica-gallium interface [1]. The increase of the interface reflectivity is in phase with the modulated pump, and the effect is more pronounced at higher temperatures.

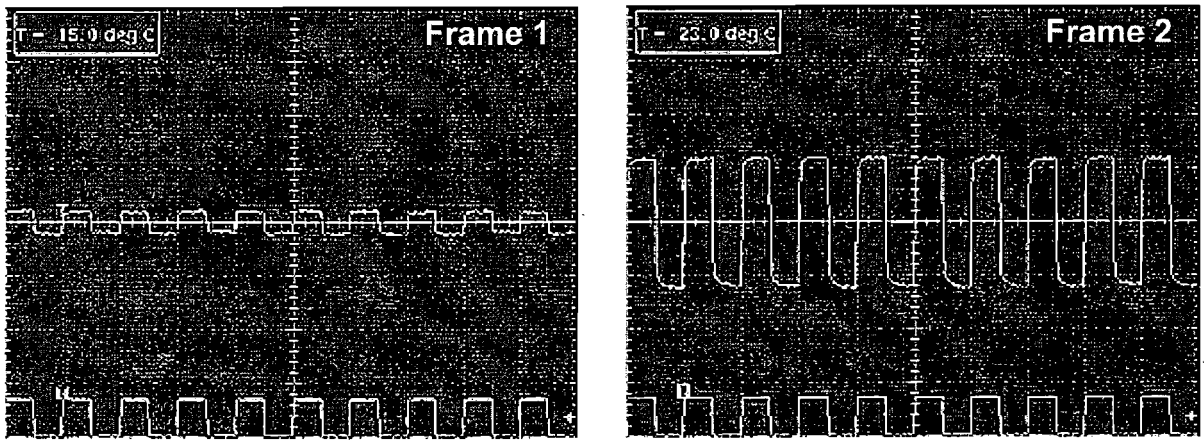


**FIGURE 3.12:** Reflected probe intensity at 15.0 $^0$C (frame 1) and at 23.0 $^0$C (frame 2) showing the light-induced reflectivity increase.

Frame 3, taken at 28.1$^0$C shows the initial stages of the reflectivity suppression effect: an immediate increase of the interface reflectivity in phase with the pump pulse, followed by a rapid but relatively small decrease from the peak level to an intermediate level. In frame 4, recorded at 28.5 $^0$C, this dynamic behaviour continues but it now shows stronger features than in figure 3.12.

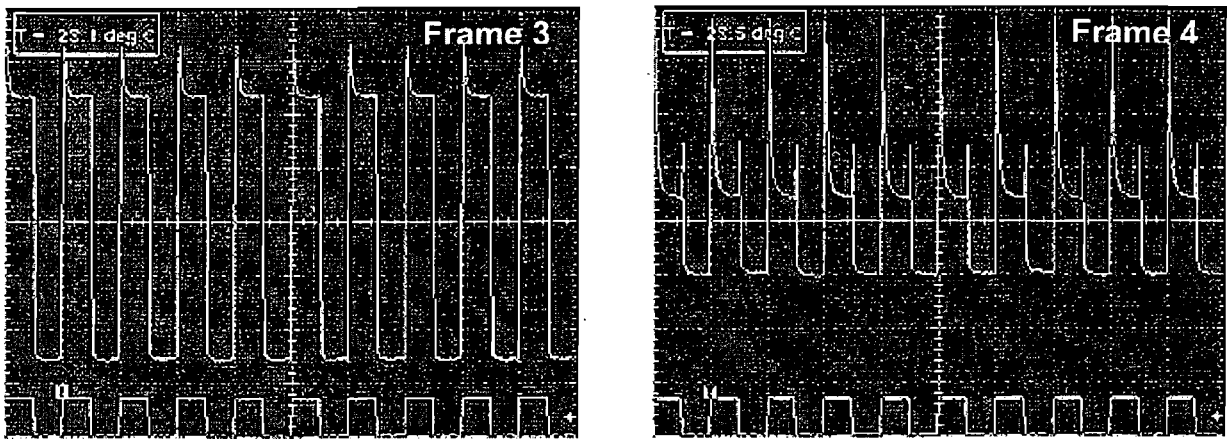


**FIGURE 3.13:** Interface reflectivity at 28.1 $^0$C (frame 3) and at 28.5 $^0$C (frame 4), showing the initial stages of the light-induced reflectivity suppression.

Frame 5, taken at T=28.9°C shows the, fully developed, light-induced low reflectivity state. In contrast with the previous frames the interface reflectivity can be seen to start in a decreasing immediately after the pump pulse arrives at the interface. It then drops sharply to a new level below the original initial reflectivity. When the pump pulse ends, the interface reflectivity starts recovering, very sharply towards the initial level, before the arrival of the pump pulse. The effect is then repeated as soon as the next pump pulse arrives at the interface and initiates the reflectivity suppression cycle again. Finally, in frame 6, the light-induced probe reflectivity modulation disappears above the melting temperature of the gallium film. The low reflectivity state is fully developed in a few hundred microseconds (~200 μs as seen on frame 5), and recovers to the initial level within a few microseconds time, figure 3.13.

## 3.9 Conclusion

The light-induced reflectivity decrease was observed in a fiberised silica-gallium interface. The effect is similar to that observed in a planar silica-gallium interface. It occurs just below the melting temperature of gallium and disappears on melting.

The reflectivity decrease is reversible and reproducible. It fully develops within a few hundred microseconds, and requires very low excitation levels.

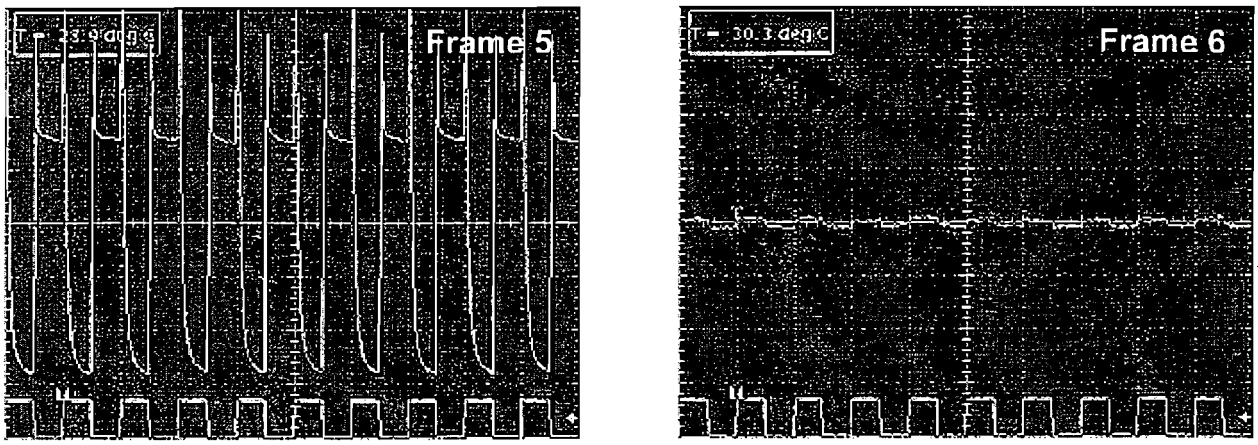


**FIGURE 3.14:** Frame 5, the fully developed low reflectivity state at 28.9 $^{0}$C showing out-of-phase modulation with respect to the pump pulses. Frame 6, the light-induced modulation has disappeared, above the melting point.

## 3.10 Discussion

The reflectivity suppression in the narrow temperature interval below the melting point is likely to result from a kind of light-induced structuring at the silica-gallium interface. The interface conditions affect the observation of the reflectivity decrease. This correlates with the fact that planar interfaces prepared by depositing gallium directly on the cover silica glass by the UPLD process do not show the low reflectivity state. The properties of this interface are governed by a transitional layer, about 3nm thick, of gallium ions that have penetrated into the silica substrate during the UPLD process [13]. Such interface is structurally rigid, preventing the formation of any kind of light-induced structuring.

Several potential candidate mechanisms may be responsible for this reflectivity suppression effect observed in a silica-gallium interface, however the exact mechanism is not known. The most likely mechanisms behind the effect, were established after lengthy discussions, especially with Professor V.I. Emely'anov of the Moscow State University during his visit to the University of Southampton, who established the initial direction of thinking.

One possible explanation of the observed reflectivity decrease is light-induced surface patterning, produced by preferential melting under illumination, forming a steady-state melt-pattern grating at the interface, with period equal to the incident light's wavelength. Bösch and Lemons [14] made the initial observations of a cw laser beam inducing melt patterns in a thin film of silicon. The molten-solid pattern was produced using an argon ion laser at 514nm, and a Nd:YAG at 1.064 μm, both focused down to spot sizes between 50 and 300μm in diameter. Laser-induced melt patterns in polycrystalline and amorphous silicon films, with solid lamellae of silicon coexisting with the melt, appearing and disappearing dynamically were observed by [14]. In another case using light from a $CO_2$ laser at 10.6 μm, an ordered melt pattern comprising of alternate strips of molten and solid silicon was observed, having a periodicity equal to the incident light's wavelength was observed [15]. The observation of periodic structures is a light-induced self-organization process. It is associated with a periodic power distribution resulting from interference between the coherent incident beam and the surface scattered beam [16]. Under these conditions the optical absorption of the interface is increased which can reduce the reflectivity substantially [15].

In the silica-gallium interfaces examined here, a similar light-induced grating structure with period equal to the incident light's wavelength may be formed, by preferential melting of the gallium film under illumination, reducing the reflectivity of the interface. However, the low reflectivity state, in the planar gallium mirror, was observed with circularly polarised light at normal incidence. The distribution of power in the molten-solid grating is polarization sensitive [17]. Circularly polarized light prevents the creation of the ordered pattern. Under these conditions [16] reported the creation of disordered patterns. Figure 3.15 shows a cross section of the silica-gallium interface with the molten-solid forming under illumination.

Another possible mechanism for the observed low reflectivity state, resulting from the same electrodynamic process that creates the melt patterns is surface rippling [17]. Surface rippling has been observed when a laser beam heats the surface of thin metal films [18]. It is considered a disadvantage of the laser treatment of metals, by creating unwanted surface roughening. Figure 3.16, shows the ripple effect at the silica-gallium interface.

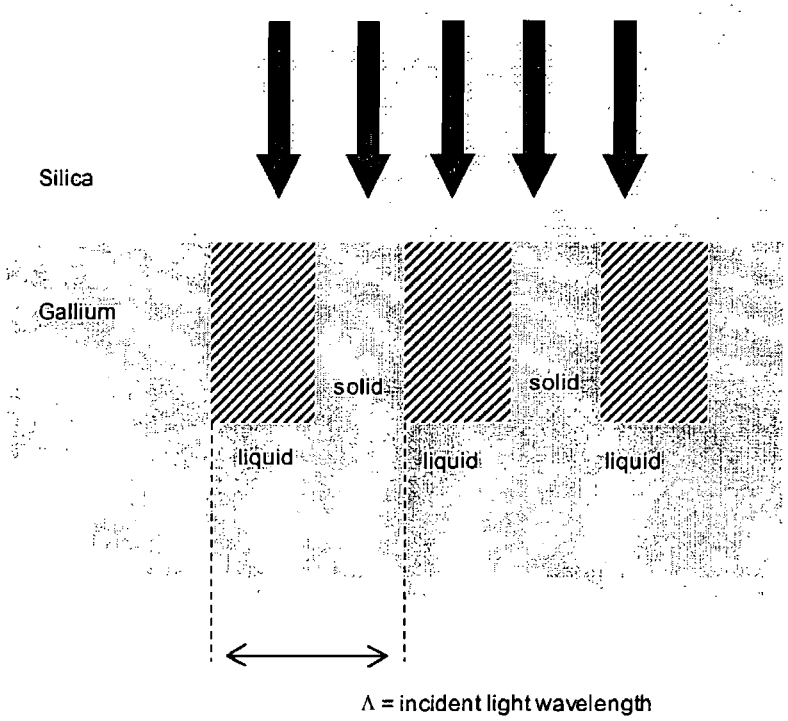


**FIGURE 3.16:** Light-induced surface patterning at the silica-gallium interface, appearing as a molten-solid grating. The period of the grating structure, Λ, is of the order of the incident light wavelength.

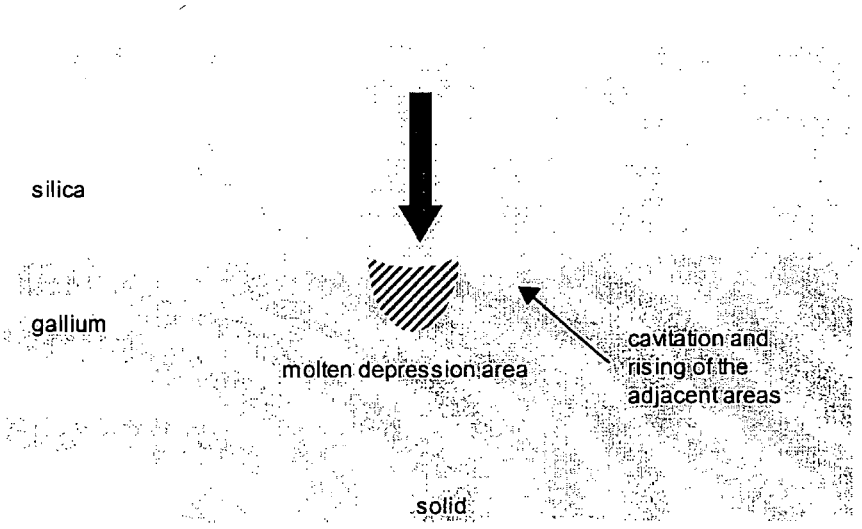


**FIGURE 3.17:** Cross section of the surface ripple effect, showing the molten depression area under the laser beam, and the adjacent roughened areas.

During surface melting, the surface of the thin film is subjected to a temperature gradient running radially outwards out from the spot area. At the centre of the laser spot the surface tension is at its lowest whereas away from the spot area increases with distance. This surface tension differential can result in a depression of the film under the beam and the subsequent rise in another part, creating a roughened surface. Rippled grating patterns were reported by [16] for pulsed laser illumination at normal incidence

The creation of a stratified planar structure at the interface of silica with gallium may also explain the observed reflectivity decrease. Such a structure could result from the formation of a quasi-liquid layer, separated from the α-gallium bulk by an α-gallium layer containing metallic inclusions. The appearance of such layering is predicted to happen at the surfaces of most metals, and has been observed in a free gallium surface (Chapter 2 and references therein). It has been shown that for a particular dielectric coefficient of the layers, the reflectivity of such a three-layer structure can be greatly reduced.

Finally, another mechanism of the reported low reflectivity state can be light-induced roughening of the silica-gallium interface. Roughening of solids near the melting point is known to appear even in the absence of any light excitation [19].

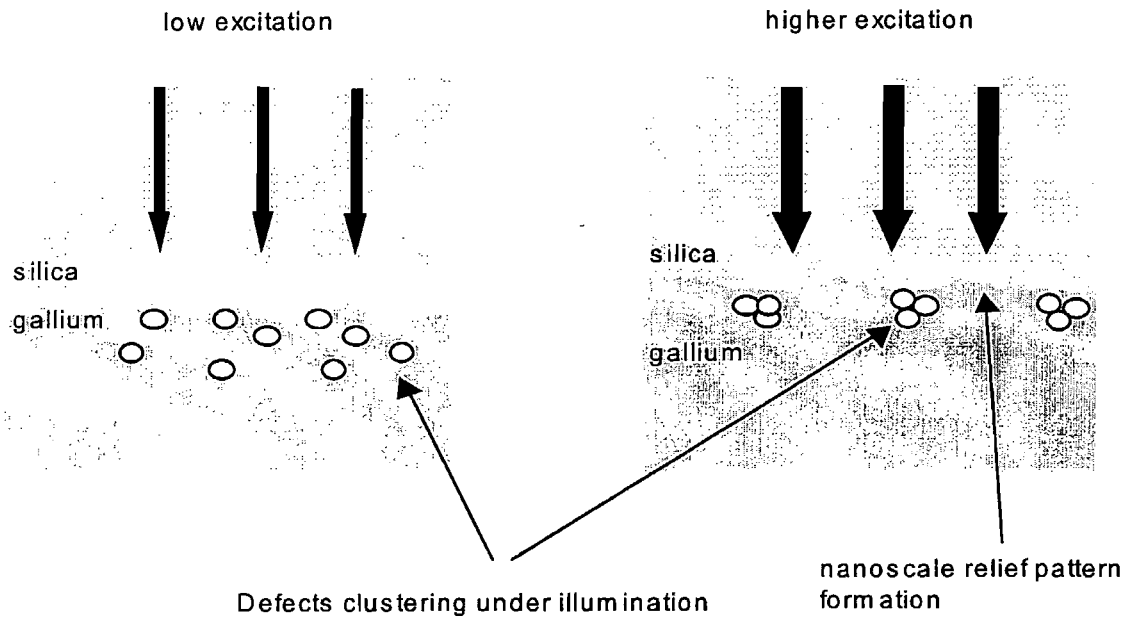


**FIGURE 3.17:** Light-induced roughening of a silica-gallium interface, showing clustering defects and relief pattern formation.

The exact mechanisms underpinning such light-induced roughening are being investigated and relief formation along with clustering of defects, figure 3.17 above, and nanoscale phase separation on the surface are being considered. If such nanoscale quasi-periodic disturbance of the surface layer occurs, its effective dielectric permittivity will have a resonance depending on the bulk plasma frequency of the metal, and on the shape and characteristic size of the nanoscale modulation [19]. If the conditions are correct, this may lead to a decrease in reflectivity [20].

Finally, intense light scattering can be responsible for the reflectivity decrease. Such scattering is known to occur when the dielectric parameters of the material show pronounced spatial-temporal fluctuations, with a characteristic correlation length equal to the wavelength. This mechanism relies on the hypothesis that such fluctuations at a silica-gallium interface may take place near the melting point and are stimulated by light.

## 3.11 Summary of Chapter 3

A silica-gallium interface exhibits a strong nonlinear behaviour close to the melting temperature of gallium, $T_m = 29.8\ ^0C$. The silica-gallium interface was prepared at the tip

of an optical fibre. The nonlinearity manifests itself as a fast light-induced structural phase transition. The transition involves the stable α-gallium phase converting into a metallic phase of considerably higher reflectivity.

Using this nonlinearity of the silica-gallium interface switching properties were investigated. All-optical switching, at wavelengths of 1.3 μm and 1.55 μm was demonstrated. Sub-microsecond switching times, and signal modulation up to 45% were observed. The all-optical switching was demonstrated with a compact, fully fiberized setup, readily customizable with existing telecommunications technology.

A potential problem associated with this type of structure can be the low contrast of the modulated signal. This can be solved with the fabrication of a Fabry-Perot resonator cavity, in which the mirrors are constructed by gallium. By adjusting the temperature of the mirrors close to the melting temperature of gallium the intensity of light within the cavity can be multiplied many times. Moreover, the polarisation dependence of the silica-gallium interface can be a limiting factor on the performance. Recent research has demonstrated that the use of gallium nanoparticles offers solutions to this problem, see Chapter 5.

Using this nonlinearity there is tremendous potential for the development of a wide range of truly practical nonlinear optical devices, compatible with existing waveguide technology, and especially all-optical switches for fully optical data processing, in the field of integrated optics.

An additional light-induced effect, at the silica-gallium interface was also observed and investigated namely, a light-induced low reflectivity state. The reflectivity decrease was observed in silica-gallium interfaces, prepared on an optical flat, or at the tip of an optical fibre. The effect is reversible, and has been observed with cw and pulsed excitation. It occurs within a narrow temperature interval just below the melting temperature of gallium ($T_m = 29.8\ ^0C$). It requires very low excitation levels.

The reflectivity decrease exhibits threshold behaviour under cw excitation. The magnitude of the reflectivity drop, and the width of the temperature interval increase with increasing

incident light intensity. Saturation occurs at higher intensities. The effect has also been observed with pulsed excitation. It is dynamically light-induced and exhibits microsecond response times.

The low reflectivity state is possibly due to light-induced structuring of the silica-gallium interface. Potential mechanisms, such as formation of a molten-solid grating and surface rippling, stratified structure, light-induced roughening and surface scattering have been considered. However, the exact mechanism behind the observed effect is unknown.

Such dynamic, reversible light-induced reflectivity suppression can be of interest as a potential power-limiting device in integrated optoelectronic applications. It can be fully integrated with current fibre optics technology and with integrated optics devices.

## References


[1] P. J. Bennett, S. Dhanjal, P. Petropoulos, D. J. Richardson, N. I. Zheludev, V. I. Emel'yanov, Applied Physics Letters, page 1787, vol. 73 no. 13, 1997

[2] P. Petropoulos, H. S. kim, D. J. Richardson, V. A. Fedotov and N. I. Zheludev, Physical Review B., page 193312, vol. 64, 2001.

[3] V. Albanis, V. A. Fedotov, K. F. MacDonald, V. I. Emely'anov, N. I. Zheludev, R. J. Knize, B. V. Zhdanov, A. V. Rode, Conference on Laser and Electro-Optics Europe 2000, Nice, France.

[4] P. Petropoulos, H. L. Offerhaus, D. J. Richardson, S. Dhanjal, and N. I. Zheludev, Applied Physics Letters, page 3619, vol. 74, 1999.

[5] N. J. C. Libatique, J. D. Tafoya, S. H. Feng, D. J. Mirell, R. J. Kain, in : Advanced Solid State Lasers, vol. 34, Opt. Soc. America, Washington DC, 2000, p. 417

[6] H. G. von Schnering, R. Nesper, Acta Chemica Scandinanica, page 870, vol. 45, 1991.

[7] M. Bernasconi, G. L. Chiarotti, E. Tosatti, Physical Review B., page 9999, vol. 52, no. 14, 1995

[8] F. J. Bermejo, P. R. Fernandez, M. Alvarez, B. Roessli, H. E. Fischer, J. Bossy, Physical Review E., page 3358, vol 56, 1997

[9] B. Pluis, D. Frenkel, J. F. van der Veen, Surface Science, page 282, vol. 239, 1990.

[10] R. Trittibach, Ch. Grutter, J. H. Bilgram, Physical Review B, page 2529, vol. 50, 1994.

[11] W. Huisman, J. F. Peters, M. J. Zwaneburg, S. A. de Vries, T. E. Derry, D. Abernathy, J. F. van der Veen, Nature, page 379, vol. 370 no. 27, 1997

[12] S. Dhanjal, University of Southampton Thesis, 1999

[13] K. F. MacDonald, V. A Fedotov, R. W. Eason, N. I. Zheludev, A. V. Rode, B. Luther-Davies, V. I. Eme'yanov, J. Opt. Soc. Am., page 331, vol 18. 2001

[14] M. A. Bosch, R. A. Lemons, Physical Review Letters, page 1151, vol. 47 no.16, 1981

[15] J. S. Preston, H. M. van Driel, J. E. Sipe, Physical Review B, page 3942, vol. 40 no. 6, 1989

[16] J. Dworschak, J. E. Sipe, H. M. van Driel, J. Opt. Soc. Am. B., page 981, vol. 7 no. 6, 1990

[17] J. S. Preston, J. E. Sipe, H. M. van Driel, J. Luscombe, Physical Review B, page 3931, vol. 40 no. 6, 1989

[18] T. R. Anthony, H. E. Cline, Journal of Applied Physics, page 3888, vol. 48 no. 9, 1977

[19] V. I. Emel'yanov, Laser Physics, page 937, vol. 8 no. 4, 1998

[20] J. G. Bergman, D. S. Chemla, P. F. Liao, A. M. Glass, A. Pinczuk, R. M. Hart, D. H. Olson, Optics Letters, page 33, vol. 6 no. 1, 1981

# Chapter 4

# Broadband Optical properties of an Ultrafast Pulsed Laser Deposited Silica-Gallium Interface - Optical Switching in the Blue-Green Spectral Region

## 4.1 Synopsis

The broadband optical properties of gallium were examined across the melting transition. The linear reflectivity of a silica-gallium interface on transition from solid to liquid was examined over a broad wavelength range. The results show a considerable broadband interface reflectivity increase on melting.

The linear reflectivity change on transition from the solid to the liquid gallium phase of a silica-gallium interface, prepared by Ultrafast Pulsed Laser Deposition (UPLD), was investigated over a broad wavelength range. A substantial broadband reflectivity increase was observed on melting.

The light-induced reflectivity change of the UPLD prepared silica-gallium interface was studied, in the blue-green spectral region. A considerable interface reflectivity increase is seen at fluences of about 1 $mJ/cm^2$. The effect peaks at temperatures just below the gallium melting point, $T_m = 29.8\ ^0C$. The interface reflectivity was studied using pulsed excitation. The reflectivity recovery times were observed to increase critically.

## 4.2 Overview of the Linear Optical Properties of Gallium

The linear optical properties of gallium are reviewed here, in relation to the spectral characteristics of the silica-gallium interface. The linear reflectivity is calculated across the melting transition for a very broad wavelength range.

The optical properties of the solid and liquid phases of gallium have been investigated in the past by various researchers [1]-[8]. However, so far in the above references only the properties of air-gallium and vacuum-gallium surfaces have been examined. These interfaces are very susceptible to surface oxidization and degradation that can alter the observed optical properties.

The work presented herein concentrates on the optical properties of the interface between silica and gallium. Confinement can change the properties of bulk gallium significantly, by modifying its surface energy inducing premelting effects that can influence the melting transition. As a result of the change in the surface energy and interface chemistry, the interfacing dielectric can considerably change the optical and nonlinear optical characteristics of gallium at the interface. It can also be expected that the crystallographic alignment at the interface can be different from a free gallium surface (see Chapter 2).

The optical properties of such an interface can be predicted using simple Fresnel formulae and data from vacuum-gallium interface experiments. Comparing the calculated values with values obtained experimentally can give an insight on the effect the dielectric interface has on the properties of the material. Nevertheless, a considerable departure between the calculated and experimental values has been seen.

In this section, data from the published works above are presented. Gallium is a polymorphic material, possessing a number of metastable phases. Under normal conditions its stable crystalline phase is the α-gallium phase. The data for the solid, α-phase, of gallium were obtained from [4] in the form of the complex dielectric constants of gallium monocrystals in the spectral range corresponding to the 0.3 eV to 3.5 eV energy range. Figure 4.1 below, shows the real and imaginary parts of the dielectric constants, $\varepsilon_1$ and $\varepsilon_2$ respectively, for light with its electric field vector oscillating along the three

crystallographic directions present in the α-gallium crystal, taken from [4]. See Chapter 2 for the structure of α-gallium and the definition of the axial notations.

This graph was transformed into tables containing values for the real and imaginary parts for the three crystallographic directions, with respect to wavelength. These values were fitted with polynomial functions in the spectral range from 450 nm to 1650 nm. The polynomial functions are given in Appendix A.

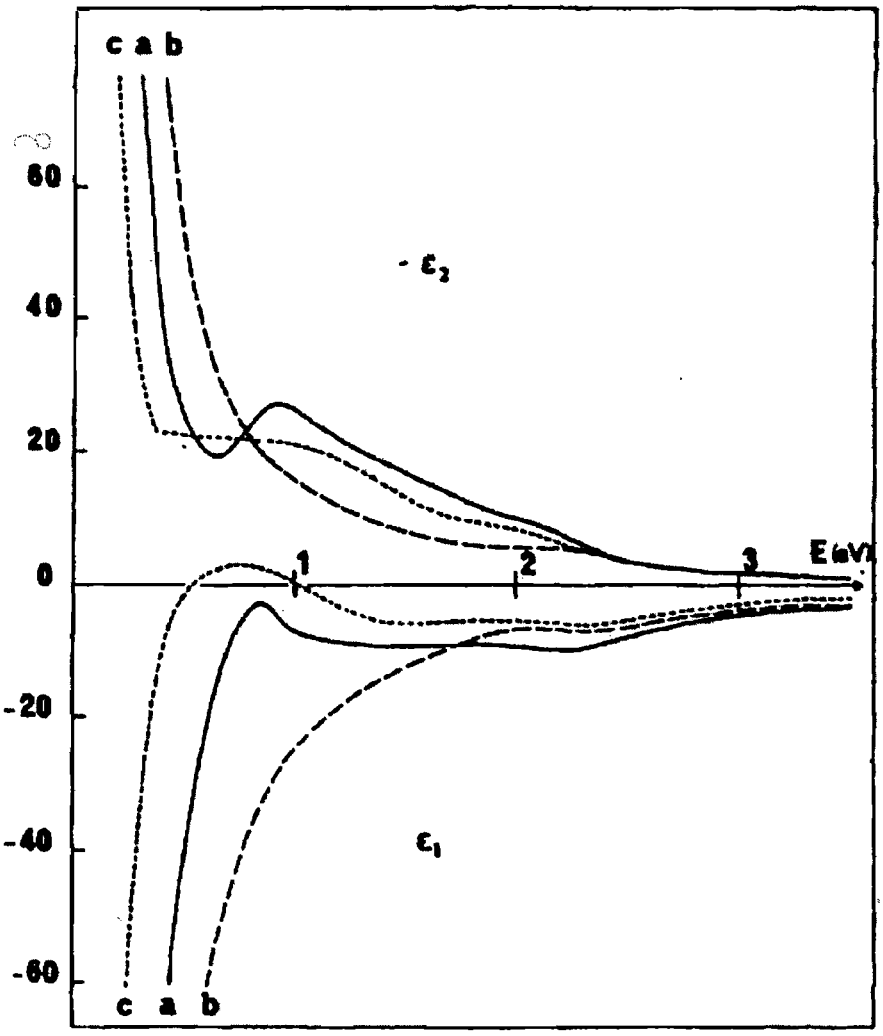


**FIGURE 4.1**: The real and imaginary parts, $\varepsilon_1$ and $\varepsilon_2$ respectively, of the complex dielectric constants of α-gallium for light polarised along the three crystallographic directions defined as a [100], b [010] and c [001] as taken from [4].

In the case of liquid gallium, values for the real and imaginary parts of the complex refractive index were obtained from [8], who investigated the optical constants of liquid gallium with respect to wavelength. The values for the optical constants of liquid gallium were fitted with polynomial functions in the range from 450 nm to 1650 nm. The polynomial functions are given in Appendix B. Figure 4.2 below shows the experimental values of the optical constants of liquid gallium, represented by , as taken from [8] compared with the values obtained from the fitting of the polynomial functions.

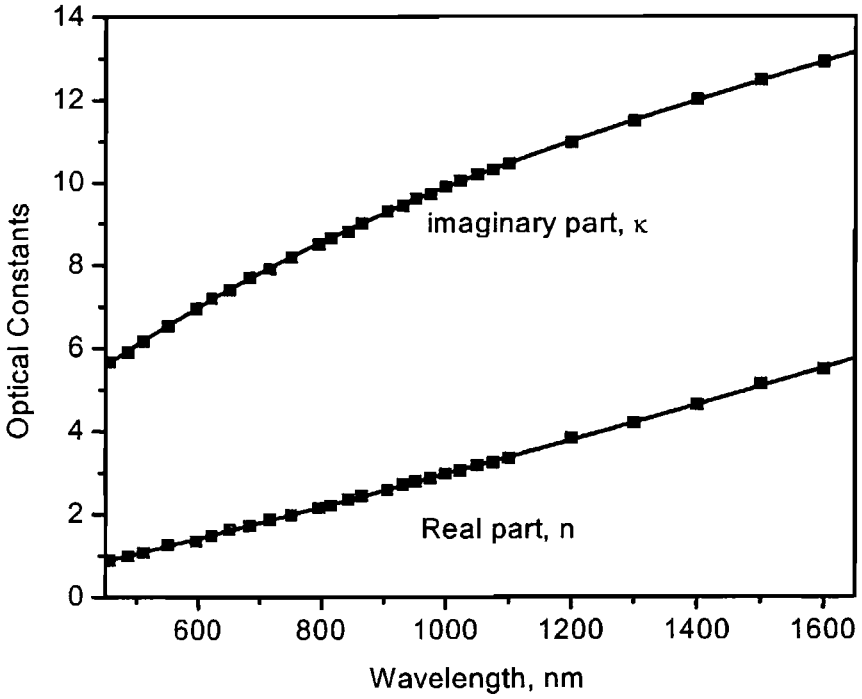


**FIGURE 4.2:** The values for the optical constants of liquid gallium, as a function of wavelength. The line shows the values obtained from the polynomial functions fitting, whereas " " show the data taken from [8].

From these values the real and imaginary parts of the complex dielectric constant of liquid gallium, $\varepsilon_1$ and $\varepsilon_2$ respectively, were calculated using equations (4.1) and (4.2) below. Figure 4.3, shows the complex dielectric constants of liquid gallium as a function of energy.

$$\varepsilon_1 = n^2 - \kappa^2 \qquad (4.1)$$

$$\varepsilon_2 = -2n\kappa \qquad (4.2)$$

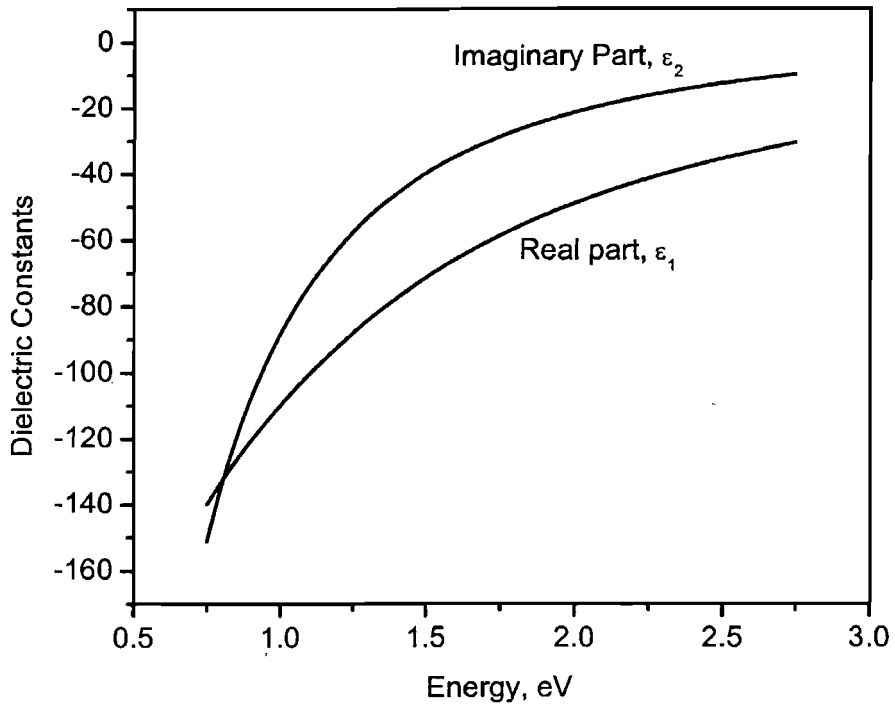


**FIGURE 4.3**: The real and imaginary parts, $\varepsilon_1$ and $\varepsilon_2$ respectively, of the complex dielectric constants of liquid gallium, as a function of energy. Calculated from equations (4.1) and (4.2) above.

The values for the dielectric properties of α-gallium, obtained from the polynomial fittings, were used to calculate the real and imaginary parts of the complex refractive index, n and κ respectively, for the three crystallographic directions of an α-gallium crystal. Figures 4.4, 4.5 and 4.6 below show the calculated values of the optical constants.

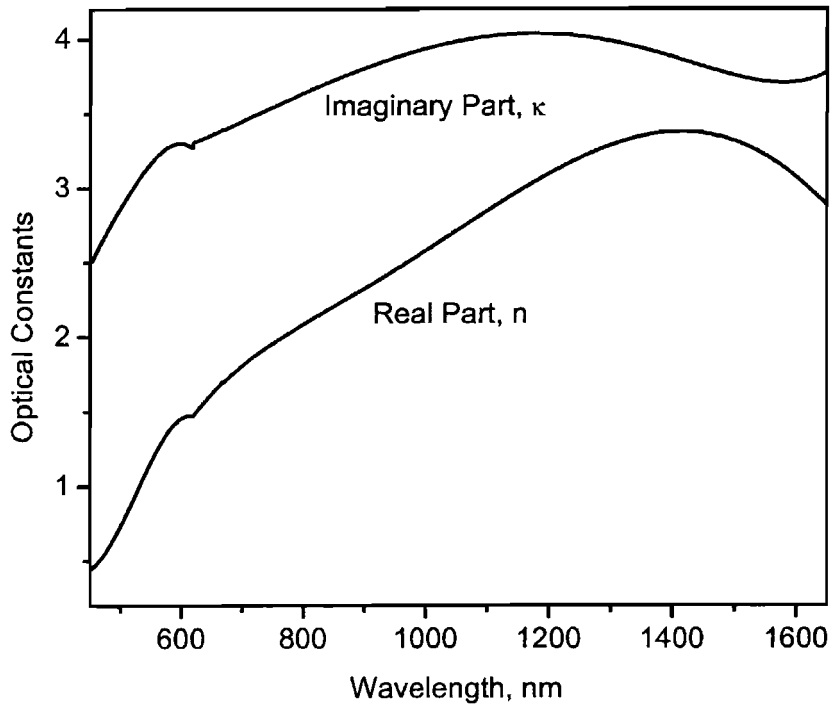


**FIGURE 4.4:** The calculated optical constants for light polarised along the [100] crystallographic direction.

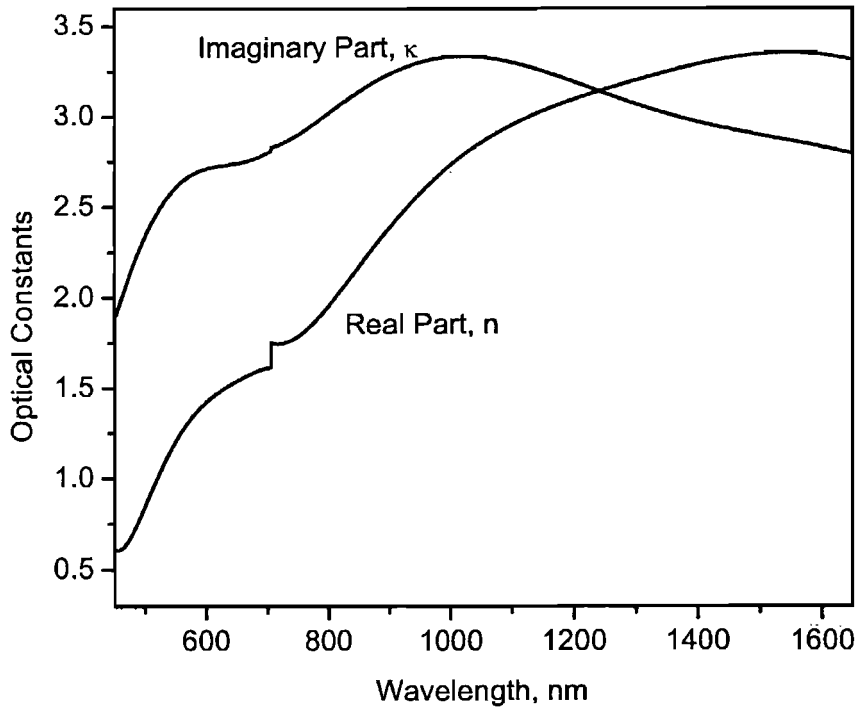


**FIGURE 4.5:** The calculated optical constants for light polarised along the [010] crystallographic direction.

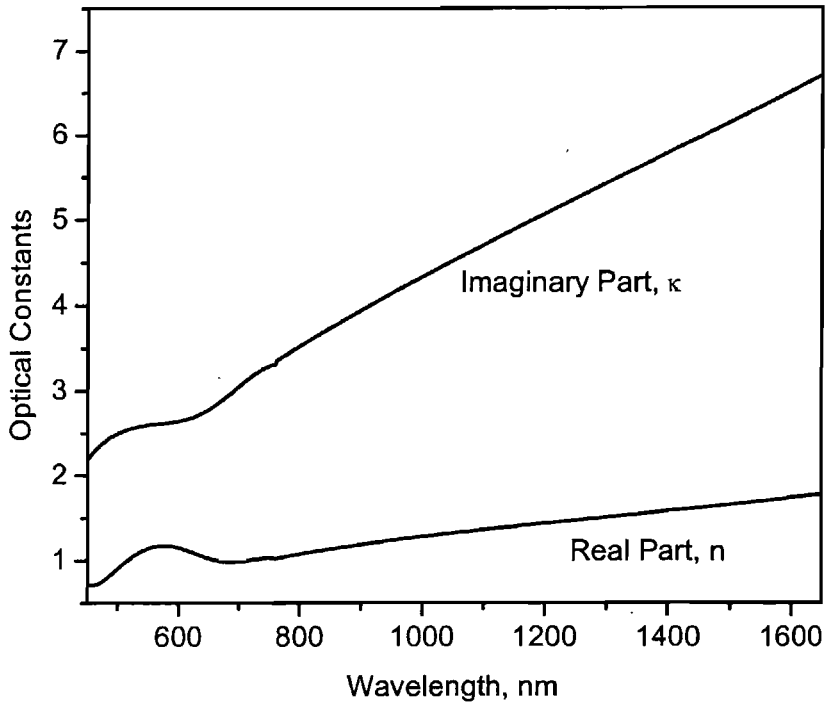


**FIGURE 4.6:** The calculated optical constants for light polarised along the [001] crystallographic direction.

Using the calculated values for the optical constants of α-gallium (figures 4.4, 4.5 and 4.6), and liquid gallium (figure 4.3) it was possible to predict the spectral characteristics of the reflectivity of a silica-gallium interface for the solid and liquid phases of gallium, using equation (4.3) below. In the solid phase reflectivity was calculated assuming light with electric field vector polarized along the three crystal directions.

$$R = \frac{(n - n_{GLASS})^2 + \kappa^2}{(n + n_{GLASS})^2 + \kappa^2} \qquad (4.3)$$

Figure 4.7 below, shows the calculated reflectivity of a silica-gallium interface for the three crystal directions of α-gallium, and liquid gallium, as a function of wavelength. Note the similarity of the a and c axes. Indeed, in Chapter 2, it is mentioned that these two axes are very similar crystallographically.

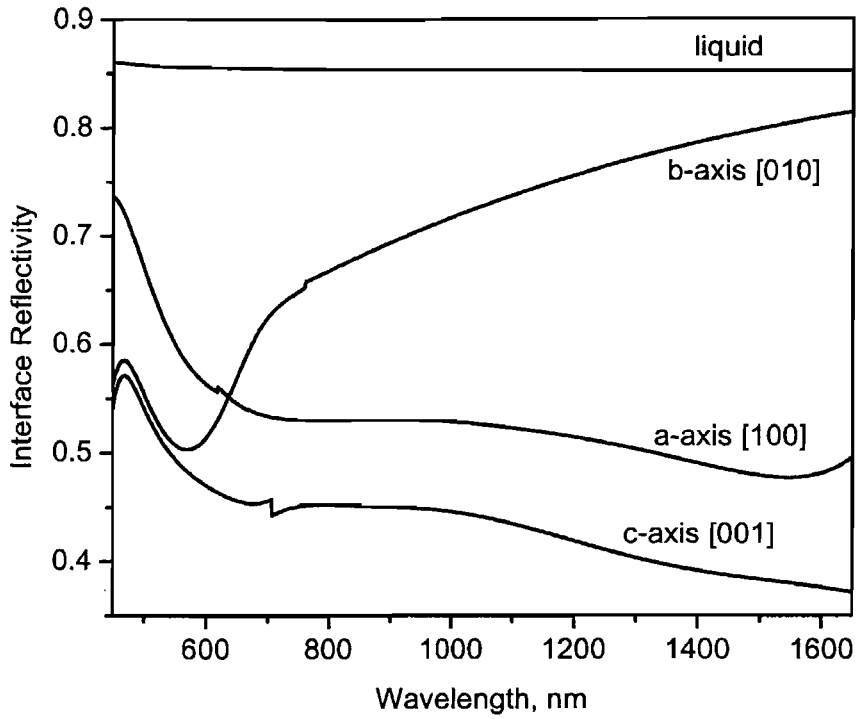


**FIGURE 4.7:** Calculated reflectivity of a silica-gallium interface for the solid and liquid phases, as a function of wavelength. Note the discontinuities in the reflectivity curves are due to the polynomial fittings and have no physical meaning.

Figure 4.7 shows the extensive change in reflectivity that takes place across the melting transition of gallium. Optical switching can be possible between the two reflective states of the material, solid (low reflectivity) and liquid (high reflectivity).

More importantly the change takes place across a very wide spectral region. This demonstrates the great potential across this wide wavelength band, spanning from visible wavelengths up to the infrared part of the spectrum that a silica-gallium interface can offer for optoelectronic applications.

## 4.3 The Optical Properties of the Silica-Gallium Interface

In this section the optical properties of a silica-gallium interface were examined. The interface was prepared by confining a small amount of molten gallium between two Corning cover glass slides (0.13 to 0.16 mm thickness, 22 $mm^2$ area, refractive index 1.532 at 632 nm). The spectral characteristics of the interface were investigated in the 450 nm to 1650 nm region across the melting transition.

A reflectometer, based on a modified optical microscope fitted with an Ealing Electro-Optics white light source, was used to obtain the broadband reflectivity measurements with respect to interface temperature. Figure 4.8 below, shows the outline of the setup used to examine the linear reflectivity of the silica-gallium interface.

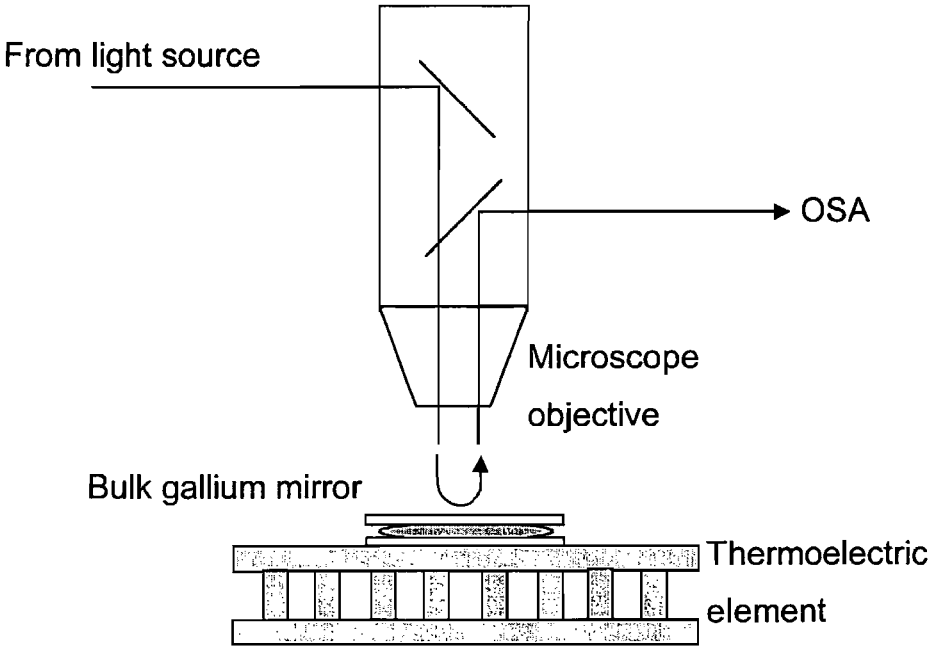


**FIGURE 4.8:** The outline of the setup used to examine the broadband interface reflectivity of a silica-gallium interface

In this setup a 3 mm area of the silica-gallium interface was illuminated with white light at normal incidence using a x10 microscope objective. To overcome the anisotropy of

gallium at the interface with silica unpolarised light was used. The reflected light was launched into a multimode optical fibre. Acquisition of the data was done using a ANDO AQ-6315 Optical Spectrum Analyser (OSA) in the range from 450 nm to 1650 nm, with 2 nm resolution. Thermal control of the silica-gallium interface was provided by a thermoelectric heat pump (Peltier element) in the range from 20 $^0$C to 33 $^0$C with an accuracy of 0.1 $^0$C. In a typical measurement the temperature of the silica-gallium interface was kept constant while the OSA obtained the reflectivity of the interface across the spectrum. Measurements were obtained this way for increasing and decreasing interface temperature. The data were calibrated against the known reflectivity of a gold mirror, to obtain the absolute values of the silica-gallium interface reflectivity. A considerable broadband increase was observed in the interface reflectivity upon melting across the wavelength range examined.

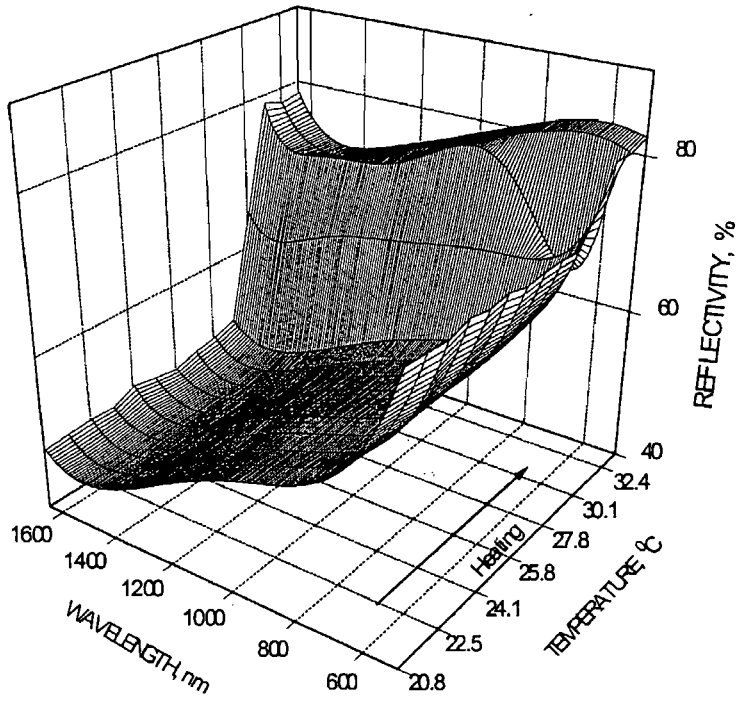


**FIGURE 4.9:** The broadband reflectivity increase of a silica-gallium interface with respect to temperature, for low intensity, unpolarised light. The graph shows the heating cycle.

No premelting phenomena were observed, within the temperature resolution used, and the transition from solid to liquid reflectivity happened in an abrupt manner. Figures 4.9 and 4.10 show the observed linear reflectivity change on melting, across the broad wavelength range.

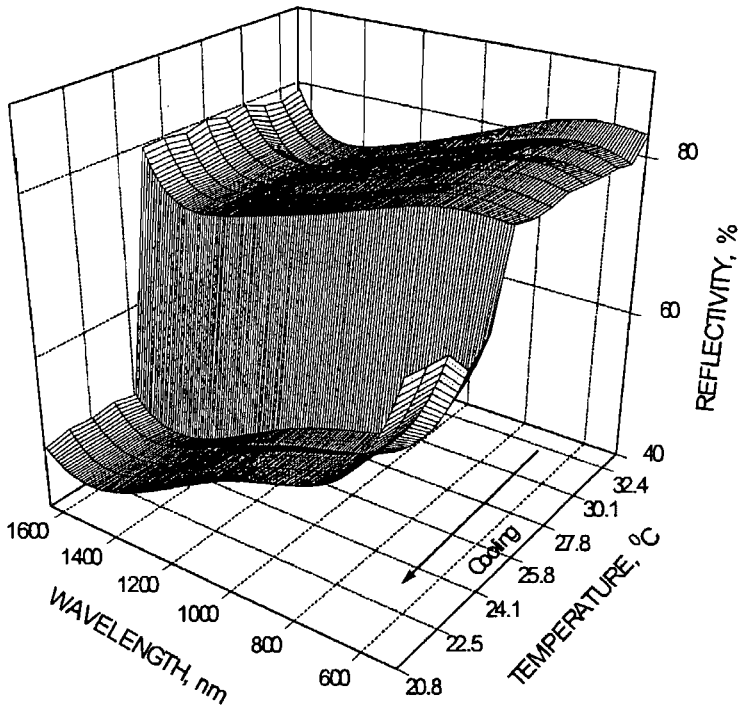


**FIGURE 4.10:** The broadband reflectivity increase of a silica-gallium interface with respect to temperature, for low intensity, unpolarised light. Here the cooling cycle is shown.

## 4.4 The Optical Properties of a Silica-Gallium Interface Prepared by Ultrafast Pulsed Laser Deposition

Silica-gallium interfaces in which gallium has a low affinity at the interface, have been used to demonstrate the enhanced nonlinear optical properties of the material. However, such contact interfaces prepared at the tip of an optical fibre, or by simply squeezing gallium between cover glass slides, lack the reliability needed in demanding applications.

Indeed, these interfaces show degradation after a few heating and cooling cycles, and are susceptible to the ambient environmental conditions. It was decided to concentrate on silica-gallium interfaces, in which gallium exhibits a high degree of stability due to the presence of a transitional layer at the silica interface.

Early attempts to produce high quality, thin gallium films by means of evaporation condensation in vacuum onto silica substrates, and by sputtering of gallium failed. The films were deposited in a structural state that did not exhibit a phase transition at the normal melting temperature. Broadband reflectivity measurements revealed that gallium was deposited in a highly reflective form, with reflectivity similar to that of liquid gallium.

A new type of confined silica-gallium structure was developed using Ultrafast Pulsed Laser Deposition (UPLD). The silica-gallium interface was manufactured at the facilities of the Laser Physics Centre, The Australian National University, Canberra Australia, by A. V. Rode and B. Luther-Davies. The samples were prepared during the visit to the Australian National University by Professor N. I. Zheludev, as part of a collaboration project sponsored by the Royal Society and the Australian Academy of Sciences.

Using this method, gallium films of about 1 – 2 μm thickness were manufactured by gallium ablation under vacuum (~2 x $10^{-6}$ Torr) directly on a silica substrate using a q-switched, mode-locked Nd:YAG laser at 1064 nm with 60 ps pulse duration. It was found that the substrate required cooling to about –100 $^0$C during deposition. This is a standard technique in the deposition of non-scattering films [3], for metals with low-melting point such as gallium. Using this method the thin gallium film was deposited in the correct crystalline phase, α-phase, and showed the required phase transition.

The UPLD silica-gallium interface linear reflectivity was examined over a broad wavelength range, from 450 nm to 1650 nm, for temperatures close and above the gallium melting point similarly as above. The temperature of the gallium sample was controlled, in the range of 14 $^0$C to 32 $^0$C, by a miniature Peltier element with a nominal accuracy of 0.1 $^0$C. Figures 4.11 and 4.12 below present the linear reflectivity of the UPLD prepared silica-gallium interface. The results show a considerable increase of the interface reflectivity, on melting, across the whole spectral region examined.

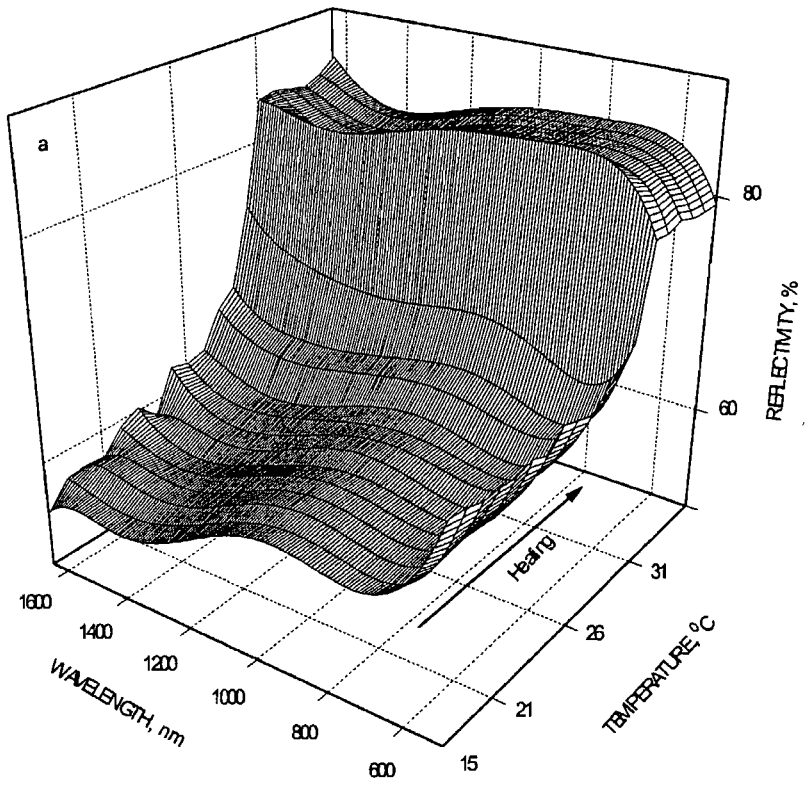


**FIGURE 4.11:** The broadband reflectivity increase of the UPLD prepared silica-gallium interface with respect to increasing temperature, for low intensity, unpolarised light. Strong premelting is observed.

In these measurements, strong premelting phenomena in the transition from solid to liquid were observed see (figure 4.11) indicated by the gradual rise of reflectivity before the melting temperature was reached. On cooling, solidification happens in an abrupt manner and reflectivity returns to its original values. This type of interface has shown exceptional structural stability, able to withstand numerous heating and cooling cycles. The stability is thought to be due to the presence of a transitional layer, at the interface between silica and gallium formed by energetic gallium ions penetrating into the silica substrate during deposition. Optical measurements of the silica-gallium interface, at a wavelength of 810 nm, have suggested the presence of a thin wetting layer of a highly reflective metallic phase forming between the silica and gallium. These results in combination with standard thin-film formulae, assuming that the optical properties of this layer are the same as those of free-electron gallium and that there is a sharp boundary between the metallic and $\alpha$-gallium phases, were used to estimate the thickness of this layer. The results have indicated that a layer of 3 nm thickness is always present at the interface, contributing to

the stability of the interface observed in the experiments. This thickness is much deeper than would be expected from a thermal evaporation process. Using a Monte-Carlo program it was found that the kinetic energies required were in the order of 600 eV. However an ion acceleration mechanism has been proposed that allows the ions to have kinetic energies of up to 1 keV during the deposition process [9 and references therein].

The results shown in figures 4.11 and 4.12 demonstrate the high optical quality of the UPLD prepared interface, and the possibilities it offers for nonlinear optical research.

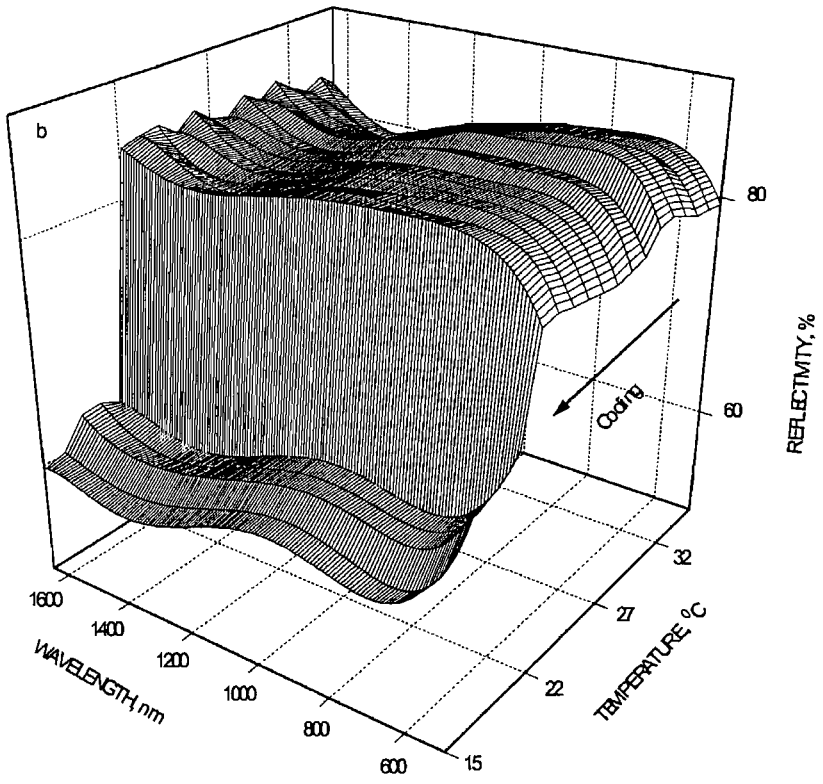


**FIGURE 4.12:** The broadband reflectivity increase of the UPLD prepared silica-gallium interface with respect to decreasing temperature, for low intensity, unpolarised light.

## 4.5 Review of the Optical Properties of a Silica-Gallium Interface

In previous sections the spectral response of the optical properties of gallium at an interface with silica were calculated for the solid and liquid phases of gallium, using data from previously published works. Moreover, the reflectivity of two types of silica-gallium

interfaces was measured across the melting transition of gallium, as a function of wavelength. In this section the results of the measurements of the spectral response of reflectivity with temperature are compared with theoretical predictions derived from previously measured data from [4].

Figure 4.13 below, shows a comparison between measured vacuum-gallium reflectivity values taken from [4], and calculated vacuum-gallium reflectivity values obtained from dielectric data using polynomial approximations. A good agreement between the measured and calculated values can be seen. Using the same polynomial approximations the reflectivity of a silica-gallium interface was calculated and is also shown in figure 4.13. The interface reflectivity is presented for light polarised along the a-axis, [100] crystallographic direction at the interface. The calculated reflectivity values for the other two crystallographic directions, b [010] and c [001] axes, show similar agreement when compared with values taken from [4].

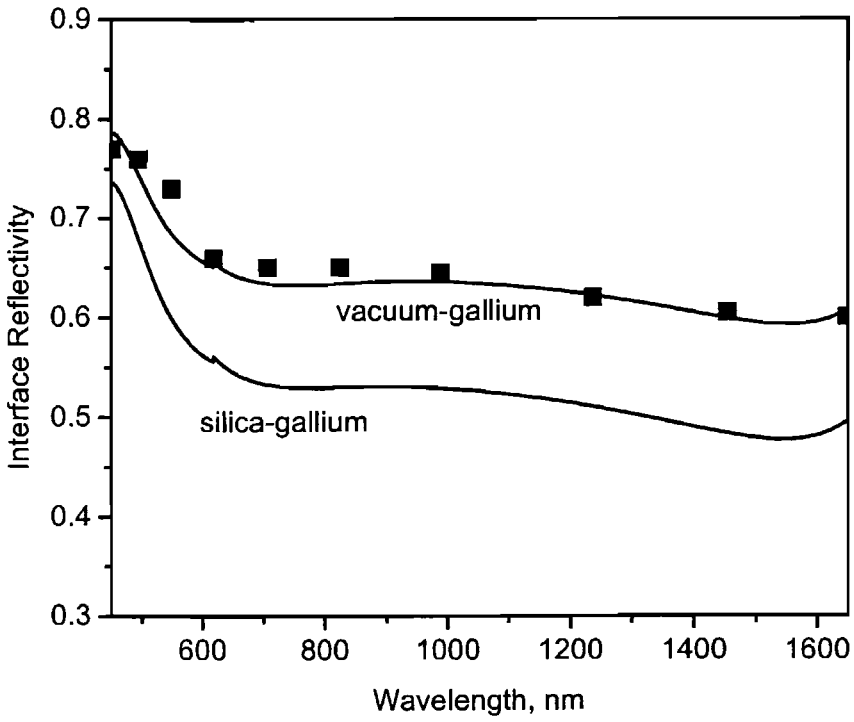


**FIGURE 4.13:** Comparison of measured reflectivity values from [4], and values obtained from polynomial approximations of dielectric data. Shown from light polarised along the a-axis of gallium, [100] crystallographic direction.

Furthermore, interesting comparisons can be made between the measured reflectivity values of the two silica-gallium interfaces examined. Both interfaces show melting at approximately 30 $^0$C, with the UPLD prepared interface exhibiting premelting beginning from 22 $^0$C. Solidification for the bulk gallium mirror is at about 24 $^0$C showing overcooling of 6 $^0$C. In the case of the UPLD prepared interface solidification takes place at 21 $^0$C, showing overcooling of 9 $^0$C. Figure 4.14, compares the spectral response of the measured reflectivity values for the two interfaces, at solid and liquid temperatures, as measured in figures 4.9, 4.10 (bulk gallium mirror) and 4.11, 4.12 (UPLD).

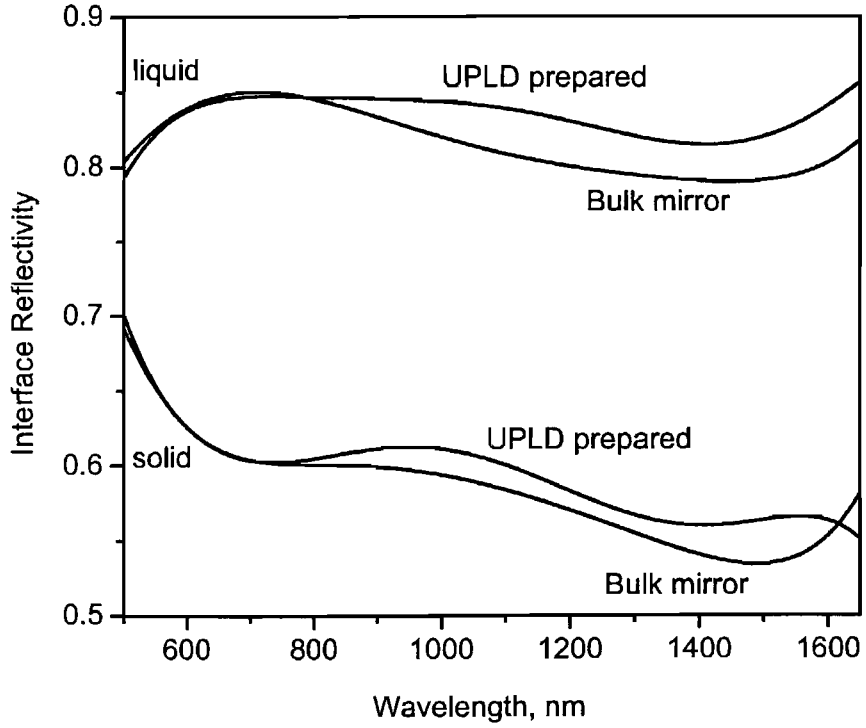


**FIGURE 4.14:** Spectral response of the measured interface reflectivity of the bulk gallium mirror and the UPLD prepared interface as a function of wavelength.

From figure 4.14 a similar behaviour between the UPLD prepared interface and the bulk gallium mirror, can be seen. In the case of solid reflectivity values, both UPLD and bulk mirror show high reflectivity in the visible region which then drops off towards the infrared (IR). Also reflectivity is very similar in the visible and the near-IR for the two interfaces. In the case of liquid gallium the reflectivity of the two interfaces shows similar response at the visible and up to the near-IR. Reflectivity of the UPLD prepared interface

shows less variation than the bulk gallium mirror. Furthermore, in the liquid a flat spectral response of reflectivity was expected (see figure 4.7). In fact, the measured liquid reflectivity shows a spectral dependence possibly due to the presence of crystalline order at the silica-gallium interface, even at liquid temperatures.

Indeed, this corroborates observations discussed in Chapter 2, and references therein, suggesting surface layering of liquid gallium and the existence of short-lived gallium dimer units in the liquid phase, representing remnants of the α-gallium covalent character. Moreover, the preferential wetting of an interface by liquid gallium has been mentioned earlier in this chapter [10], with layers of gallium dimer units orientated roughly perpendicular to the interface, forming planes of dimers in an increasingly disordered fashion moving away from the interface. These observations of the presence of the dimer structure, give rise to weak covalent absorption, which can explain the spectral response of the silica-gallium interface when gallium is in its liquid phase.

Moreover, the latter observation can be used to determine the crystallographic arrangement at the silica-gallium interface, and the spectral response of the measured solid reflectivity. Assuming that the dimer units (b-axis [010] crystallographic direction) will be roughly perpendicular to the interface, this allows for the two existing crystallographic directions to occupy the plane parallel to the interface. Using the calculated reflectivity values for the a [100] and c [001] crystallographic directions from figure 4.7, the average in-plane interface reflectivity can be calculated. Figure 4.15 compares the measured reflectivity for the UPLD prepared interface, with the average calculated in-plane reflectivity.

The spectral response of the solid reflectivity can be seen to agree with the calculated values for reflectivity. However, the two sets of data show a discrepancy in the reflectivity values reached. Indeed, the measured reflectivity exhibits higher values that the calculated one. The difference in reflectivity values is possibly due to oxidization of the interface, or calibration differences. An additional reason can be the existence of a different metastable phase of gallium at the interface, such as β-gallium, GaII or GaIII. In the liquid phase the above-mentioned spectral response of the measured values can be clearly seen.

In conclusion, the calculated and measured reflectivity across the melting transition and as a function of wavelength, of a silica-gallium interface was examined, and the differences and similarities were reviewed. A good agreement between the calculated and measured values can be seen across the spectral region examined.

The measured reflectivity of two silica-gallium interfaces prepared by different procedures were examined and compared. A good agreement between the reflectivity response of the two interfaces can be seen. This indicates that the optical properties of a UPLD prepared silica-gallium interface are similar to those of bulk gallium. Finally, the results suggest that the optical properties of a silica-gallium interface can be reasonably estimated using data from vacuum and air-gallium surfaces and Fresnel formulas.

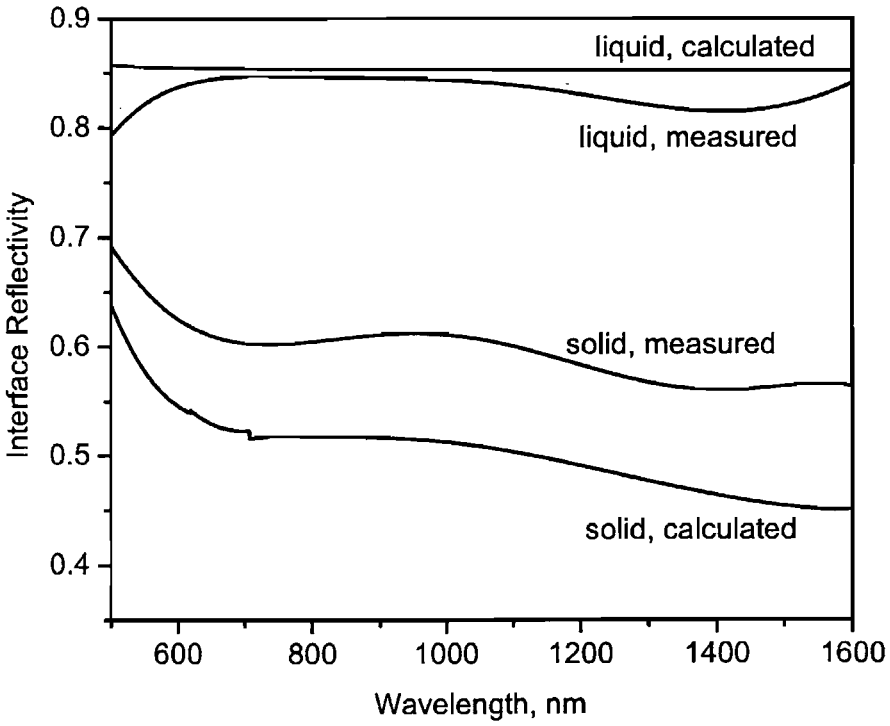


**FIGURE 4.15:** Comparison of the measured interface reflectivity of the UPLD prepared interface, and the calculated average in-plane reflectivity.

## 4.6 Light-Induced Reflectivity Increase at the Blue-Green Part of the Spectrum

In this experiment the nonlinear optical properties of the same UPLD prepared silica-gallium interface are examined. The light-induced reflectivity increase was investigated at the blue-green part of the spectrum. The dependence of the interface reflectivity with incident light was measured, at wavelengths of 488, 496, 501 and 514 nm, for a range of temperatures starting well below the melting temperature of gallium ($T_m$ = 29.8 $^0$C) and reaching a few degrees above $T_m$. Some of the measurements reported herein were obtained in collaboration with Mr V. A. Fedotov.

To examine the reflectivity of the UPLD silica-gallium interface in the blue-green region, light from a Spectra Physics argon ion laser (Model 2060-10S) at 488, 496, 501 and 514 nm, in a single beam setup was used. The light was focused on the gallium film, through the silica substrate, at near to normal incidence to a spot of approximately 50 μm in diameter. The temperature of the interface was controlled by a thermoelectric (Peltier) element, as mentioned earlier, in the range between 14 $^0$C to 32 $^0$C with a nominal accuracy of 0.1 $^0$C.

To avoid any problems due to the anisotropic character of the silica-gallium interface, the incident light was circularly polarised. The beam intensity was modulated at 200 Hz. The experimental setup used to investigate the linear reflectivity of the silica-gallium interface with respect to incident light intensity is shown in figure 4.16.

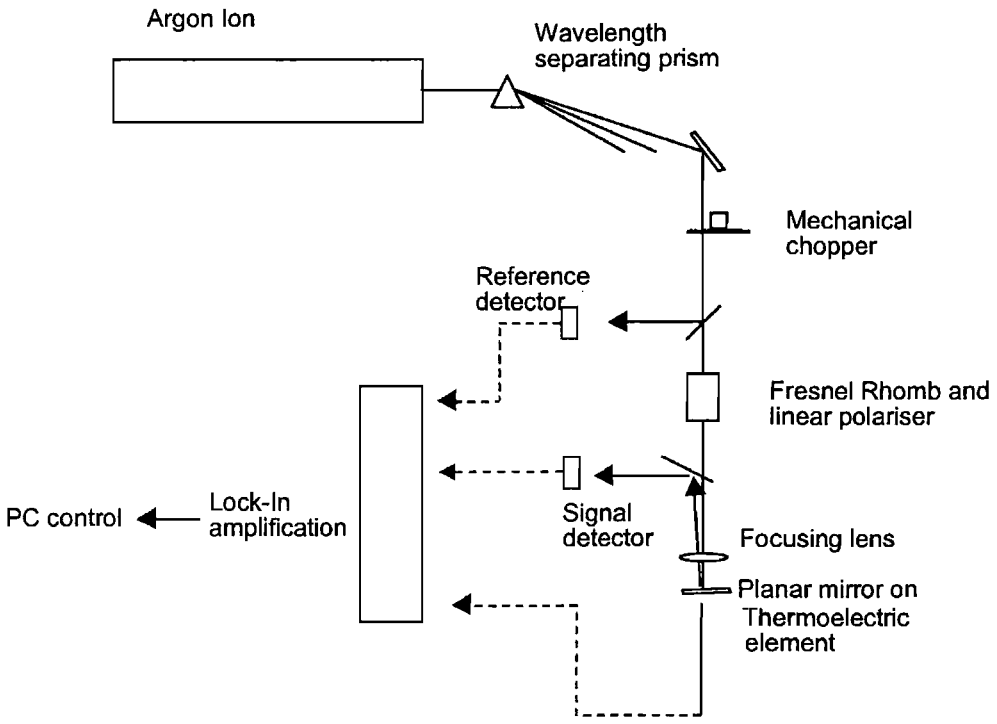


**FIGURE 4.16:** The experimental setup used to investigate the linear reflectivity for wavelengths in the blue-green spectral region.

In figure 4.17, the change of the silica-gallium interface reflectivity on melting, for low intensity light, is shown for the different wavelengths used. The experimental data are shown in comparison with the values for the change of reflectivity of the silica-gallium interface calculated using values for the optical constants from figures 4.4, 4.5 and 4.6. In figure 4.17, the calculated reflectivity values account for the presence of a transient metallic layer, 3nm thick. A good agreement between our experimental and calculated values, of the silica-gallium interface reflectivity change on melting, can be seen.

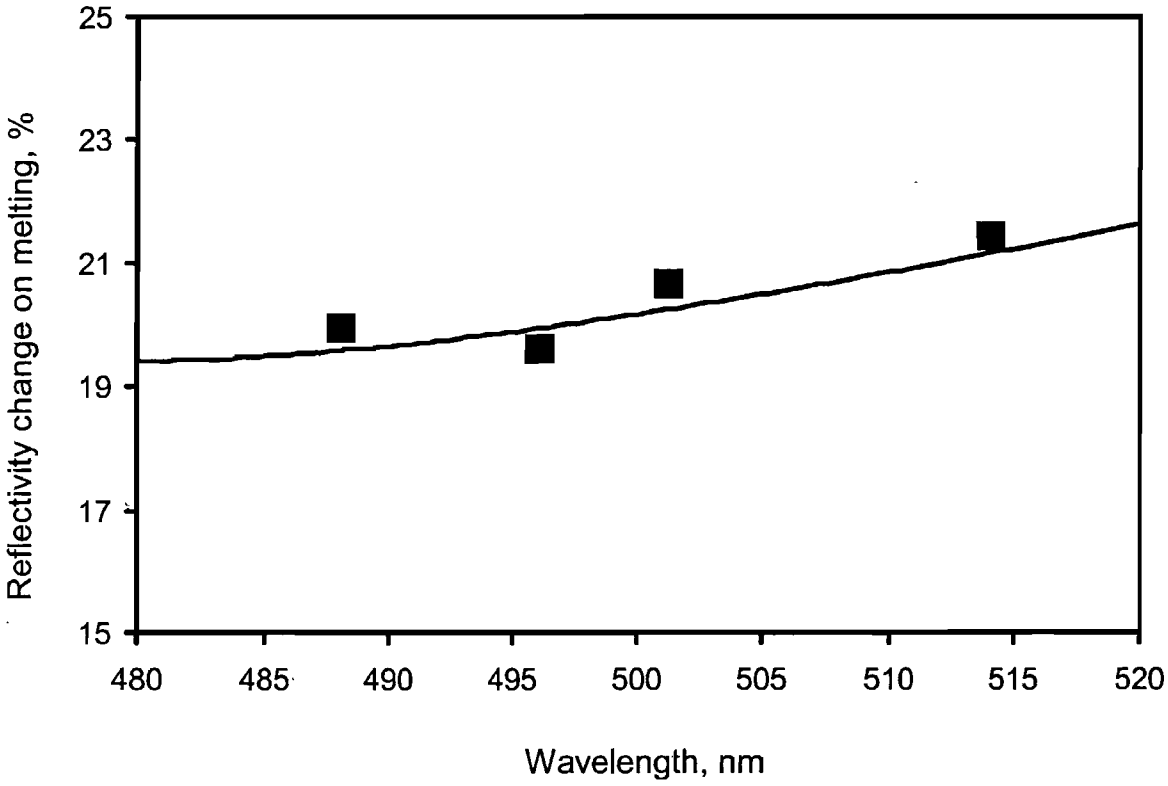


**FIGURE 4.17:** Reflectivity change at the UPLD silica-gallium interface on melting in the blue-green spectral region. The solid line represents the calculated value of the reflectivity change whereas the " " are the experimental results.

The nonlinear response of the UPLD silica-gallium interface is shown in figure 4.18. Here, the reflectivity of the silica-gallium interface, as a function of temperature, for different light intensities at a wavelength of 514 nm is presented. Curves i to iv correspond to silica-gallium interface reflectivity at incident light intensities of 100 W/cm$^2$, 500 W/cm$^2$, 1.5 kW/cm$^2$ and 3 kW/cm$^2$, curve v corresponds to decreasing temperature. Liquid gallium reflectivity is reached at approximately 30 $^0$C, with solidification occurring at 24 $^0$C. The results show a strong modification of the interface reflectivity as the light intensity is increased, with respect to increasing temperature. Indeed, the reflectivity change can be seen to become less abrupt with increasing intensity, however, the temperature at which the liquid gallium reflectivity (~76 %) is reached, remains constant for all excitation levels used in the experiment.

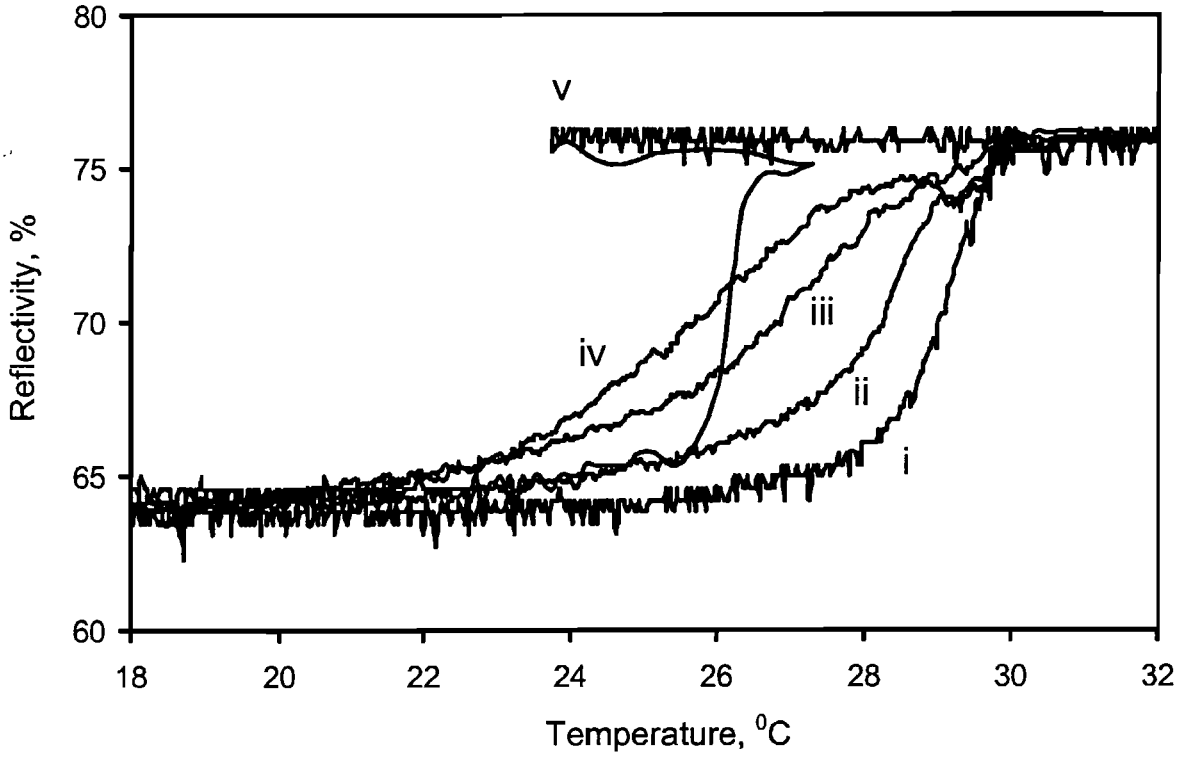


**FIGURE 4.18:** Interface reflectivity at 514 nm with increasing temperature, and for various light intensities (curves i-iv) across the melting point of gallium. Curve v shows reflectivity with decreasing temperature.

Note the interesting behaviour, seen in curve v, of the interface reflectivity with decreasing temperature, caused by the heat released when the gallium films recrystallises. Recrystallisation from melt is an avalanche process which develops through the formation of crystallisation seeds. As a result a substantial amount of energy is released in the form of heat. In the absence of a heat sink this could lead to an abrupt increase in the temperature of the sample. Such an effect is often used as experiment with various substances to illustrate the thermodynamical peculiarities of first order melting. Simple thermodynamic calculations can show that such heat release can cause an increase in temperature of several tens of degrees. Indeed, in the case of gallium and if an adiabatic process is considered, the temperature difference going from liquid to solid is

$$\Delta T = L/C \qquad (4.4)$$

Where L = 80 $Jg^{-1}C^{-1}$ is the latent heat of gallium, and C = 0.371 $Jg^{-1}$ is the specific heat of gallium, giving $\Delta T = \sim 215\ ^0C$. However, in reality a much smaller temperature rise can be expected due to the presence of a heat sink in the form of the thermoelectric element (Peltier unit). Nevertheless, such a temperature increase is what is observed in fig. 4.18. It is a transitional effect which confuses the thermal stabilisation circuitry, which can not cope immediately and registers a rise in the temperature axis.

To illustrate the light-induced reflectivity change for increasing temperatures at a wavelength of 514 nm, figure 4.19 is presented, below. It is shown as the difference between reflectivity at the higher intensity levels (curves ii to iv) and the lowest intensity level (curve i). The maximum change is achieved a few degrees below the melting point of gallium, $T_m$, while the effect disappears on melting. From this figure, it can be seen that a reflectivity change of about 15 % can be induced at the silica-gallium interface, under illumination of a laser beam of 3 $kW/cm^2$ intensity.

## 4.7 Conclusion

The nonlinear reflectivity of a UPLD prepared silica-gallium interface was investigated in the blue-green spectral region. The light induced interface reflectivity change was measured with respect to increasing and decreasing temperature, at wavelengths of 488, 496, 501 and 514 nm. Results show that reflectivity can be modified by as much as 15% at a wavelength of 514 nm, close to the melting point of gallium.

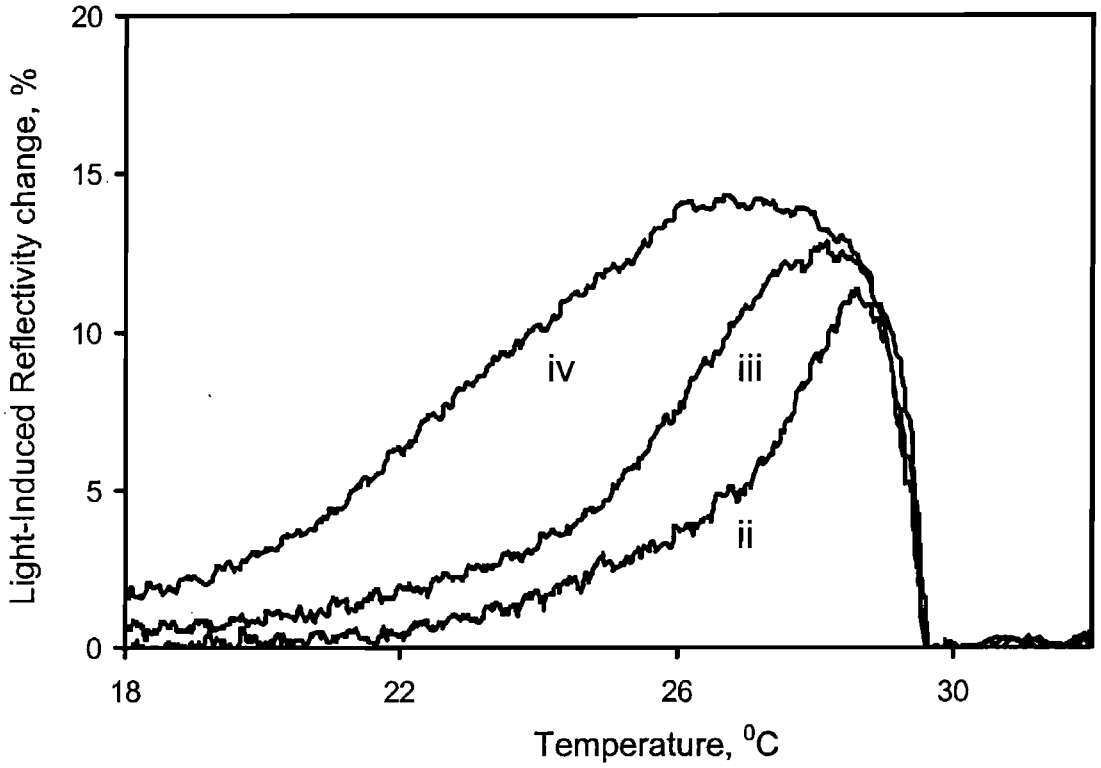


**FIGURE 4.19:** The magnitude of the light-induced reflectivity change with increasing temperature as the difference between reflectivity at higher intensity levels (curves ii to iv) and the lowest intensity level (curve i).

## 4.8 Discussion

An obvious mechanism that could be used to explain the observed reflectivity behaviour, shown in figures 4.18 and 4.19, is laser-induced melting in which the laser beam heats the thin gallium film at the interface with silica, causing it melt. To understand the exact nature of the mechanism behind the observed reflectivity increase, it was decided to investigate the temperature change due to the presence of the laser beam heating the interface. To do so, the temperature distribution and heat flow at the interface were modelled, using a method based on Green's function. The model was adapted to the specific case of a silica-gallium interface, and all calculations were performed by V. A. Fedotov under the supervision of Prof. Zheludev. The equations included here and the relevant thermal calculation results can be found in [11]. Using these calculations the rise in the local interface temperature was evaluated, in order to understand whether the

observed reflectivity increase was a result of the presence of the laser beam at the interface.

The three-dimensional heat conduction equation of the silica-gallium interface was analytically solved for the steady state regime of laser illumination. Initially, the use of numerical solvers based on the finite element method was found to be problematic. The dimensions of the gallium film are considerably smaller than the dimensions of the silica substrate, and at the same time the diameter of the laser spot is but a fraction of the sample width. To overcome this difficulty, an axial symmetry of the sample was introduced, approximated by a cylinder with a diameter equal to the typical width of the sample [11]. Such approximation does not affect the actual temperature distribution near the laser spot. In addition, convection and radiative losses from the sides of the silica-gallium interface were ignored, making the calculated values of the temperature increase to be an overestimate of the actual values of temperature.

Using the axial symmetry in the cylindrical co-ordinate system, the heat conduction equation is as follows:

$$\frac{1}{\rho}\frac{\partial}{\partial\rho}\left[\rho\frac{\partial T_i(z,\rho)}{\partial\rho}\right]+\upsilon^2{}_1\frac{\partial^2 T_i(z,\rho)}{\partial z^2}=0 \qquad (4.5)$$

where $i$ is an index referring to the substructure, i.e. ceramic plate, gallium film and silica glass, and $\upsilon_i=\sqrt{\lambda_i^{\,z}/\lambda_i^{\rho}}$ where $\lambda_i^{\,z}$ and $\lambda_\rho{}^z$ are the thermal conductivities in the axial, $z$, and radial directions, $\rho$, of the cylinder element used to approximate the silica-gallium structure. Next, the appropriate boundary conditions were introduced, considering that any losses from the sides of the samples are neglected, and the laser energy absorbed by the gallium film is confined in the optical skin depth, which is negligible compared to the thickness of the film.

In the calculations the sample temperature was taken to be 26 $^0$C as set by the thermal element. The initial reflectivity of the silica-gallium interface was taken to be about 60%, as suggested by the theoretical predictions and the measured values discussed earlier in

this chapter. The calculations were performed for an incident light intensity of 3 $kW/cm^2$, which was the highest intensity used in the experiment. Furthermore, gallium's characteristics and thermal properties were taken into account. As discussed in Chapter 2 a specific orientation prevails at the interface with silica, the optical properties of which were examined in the beginning of this chapter. The thermal properties of gallium are, similar to the optical properties, dependent on the crystal orientation at the interface. In the calculations the thermal conductivity of α-gallium, was taken as $\lambda_c$ = 15.9 $Wm^{-1}K^{-1}$ perpendicular to the interface and as 64.6 $Wm^{-1}K^{-1}$ in the plane of the interface, an average of $\lambda_a$ = 41 $Wm^{-1}K^{-1}$, $\lambda_b$ = 88 $Wm^{-1}K^{-1}$.

The results of the thermal calculations indicated that the local rise in the interface temperature, under the laser spot, would be ~2 $^0C$, above the set sample temperature regulated by the thermoelectric element (see above). In practice the temperature rise would be smaller since in the model the relatively low value of 0.8 $Wm^{-1}K^{-1}$ was used for the thermal conductivity of glass, and all radiative and convection losses have been ignored. Such a temperature rise cannot explain the reflectivity behaviour observed in the experiment. However, such a calculation does not firmly exclude the possibility of thermal melting as the mechanism behind the reflectivity behaviour of the silica-gallium interface observed in figures 4.18 and 4.19.

Nevertheless, such an explanation has some obvious problems. Namely, if the presence of the laser beam at the silica-gallium interface would melt the whole gallium film, then the low intensity reflectivity, illustrated by curve i in figure 4.18, would be shifted down towards lower temperature values along the temperature axis. This downward shift would be equal to the increase in temperature of the film caused by the laser heating the interface. However, in the case of the reflectivity behaviour observed, instead of a temperature shift, a modification of the reflectivity curve was seen, while most importantly the melting temperature remained the same even at the higher incident light intensities.

Therefore, the observed modification of the reflectivity curves, which happen across a wide range of temperatures as shown in figure 4.18, and the observed reflectivity increase at the silica-gallium interface cannot be explained by a thermal effect, and there should be

another mechanism of most likely a non-thermal nature. Indeed, such a non-thermal mechanism, involving metallic film formation through light excitation, has recently been found to be an accurate model explaining the reflectivity behaviour of a silica-gallium interface under cw excitation [9]. The measurements performed in the blue-green spectral region in this experiment are consistent with the non-thermal mechanism proposed in [9]. According to that model, gallium will undergo a non-thermal, surface-assisted phase transition when illuminated with light. During this transition, the reflectivity of the silica-gallium interface depends on the presence of a thin wetting layer of a highly reflective metallic phase that forms at the interface between the silica and gallium. In chapter 1, it was shown that a thin layer of a metallic phase of gallium, known as Ga(III), forms readily at a surface of α-gallium without any external stimulation.

The light-induced transition of the silica-gallium interface is made possible by the crystalline structure of α-gallium. In chapter 1, the energy band structure of the material was discussed, and the existence of distinct transitions within the band structure was related to the presence of covalent bonding in the α-gallium structure. The covalent bonding results in a broad absorption band which makes the silica-gallium interface sensitive to external stimulation through light excitation at wavelengths spanning from ~310 nm to ~1820 nm.

The measurements of the, UPLD prepared, silica-gallium light-induced interface reflectivity were within this range, at 514 nm, and close to the peak of the optical absorption band. In this case, absorption of light is highly localised and leads to the excitation of the Ga dimers, from the bonding to the antibonding state, reducing the stability of the surrounding crystalline cell, which subsequently undergoes a transition to a new phase of considerably different optical properties in the form of a microscopic inclusion. The presence of the microscopic inclusions of the metallic phase shifts the energy balance at the silica-gallium interface, and as a result leads in the creation of a metallic layer.

As the incident light intensity increases, the thickness of the new metallic phase's layer increases accordingly. The new phase is stable under light illumination, and grows epitaxially as a layer at the interface between silica and gallium, propagating towards the

bulk α-gallium film. The increase in the interface reflectivity is a result of the increasing thickness of the metastable phase. The exact identity of this phase is not yet clear, but it is most likely to be one of the material's existing metastable phases, such as β-gallium, Ga(II) and Ga(III). These phases exhibit metallic characteristics as discussed in chapter 1, similar to those of the liquid state and are involved in the continuous transition from the solid crystalline α-phase to the liquid (α-gallium β-gallium Ga(II) Ga(III) liquid) [12].

## 4.9 Dynamic Measurements of the Light-Induced Reflectivity Change at a Silica-Gallium Interface

In this part of the experiment, the interface reflectivity of the silica-gallium interface was studied using pulsed excitation. A pump-probe setup, with a modulated pump and a cw laser as the probe source, was used. The reflectivity of the interface was examined using pump pulses of different intensities, for various sample temperatures up to the melting point of gallium.

The 514 nm line, from the Spectra Physics argon ion laser (Model 2060-10S), was used as the pump to investigate the switching properties of the silica-gallium interface. The reflectivity of the interface was monitored using a cw HeNe laser at 633 nm. An acousto-optical modulator was used to alter the pump into pulses of duration, $\tau_p$, 150 ns, 400 ns and 1 μs, with a repetition rate of 100 Hz. In this experiment, the intensity modulation of the pump beam induces a change in the reflectivity of the silica-gallium interface, causing a modulation on the probe intensity.

Both the pump and probe beams were focused at the gallium film, through the silica substrate, at spot diameters of about 50 μm and 35 μm, respectively. The polarisation of the pump was circular. A digital oscilloscope was used to register and record the reflected probe signal, detected by a fast photodiode. The overall bandwidth of the detection system was 150 MHz. The pump-probe setup used is shown in figure 4.20.

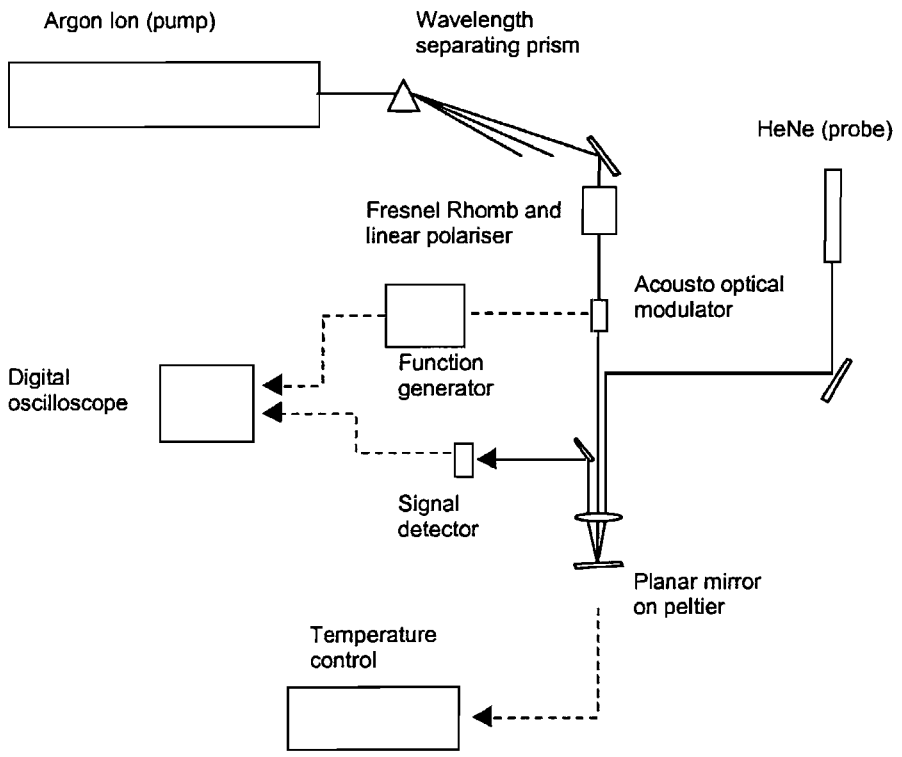


**FIGURE 4.20:** The pump-probe setup used to investigate the switching properties of the silica-gallium interface between 514 nm (pump) and 633 nm (probe).

The transient measurements show the behaviour of the silica-gallium reflectivity under pulsed optical excitation, with pulse duration in the nanosecond/microsecond range, and illustrate the typical response of the interface reflectivity, similar to that observed in Chapter 3. Figure 4.21, below, shows the dynamics of the silica-gallium interface reflectivity response, as measured for different pump pulse durations. The results indicate that the interface reflectivity rises immediately after the start of the pump pulse (shown by the dashed vertical line in figure 4.21). Furthermore, the relaxation of the interface reflectivity after the pump pulse ends can be seen. Here the recovery time, $\tau$, is taken at

the full width at half maximum of reflectivity, indicated by the arrow, when the pump pulse is no longer present and the reflectivity starts to recover. The measurements indicated that the recovery time is dependent on temperature, see figure 4.23 below.

Figure 4.22 shows the magnitude of the pump-induced, probe reflectivity change as a function of sample temperature, for three pump pulse durations. The results show that the maximum light-induced change occurs just below the melting point, at a temperature of 27.8 $^0$C. Moreover, when the melting temperature is reached the effect disappears.

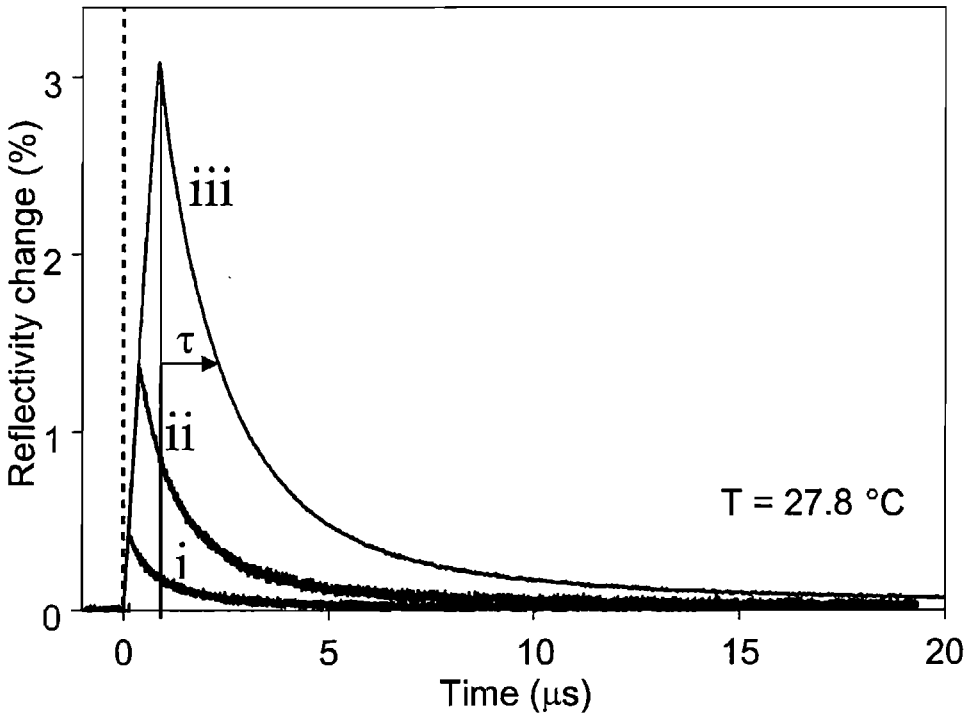


**FIGURE 4.21:** The dynamics of the light-induced reflectivity change plotted for three different pump pulse durations at T = 27.8 $^0$C. Curves i, ii and iii correspond to different pump pulse durations, 0.15 μs, 0.40 μs and 1.00 μs, while τ indicates the recovery time.

## 4.10 Conclusions

The transient dynamics of the silica-gallium interface were investigated using a pump-probe setup. The results indicate that reflectivity rises immediately after the start of the

pump pulse. The maximum light-induced change occurs just below the melting point, and disappears above melting.

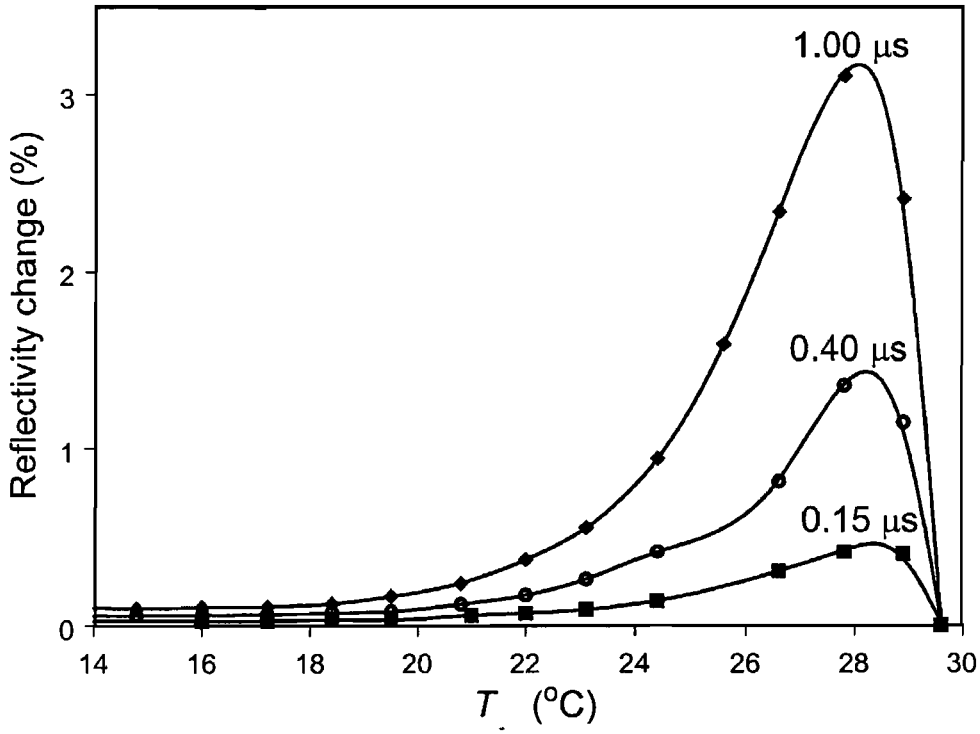


**FIGURE 4.22:** The magnitude of the reflectivity change for the different pump pulse durations, 0.15 μs, 0.40 μs and 1.00 μs, with increasing temperature.

## 4.11 Discussion

The transient measurements shown in figures 4.21 and 4.22 above, illustrate the typical response of the silica-gallium interface reflectivity under pulsed laser excitation. The results presented therein, can be explained by a nonthermal mechanism similar to that introduced in the case of the cw measurements discussed earlier. This mechanism has been used to successfully explain the dynamic behaviour of a silica-gallium interface under pulsed laser excitation for pulse durations longer than 10 ns [13]. According to this mechanism, the behaviour of the silica-gallium interface reflectivity is associated with a fast light-induced, surface-assisted, structural phase transition, involving a transition to a new metastable phase, which becomes stable in the presence of the pump pulse. This transition is made possible by the sensitivity of the silica-gallium interface under illumination, when close to the melting temperature of gallium. Recent work suggests that

the metallic phase grows during the pulse duration, forming a well-defined metallic layer at the interface [14].

The rapid increase of reflectivity, shown in figure 4.21 for the three different pulse durations, is a result of the increased density of the metallic phase at the interface. When the pump excitation is no longer present, the metallic phase becomes metastable and begins to recrystallize back to the α-phase, with reflectivity recovering its initial value.

If the observed behaviour was temperature driven, due to the presence of the laser beam heating the interface locally and involving no change in the structure of α-gallium, reflectivity would relax as the temperature of the interface relaxed. In this case the recovery time of the interface reflectivity would be independent of temperature, since the heat conduction equation, equation (4.5), is not a function of temperature. In the measurements presented here, the interface reflectivity recovers exhibiting temperature dependent recovery times as shown in figure 4.23, below. As with previous case the recovery time is measured when the pump pulse ends and reflectivity starts recovering to its initial value, and is measured at roughly the full width at half maximum.

The reflectivity recovery time is a function of the velocity, $v_r$, with which the α-phase/metallic phase front moves towards the silica substrate. It also depends on the rate of thermal diffusion, i.e. the rate at which the interface cools, and also on the thickness of the metallized layer. In the case of the measurements presented here, the growth velocity is the dominant factor, since the thermal diffusion time is much shorter than the recrystallization time.

The growth velocity depends on the sample temperature: $v_r = g(1 - T/T_m)$, where $g$ is a function of the recrystallisation mechanism and $T_m$ is the bulk melting temperature [9]. From the transient reflectivity measurements corresponding to sample temperature of 27.8 $^0$C, (figure 4.22) $v_r$ was found to be $4 \times 10^{-4}$ ms$^{-1}$. The recovery time $\tau = d / v_r$, where d is the thickness of the metallized layer, is expected to be longer for larger induced reflectivity changes, i.e. thicker metallized layers and increase critically on approaching $T_m$. All of these features have been observed in the experiment, in particular the recovery time increases as $\sim 1 / (T_m - T)$, see figure 4.23 below.

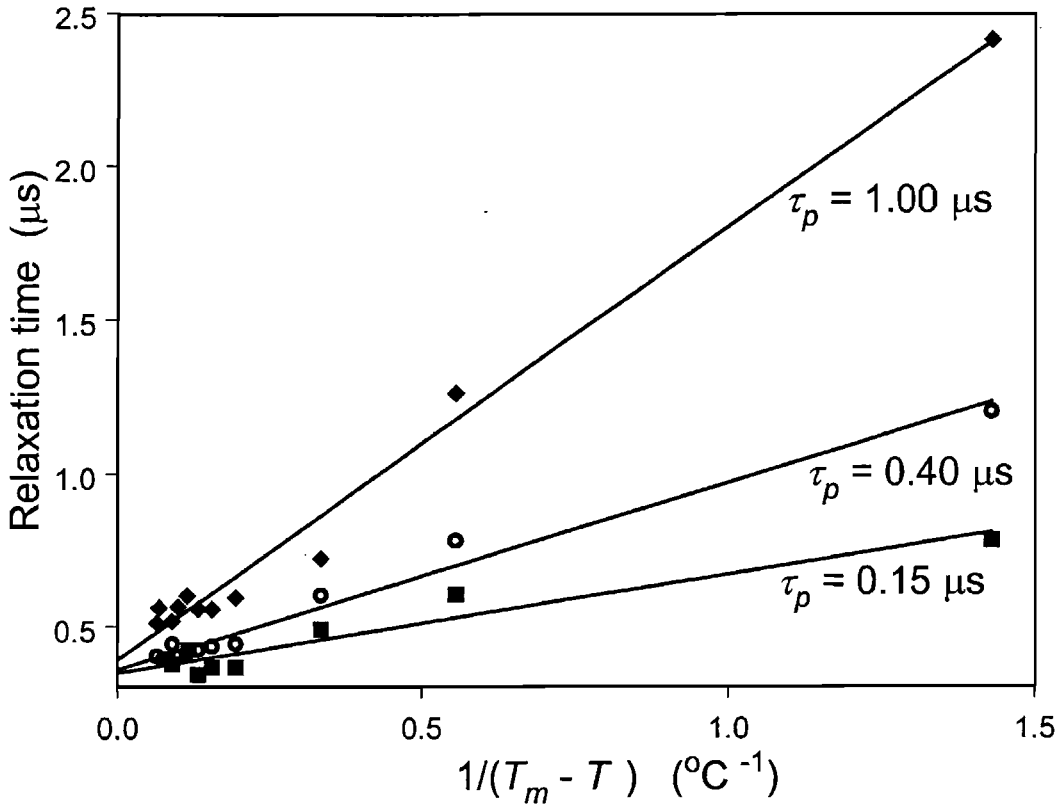


**FIGURE 4.23:** The recovery time, $\tau$, of the pump-induced probe reflectivity change presented as a function of $1/(T_m - T)$, for three pump pulse durations.

## 4.12 An Additional Dynamic Behaviour

The results presented in figures 4.21, 4.22 and 4.23 represent a typical response observed at the silica-gallium interface. However, some areas of the UPLD silica-gallium interface responded differently to optical excitation. Figure 4.24, below, shows the dynamics of the reflectivity change in these areas.

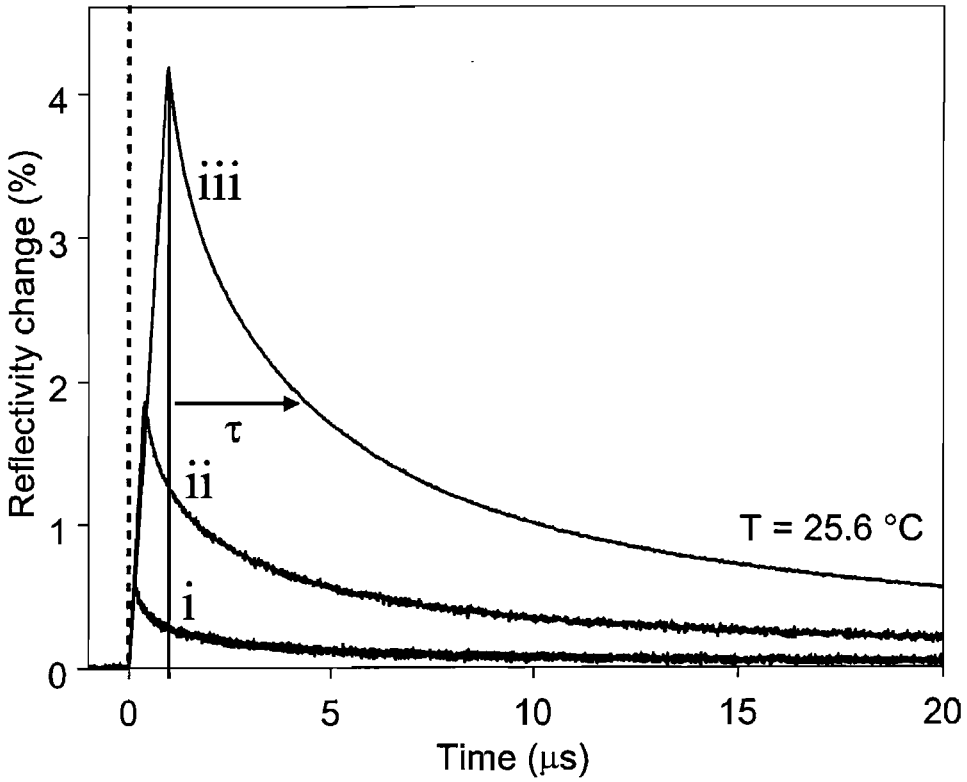


**FIGURE 4.24:** The dynamics of the reflectivity change associated with the additional behaviour observed, plotted for three different pump pulse durations at T = 25.6 $^{0}$C. Curves i, ii and iii correspond to different pump pulse durations, 0.15 μs, 0.40 μs and 1.00 μs, while τ indicates the recovery time.

In these areas under pulsed excitation the reflectivity recovery times exhibit a much longer component. The pump-induced, probe reflectivity change can be seen to disappear before $T_m$, and the maximum light-induced change occurs at a temperature of 25.6 $^{0}$C, see figure 4.25, below.

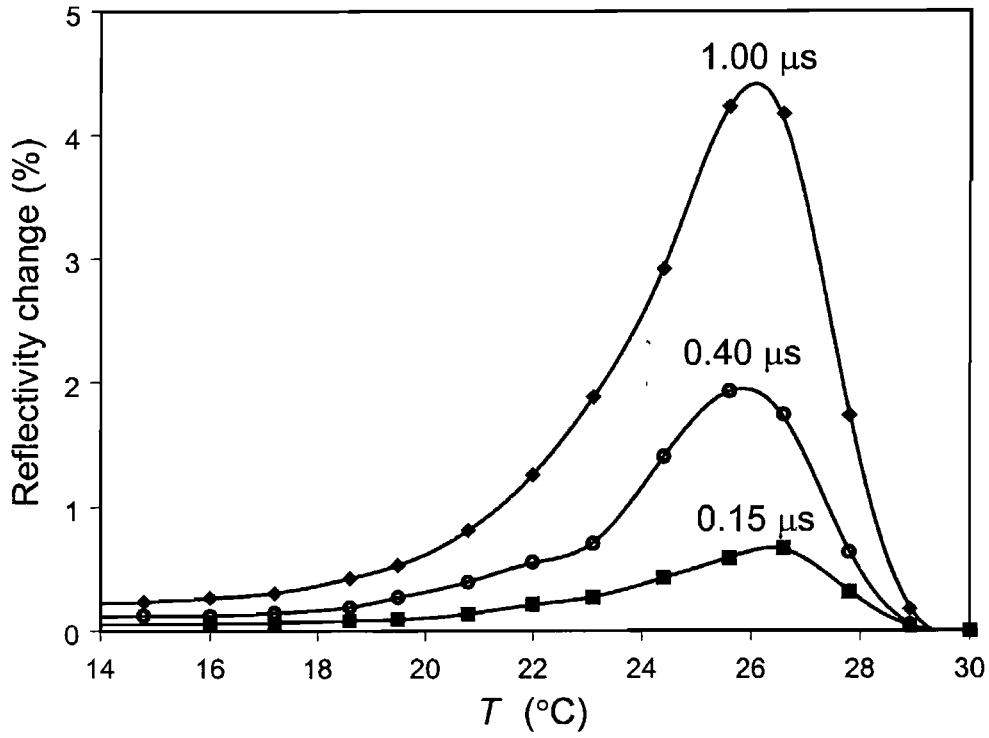


**FIGURE 4.25:** The magnitude of the light-induced change associated with the additional behaviour, plotted for three pump pulse durations used, 0.15 μs, 0.40 μs and 1.00 μs, with increasing temperature.

However, a number of features similar to the previous case can still be seen. Namely, the reflectivity starts to rise immediately after the pump pulse (dashed line) and the effect accumulates with time. Figure 4.26 shows a direct comparison of the transient dynamics of the reflectivity change, with $\tau_p$ = 1 μs, for the two types of response for increasing temperatures.

This type of interface reflectivity behaviour can be described as a predominantly thermal effect. It can be attributed to the poor thermal properties at the areas exhibiting the additional effect. As a result, the gallium film at the interface undergoes melting before the bulk melting temperature is reached. Nevertheless, the non-thermal mechanics described above, still play an important role. This is indicated by the immediate rise of the interface reflectivity after the arrival of the pump pulse.

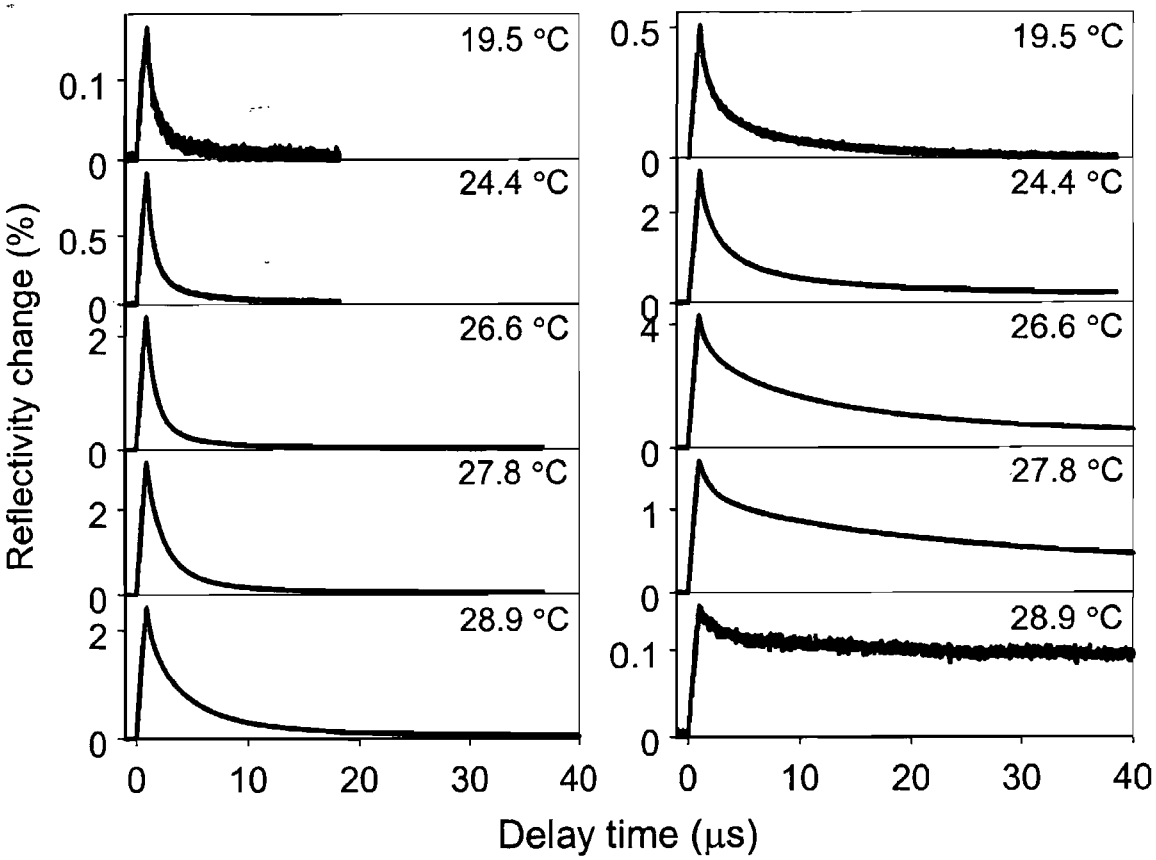


**Figure 4.26:** Direct comparison of the transient dynamics of the pump-induced probe reflectivity change, showing the non-thermal (left) and thermal effect (right). Presented as a function of the sample temperature T, for pump pulse duration $\tau_p$ = 1.00 μs. Note the increasing difference in the reflectivity change dynamics with respect to increasing temperature.

If the effect was a fully thermal one, then there would be a delay before the interface reflectivity starts to rise, equal to the time needed to bring the local temperature above the melting point. When the pump excitation is no longer present the interface reflectivity starts to recover. The reflectivity relaxation times can be seen to increase as temperature approaches the melting temperature, exhibiting, though, much longer recovery dynamics.

The results presented in figures 4.24 and 4.25 suggest that in these areas the growth velocity is no longer the dominant factor in the recovery of interface reflectivity. Under these conditions, both the recrystallisation dynamics and thermal diffusion rate are active while reflectivity recovers. Indeed, due to the poor thermal quality of the interface at these

points, thermal diffusion is unable to remove the heat accumulated locally and the film temperature is maintained higher than the Peltier element temperature keeping reflectivity at higher values and resulting in the long recovery times observed.

## 4.13 Summary of Chapter 4

In summary, the linear reflectivity of the Ultrafast Pulsed Laser Deposition prepared silica-gallium interface was examined in the broadband spectral region, from 400 nm to 1650 nm. The results show a considerable increase of the interface reflectivity on melting across the whole spectral region.

Moreover, the nonlinear optical properties of the same UPLD silica-gallium interface, were investigated in the blue-green spectral region. Single beam, cw measurements, of the interface reflectivity at wavelengths, $\lambda$ = 488, 496, 501 and 514 nm, and with different incident light intensities, were performed. The results show that reflectivity can be modified by as much as 15%, by incident light of 3 kW/cm$^2$ intensity at a wavelength of 514 nm, close to the melting point of gallium, $T_m$ = 29.8 $^0$C. The transient dynamics of the interface reflectivity under pulsed excitation, using a modulated pump at 514 nm and cw probe at 633 nm were also investigated. Two types of reflectivity response, depending on the silica-gallium interface properties, were observed. The mechanisms behind these phenomena were identified as a non-thermal and a predominantly thermal one. In the case of the non-thermal behaviour, the results indicate that reflectivity rises immediately after the pump pulse. In the range of pulse durations used the effect was observed to accumulate with time. The maximum light-induced change occurs just below the melting point at 27.8 $^0$C, and the effect disappears above melting. The predominantly thermal behaviour shows much longer reflectivity recovery times, whereas the maximum light-induced effect occurs earlier at 25.6 $^0$C, and disappears before the melting temperature is reached.

The results presented in this chapter, indicate that the UPLD prepared silica-gallium interface is very sensitive to low power excitation across a very broadband region of the spectrum. Switching between any wavelengths in the 400-1800 nm is possible, and offers an opportunity for a broadband optoelectronics material.

## References


[1] J. Bor. C. Bartholomew, Proceedings of the Physical Society, page 115, vol. 90, 1967

[2] P. Cheyssac, R. Kofman, R. Garrigos, Solid State Communications, page 1583, vol. 44 no. 12, 1982

[3] G. Jezequel, J. Lemonnier, J. Thomas, Journal of Physics F: Metal Physics, Page1613, vol. 7 no. 8, 1977

[4] R. Kofman, P. Cheyssac, J. Richard, Physical Review B, page 5216, vol. 16 no.12, 1977

[5] R. Kofman, P. Cheyssac, R. Garrigos, Journal of Physics F: Metal Physics, page 2345, vol. 9 no. 12, 1979

[6] A. P. Lenham, Proceedings of the Philosophical Society, page 933, vol. 82, 1963

[7] Yu. I. Rapp, R. G. Yarovaya, L. A. Bondarenko, UDC (Fiz. Metal. Metalloved, 32, 4, 728, 1971), 1971

[8] R. Sh. Teshev, A. A. Shebzukhov, Optics and Spectroscopy (USSR), page 693, vol. 65, 1988

[9] K. F. MacDonald, V. A. Fedotov, R. W. Eason, N. I. Zheludev, A. V. Rode, B. Luther-Davies, V. I. Eme'yanov, J. Opt. Soc. Am., page 331, vol 18. 2001.

[10] W. Huisman, J. F. Peters, M. J. Zwaneburg, S. A. de Vries, T. E. Derry, D. Abernathy, J. F. van der Veen, Nature, page 379, vol. 370 no. 27, 1997

[11] Photonics of the nanoscale structural transitions in confined gallium, V. A. Fedotov, University of Southampton Thesis, 2002

[12] F. J. Bermejo, P. R. Fernandez, M. Alvarez, B. Roessli, H. E. Fischer, J. Bossy, Physical Review E., page 3358, vol. 56, 1997

[13] V. Albanis, S. Dhanjal, V. A. Fedotov, K. F. MacDonald, N. I. Zheludev, P. Petropoulos, D. J. Richardson, V. I. Emely'anov Physical Review B., page 165207, vol. 63, 2001

[14] P. Petropoulos, H. S. kim, D. J. Richardson, V. A. Fedotov and N. I. Zheludev, Physical Review B., page 193312, vol. 64, 2001.

# Chapter 5

# Summary and Further Work

## 5.1 Summary

The light-induced reflectivity change of gallium confined at an interface with silica, close to the melting transition of gallium, has been investigated. The behaviour can be attributed to a surface assisted, reversible, light-induced structural phase transition. Using this nonlinear behaviour the following effects were presented and discussed in the thesis:

- Cross-wavelength, all-optical switching between 1.3 and 1.55 μm was achieved for the first time.
- The effect of reflectivity suppression at a silica-gallium interface, due to a light-induced low-reflectivity state was studied in detail for the first time, with cw and pulsed excitation.
- A light-induced reflectivity increase, previously reported at the infrared part of the spectrum, was observed and studied in the blue-green part of the spectrum with cw excitation for the first time.
- The dynamics of the light-induced reflectivity change at a silica-gallium interface were studied in the visible part of the spectrum for the first time, revealing a thermal and non-thermal behaviour.

The results presented in this thesis suggest that the nonlinear behaviour of a silica-gallium interface is strong and it offers potential for the realisation of a number of practical optoelectronics devices. The summary of the chapters follows below.

## 5.2 Summary of Chapter 2

Chapter 2 was a literature review of the physical properties of gallium. The polymorphic characteristics of gallium were presented and the stable crystalline form was identified. The main structural modifications and metastable phases of the material were also discussed. The melting of gallium crystals with the associated surface phenomena was discussed. Finally, the properties of the liquid phase of the material were examined.

## 5.3 Summary of Chapter 3

In chapter 3 the strong nonlinear behaviour of the silica-gallium interface was used to demonstrate an all-optical switch. Cross-wavelength modulation between signals at 1.3 μm and 1.5 μm was achieved, with modulation of up to 40 % in reflected light intensity and sub-microsecond switching times. It was argued that the nonlinear behaviour can be attributed to a light-induced metallization of gallium at the interface with silica.

An additional light-induced effect was also examined in chapter 3. The reflectivity of a silica-gallium interface was observed to be reduced in a reversible manner when the interface was excited by a few milliwatts of laser power. This reflectivity drop was seen with both cw and pulsed excitation. Under cw excitation the reflectivity decrease was observed to exhibit threshold behaviour, with saturation occuring at higher light intensities. With pulsed excitation the low reflectivity state was observed to be dynamically light-induced with microsecond response times. This low reflectivity state was attributed to a light-induced structuring at the interface. Some potential mechanisms were presented and discussed.

The nonlinearity at a silica-gallium interface offers potential for the development of a wide range of practical nonlinear optical devices. The dynamic, reversible light-induced reflectivity suppression can be potentially used in power-limiting applications in optoelectronic applications.

## 5.4 Summary of Chapter 4

In chapter 4, the linear and nonlinear optical properties of gallium confined at the interface with silica were examined across the melting transition. The reflectivity of a silica-gallium interface over a broad wavelength range was estimated theoretically, for the solid and liquid states, using Fresnel formulas and previously published data for the optical properties of gallium single crystals. The linear reflectivity of two silica-gallium interfaces with different degrees of confinement was measured across the melting transition of gallium as a function of wavelength. A considerable increase in interface reflectivity across the whole spectral range examined was observed. The measured values were compared with the estimated reflectivity values.

The nonlinear optical properties of a silica-gallium interface prepared by Ultrafast Pulsed Laser Deposition, in which gallium has a high degree of confinement, were investigated in the blue-green spectral region. The light induced change of the interface reflectivity was examined with single beam, cw, measurements at various wavelengths as a function of intensity and temperature. Reflectivity was modified by as much as 15% at a wavelength of 514 nm, close to the melting point of gallium, $T_m = 29.8\ ^0C$.

The light-induced reflectivity change of the UPLD prepared interface was examined with pulsed excitation in the visible part of the spectrum for the first time. The transient dynamics were investigated with a pump-probe setup. Two types of reflectivity response were observed, which depended on the properties of the interface. The mechanisms behind these phenomena were identified as a non-thermal and a predominantly thermal one. The non-thermal behaviour was attributed to a reversible, light-induced, surface-assisted metallization of the silica-gallium interface. The maximum effect was observed to occur just below the melting point at 27.8 $^0C$, and the effect disappeared above melting. In the case of the predominantly thermal behaviour it was argued that the effect was due to the poor local thermal quality of the interface. The maximum change of reflectivity was observed to occur earlier at 25.6 $^0C$, and the effect disappeared before the melting temperature was reached.

## 5.5 Further Work

By confining gallium at an interface with silica and bringing the material up to its melting transition it was shown that the interface becomes sensitive to a broad wavelength range of optical excitation. A strong nonlinear behaviour is developed, manifested as a surface-assisted, reversible light-induced reflectivity change. If this enhanced nonlinearity is to be used for practical applications where the size of the device is critical, the dimensions of the underlying nonlinear structures have to be reduced. An approach to reducing the size and increase the confinement of a material is nanostructuring.

Indeed in the case of gallium, nanoparticles are the ultimate confined geometry [1]. Confining gallium in the form of nanoparticles leads to modifications of gallium's properties and phase diagram, facilitating the reversibility of its phase transition underpinning the optical nonlinearity and offering local field enhancement effects which could improve the characteristics of gallium-based all-optical devices.

A technique for depositing gallium nanoparticles at the tip of optical fibres has been developed, and initial results have suggested that the mechanism behind the nonlinearity in gallium nanoparticles is similar but not the same as with the case of gallium films [1]. Research in ongoing and it is now being directed towards photonics of structural transformations in single gallium nanoparticles.

However, despite the exciting results through the manifestation of a strong nonlinearity at the silica-gallium interface, there are still questions regarding the microscopic properties of the interface, and the way they govern the observed nonlinear response. The lack of a clear understanding of the features of the silica-gallium interface at the atomic level, close to the structural melting transition of gallium, opens a very wide area of research in the structural characteristics. Using available materials characterisation techniques, such as X-ray diffraction and neutron scattering, the exact crystal structure and phase at the silica interface, as well as the grain size and the formation of defects and dislocations on melting, can be investigated. As a result, it might be possible to engineer a silica-gallium interface with tailored properties that could further enhance the ability of the interface to manifest an even stronger nonlinear response.

## References

[1] N. I. Zheludev, Nonlinear Optics at the Nano-Scale, Contemporary Physics, page 365, vol. 43, no. 5, 2002

# Appendix A

# Polynomial Approximations and Reflectivity Values

## A-1 Polynomial Approximations

The dielectric data for the α-gallium phase for light polarised along the three crystallographic directions taken from [1], see Chapter 4 figure 1, were fitted with polynomials. To account for the complex spectral response of the dielectric data in figure 1, the polynomial approximations were fitted to specific wavelength regions.

The polynomial approximations as a function of wavelength for the complex dielectric properties of α-gallium, for the three crystallographic directions are given below.

### A-1.1 Complex dielectric constants for light polarised along the a-axis, [100] crystallographic direction.

Real part, $\varepsilon_1$, in the range 450 nm to 618 nm

$$311.14\,x^3 - 328.25\,x^2 + 66.91\,x + 2.018$$

Real part, $\varepsilon_1$, in the range 618 nm to 1650 nm

$$-87\,x^4 + 356.55\,x^3 - 517.72\,x^2 + 319.03\,x - 79.69$$

Imaginary part, $\varepsilon_2$, in the range 450 nm to 618 nm

$$-7877.1\ x^4 + 13643.12\ x^3 - 8709.22\ x^2 + 2322.18\ x - 217.62$$

Imaginary part, $\varepsilon_2$, in the range 619 nm to 669 nm

$$313.68\ x^6 - 1885.59\ x^5 + 451.82\ x^4 - 5503.3\ x^3 + 3569.62\ x^2 - 1125.95\ x + 134.81$$

Imaginary part, $\varepsilon_2$, in the range 670 nm to 1650 nm

$$151.24\ x^5 - 856.54\ x^4 + 1860.32\ x^3 - 1995.88\ x^2 + 1027.25\ x - 206.07$$

## A-1.2 Complex dielectric constants for light polarised along the b-axis, [010] crystallographic direction.

Real part, $\varepsilon_1$, in the range 450 nm to 760 nm

$$4870.2\ x^4 - 11990.08\ x^3 + 10893\ x^2 - 4341.68\ x + 636.53$$

Real part, $\varepsilon_2$, in the range 761 nm to 1650 nm

$$-4.27\ x^3 + 4.59\ x^2 - 27.22\ x + 9.76$$

Imaginary part, $\varepsilon_2$, in the range 450 nm to 760 nm

$$-47308.4\ x5 + 144457.92\ x4 - 174477.99\ x3 + 104110.49\ x2 - 30659.13\ x - 3565.98$$

Imaginary part, $\varepsilon_2$, in the range 761 nm to 1650 nm

$$6.6\ x3 - 20.27\ x2 + 37.93\ x - 13.18$$

## A-1.3 Complex dielectric constants for light polarised along the c-axis, [001] crystallographic direction.

Real part, $\varepsilon_1$, in the range 450 nm to 706 nm

$$-595.2\ x^3 + 1104.13\ x^2 - 678.54\ x + 132.87$$

Real part, $\varepsilon_1$, in the range 706 nm to 1650 nm

$$18.69\ x^4 - 119.04\ x^3 + 261.24\ x^2 - 226.65\ x + 62.13$$

Imaginary part, $\varepsilon_2$, in the range 450 nm to 706 nm

$$-36842.67\ x^5 + 112796.67\ x^4 - 137122.04\ x^3 + 82614.84\ x^2 - 24608.84\ x + 2896.5$$

Imaginary part, $\varepsilon_2$, in the range 707 nm to 1650 nm

$$443.9\ x6 - 3457.28\ x5 + 11023.28\ x4 - 18369.78\ x3 + 16807.06\ x2 - 7954.9\ x + 1525.94$$

## A-1.4 Polynomial Approximations for the Optical Constants of Liquid Gallium

The optical constants of the liquid phase of gallium were found in [2] and fitted with polynomial approximations. The fitted polynomials are shown below.

Real part, **n**, of the complex refractive index of liquid gallium in the range 450 nm to 1650 nm

$$0.397\ x^2 + 3.23\ x - 0.66$$

Imaginary part, $\kappa$, of the complex refractive index of liquid gallium in the range 450 nm to 1650 nm

$$1.34\,x^3 - 6.46\,x^2 + 14.944\,x + 0.06$$

## A-2 Reflectivity Values Table

Reflectivity values for light polarised along the a-axis, [100] crystallographic direction.

| Wavelength | ε1 | ε2 | κ | n | R calculated vacuum-ga | R calculated glass-ga |
|---|---|---|---|---|---|---|
| 0.412 | -4.372119 | 1.9293 | 2.139041 | 0.450973 | 0.729989 | 0.680383 |
| 0.449 | -5.948904 | 2.165962 | 2.477887 | 0.437058 | 0.786932 | 0.738456 |
| 0.494 | -7.522173 | 3.904786 | 2.828202 | 0.69033 | 0.74564 | 0.681384 |
| 0.549 | -8.697217 | 7.322537 | 3.167532 | 1.155874 | 0.685071 | 0.60106 |
| 0.618 | -8.5581 | 9.604704 | 3.272801 | 1.467353 | 0.650611 | 0.556736 |
| 0.706 | -8.650798 | 12.65598 | 3.462718 | 1.827463 | 0.634232 | 0.533171 |
| 0.824 | -8.955219 | 15.77277 | 3.680551 | 2.142718 | 0.634085 | 0.529625 |
| 0.988 | -8.888587 | 20.00196 | 3.922793 | 2.549454 | 0.635622 | 0.528227 |
| 1.236 | -6.083873 | 25.57065 | 4.022953 | 3.178094 | 0.622112 | 0.509155 |
| 1.648 | -5.880102 | 21.79362 | 3.771806 | 2.889016 | 0.60628 | 0.492408 |

Reflectivity values for light polarised along the b-axis, [010] crystallographic direction.

| Wavelength | ε1 | ε2 | κ | n | R calculated vacuum-ga | R calculated glass-ga |
|---|---|---|---|---|---|---|
| 0.449 | -4.231493 | 3.144272 | 2.179828 | 0.72122 | 0.626032 | 0.556485 |
| 0.494 | -5.385053 | 4.292413 | 2.477048 | 0.866437 | 0.639711 | 0.561485 |
| 0.549 | -5.455098 | 5.935224 | 2.599656 | 1.14154 | 0.597497 | 0.507138 |
| 0.618 | -5.936955 | 5.928996 | 2.676514 | 1.107597 | 0.618257 | 0.530164 |
| 0.706 | -8.672094 | 5.817795 | 3.091512 | 0.94093 | 0.717537 | 0.642007 |
| 0.824 | -11.94174 | 8.00402 | 3.627516 | 1.103237 | 0.749015 | 0.674405 |
| 0.988 | -16.77098 | 10.87364 | 4.287104 | 1.26818 | 0.784359 | 0.714454 |
| 1.236 | -24.93455 | 15.19741 | 5.202665 | 1.460541 | 0.823617 | 0.761932 |
| 1.648 | -41.74427 | 23.81761 | 6.700944 | 1.777183 | 0.864893 | 0.814428 |

Reflectivity values for light polarised along the c-axis, [001] crystallographic direction.

| Wavelength | ε1 | ε2 | κ | n | R calculated vacuum-ga | R calculated glass-ga |
|---|---|---|---|---|---|---|
| 0.449 | -3.526567 | 2.296392 | 1.966584 | 0.583853 | 0.633721 | 0.576689 |
| 0.494 | -5.128904 | 3.70007 | 2.393027 | 0.773094 | 0.651384 | 0.579368 |
| 0.549 | -5.898811 | 6.275014 | 2.693614 | 1.164794 | 0.609846 | 0.520159 |
| 0.618 | -5.876454 | 8.049076 | 2.814464 | 1.429948 | 0.586297 | 0.488014 |
| 0.706 | -4.919843 | 9.98553 | 2.832983 | 1.76237 | 0.54974 | 0.442242 |
| 0.824 | -5.237712 | 12.76116 | 3.084797 | 2.068395 | 0.562962 | 0.451478 |
| 0.988 | -3.789222 | 18.14776 | 3.341283 | 2.715686 | 0.564977 | 0.447008 |
| 1.236 | -0.069513 | 20.30219 | 3.191538 | 3.180629 | 0.540099 | 0.416049 |
| 1.648 | 3.173118 | 20.83822 | 2.992098 | 3.482208 | 0.520404 | 0.392397 |

Reflectivity values for liquid gallium.

| Wavelength | n | κ | Reflectivity vacuum-ga | R calculated glass-ga |
|---|---|---|---|---|
| 0.45 | 0.873893 | 5.596958 | 0.8996604 | 0.86076245 |
| 0.5 | 1.05425 | 6.0825 | 0.8976872 | 0.85767121 |
| 0.55 | 1.236593 | 6.545793 | 0.896627 | 0.85591389 |
| 0.6 | 1.42092 | 6.98784 | 0.896076 | 0.85491619 |
| 0.65 | 1.607233 | 7.409648 | 0.8958043 | 0.85434864 |
| 0.7 | 1.79553 | 7.81222 | 0.8956781 | 0.85401792 |
| 0.75 | 1.985813 | 8.196563 | 0.8956191 | 0.85380929 |
| 0.8 | 2.17808 | 8.56368 | 0.8955818 | 0.85365484 |
| 0.85 | 2.372333 | 8.914578 | 0.8955406 | 0.85351531 |
| 0.9 | 2.56857 | 9.25026 | 0.8954825 | 0.85336933 |
| 0.95 | 2.766793 | 9.571733 | 0.8954021 | 0.85320697 |
| 1 | 2.967 | 9.88 | 0.8952991 | 0.85302566 |
| 1.05 | 3.169193 | 10.17607 | 0.8951766 | 0.85282766 |
| 1.1 | 3.37337 | 10.46094 | 0.8950394 | 0.85261837 |
| 1.15 | 3.579533 | 10.73562 | 0.8948941 | 0.85240524 |
| 1.2 | 3.78768 | 11.00112 | 0.8947476 | 0.85219704 |
| 1.25 | 3.997813 | 11.25844 | 0.8946076 | 0.85200333 |
| 1.3 | 4.20993 | 11.50858 | 0.8944819 | 0.85183409 |
| 1.35 | 4.424033 | 11.75255 | 0.8943783 | 0.85169947 |
| 1.4 | 4.64012 | 11.99136 | 0.8943047 | 0.85160957 |
| 1.45 | 4.858193 | 12.22601 | 0.8942686 | 0.85157427 |
| 1.5 | 5.07825 | 12.4575 | 0.8942771 | 0.85160314 |
| 1.55 | 5.300293 | 12.68684 | 0.8943374 | 0.85170528 |
| 1.6 | 5.52432 | 12.91504 | 0.8944557 | 0.85188927 |
| 1.65 | 5.750333 | 13.1431 | 0.8946382 | 0.85216304 |

## References

[1] R. Kofman, P. Cheyssac, J. Richard, Physical Review B, page 5216, vol. 16 no.12, 1977

[2] R. Sh. Teshev, A. A. Shebzukov, Optics and Spectroscopy [USSR], page 693, vol. 65, 1988

# Appendix B

# Refereed Papers Published and Conference Publications

## B-1 Published Papers

Reprints of the papers listed below are included at the back cover of the thesis

1. V. Albanis, S. Dhanjal, N.I. Zheludev, P. Petropoulos, D.J. Richardson, **Cross-wavelength all-optical switching using nonlinearity of liquefying gallium**, Optics Express, vol. 5, no. 8, 157-162, 1999.

2. P.J.Bennett, V. Albanis, Y.P. Svirko, N.I. Zheludev, **Femtosecond cubic optical nonlinearity of thin nickel films**, Optics Letters, vol. 24, no. 19, 1373-1375, 1999.

3. V. Albanis, R.T. Bratfalean, S. Dhanjal, V.I. Emelyanov, P. Petropoulos, D.J. Richardson, N.I. Zheludev, **The light-induced specular reflectivity suppression at a gallium/silica interface**, Optics Letters, vol. 25, no 21, 1594-1596, 2000.

4. V. Albanis, S. Dhanjal, K. MacDonald, P. Petropoulos, H.L. Offerhaus, D.J. Richardson, A. Rode, N.I. Zheludev, **The light induced structural phase transition confining gallium and its photonic applications**, Journal of Luminescence, vol. 87-9, 646-648, 2000.

5. V. Albanis, S. Dhanjal, V. A. Fedotov, K. F. MacDonald, N. I. Zheludev, D. J. Richardson, V. I. Emelyanov, **Nanosecond dynamics of a gallium mirror's light-induced reflectivity change**, Physical Review B-Condensed Matter and Materials Physics, vol. 63, no. 16, 165207-165214, 2001

6. V. Albanis, V. A. Fedotov, N. I. Zheludev, **Light-induced reflectivity switching in gallium-on-silica films in the blue-green spectral region**, Optics Communications, vol. 214, 271-276, 2002.

## B-2 Major Conferences Publications

1. V. Albanis, P. Petropoulos, S. Dhanjal, D. J. Richardson, N. I. Zheludev, **Confining metallic gallium - new material structure for optical data processing at milliwatt power level**, MRS Fall Meeting Boston, USA 30 November - 4 December 1998 T1.6

2. V. Albanis, S. Dhanjal, P. Petropoulos, D. J. Richardson, N. I. Zheludev, V. I. Emelyanov, **Light-induced structural phase transition in confining gallium and associated gigantic optical nonlinearity**, MRS Fall Meeting Boston, USA 30 November - 4 December 1998 W7.19

3. P.J. Bennett, V. Albanis, Yu. P. Svirko, N. I. Zheludev, **Ultrafast cubic optical nonlinearity in semitransparent nickel films: bulk versus surface contributions**, CLEO 1999, Baltimore, 23-28 May 1999, QThG16

4. V. Albanis, S. Dhanjal, V. I. Emelyanov, P. Petropoulos, D. J. Richardson, N. I. Zheludev, **Dynamics of the light-induced structural phase transition in confining gallium and associated gigantic optical nonlinearity**, QELS '99 Baltimore, 23-28 May 1999 (Invited) QME3

5. V. Albanis, B. Luther-Davies, K. MacDonald, A. V. Rode, and N. I. Zheludev, **Gigantic optical nonlinearity of gallium films deposited by ultrafast laser ablation**, Proceedings ACOFT'99, 24$^{th}$ Australian Conference on Optical Fibre Technology, IREE Society, Sydney, Australia, July 1999

6. V. Albanis, B. Luther-Davies, K. MacDonald, A. V. Rode, and N. I. Zheludev, **Gigantic optical nonlinearity of gallium films deposited by ultrafast laser ablation**, International Conference on Luminescence and Optical Spectroscopy of Condensed Matter, Osaka, Japan, 23-27 August 1999.

7. V. Albanis, V.A. Fedotov, K.F. MacDonald, V.I. Emelyanov, N.I. Zheludev, R.J. Knize, B.V. Zhdanov, A.V. Rode, **Gigantic broadband optical nonlinearity in gallium films deposited by ultrafast laser ablation**, CLEO Europe 2000, 10-15 September 2000, Nice, France.

1. is reprinted from Optics Express, vol. 5, no. 8, 157-162, 1999, with permission from Optical Society of America.
2. is reprinted from Optics Letters, vol. 24, no. 19, 1373-1375, 1999, with permission from Optical Society of America.
3. is reprinted from Optics Letters, vol. 25, no 21, 1594-1596, 2000, with permission from Optical Society of America
4. is reprinted from the Journal of Luminescence, vol. 87-9, 646-648, 2000, with permission from Elsevier Science.
5. is reprinted from Physical Review B-Condensed Matter and Materials Physics, vol. 63, no. 16, 165207-165214, 2001, with permission from the American Physical Society.
6. is reprinted from Optics Communications, vol. 214, 271-276, 2002, with permission from Elsevier Science.

# Cross-wavelength all-optical switching using nonlinearity of liquefying gallium

**V.Albanis, S. Dhanjal and N.I. Zheludev**

*Department of Physics and Astronomy, University of Southampton*
*Highfield, Southampton SO17 1BJ, UK*
*va@phys.soton.ac.uk, sd@phys.soton.ac.uk, n.i.zheludev@soton.ac.uk*

**P. Petropoulos and D.J. Richardson**

*Optoelectronics Research Centre, University of Southampton*
*Highfield, Southampton SO17 1BJ, UK*
*pp@orc.soton.ac.uk, djr@orc.soton.ac.uk*

**Abstract:** The gallium/silica interface optical nonlinearity associated with a light-induced structural phase transition from α-gallium to a more reflective, more metallic phase shows an exceptionally broadband spectral response. It allows 40% deep nanosecond/microsecond cross-wavelength intensity modulation between signals at 1.3 and 1.55μm.

© 1999 Optical Society of America

**OCIS codes:** (060.1810) Couplers, switches and multiplexers; (190.1450) Bistability; (240.4350) Nonlinear optics at surfaces

## References and links

1. P. J. Bennett, S. Dhanjal, P. Petropoulos, D. J. Richardson and N. I. Zheludev, "A photonic switch based on a gigantic, reversible optical nonlinearity of liquefying gallium," App. Phys. Lett. **73**, 1787-1789 (1998).
2. H. G. Von Schnering and R. Nesper, "Alpha-gallium - an alternative to the boron structure," Acta. Chem. Scan. **45**, 870-872 (1991).
3. P. Petropoulos, H. L. Offerhaus, D .J. Richardson, S. Dhanjal and N. I. Zheludev, "Passive Q-switching of fiber lasers using a broadband liquefying gallium mirror," App. Phys. Lett. **74**, 3619-3621 (1999).
4. M. Bernasconi, G. L. Chiarotti and E. Tosatti "Theory of the structural and electronic-properties of alpha-ga(001) and (010) surfaces," Phys. Rev B **52**, 9999-10013 (1995).
5. R. Trittibach, Ch. Grutter, and J. H. Bilgram "Surface melting of gallium crystals," Phys. Rev. B **50**, 2529-2539 (1994).

Recent discovery of a remarkably strong optical nonlinearity at a gallium-dielectric interface has already resulted in the demonstration of a fully-fiberized all-optical gate based on a nonlinear gallium mirror [1]. The mirror was manufactured on the tip of a single-mode fiber. In the gate the intensity of the light in the signal channel was modulated by the intensity of light in the control channel, both at wavelengths of about 1.55μm. The gate performance was characterized with a continuously modulated pump and modulation efficiency of about 30% with several hundred kilohertz bandwidth has been achieved.

In this paper we report that a nonlinear gallium mirror can be used for controlling light with light in pulse regime with sub-microsecond response time. We also demonstrate that the gallium/silica interface nonlinearity shows an exceptionally broadband spectral response. This broadband characteristic of the mirror has allowed us to demonstrate cross-wavelength all-optical gating between signals at wavelengths of 1.3 and 1.55μm. The gallium nonlinearity is associated with a

#11936 - $15.00 US
Received July 20, 1999; Revised September 22, 1999
(C) 1999 OSA

light-induced structural phase transition in the common form of α-gallium in solid phase. It is believed that in the nanosecond-microsecond regime of optical excitation, the mechanism of the phase transition is predominantly non-thermal. Optical excitation is highly localized and destabilizes covalent bonding within the crystalline structure of alpha-gallium thus provoking a surface assisted transition to a more reflective, more metallic metastable phase. Such excitation of bonding-anti-bonding transitions in α-gallium is associated with a broad absorption band spanning from 0.8 to 4 eV [2]. This indicates that the effect may be induced by light in the visible and infrared parts of the spectrum. The structural phase transition drives a considerable change in the electronic, and in particular, in the optical properties of the material, also across a very broad spectral range. Conventional α-gallium has a relatively low reflectivity, typical to a semi-metal, which increases dramatically when the more metallic phase is induced at the interface by light stimulation. Although the exact nature of the light-induced metastable phase is not known yet, our data shows that its optical properties are very close to those of a free electron metal. Since on melting gallium acquires nearly free electron metal characteristics, the reflectivity change associated with the light-induced phase transition may be well illustrated by the change of gallium reflectivity on melting. Such reflectivity change is presented on Fig.1, which shows that a considerable effect across visible and infrared parts of the spectrum.

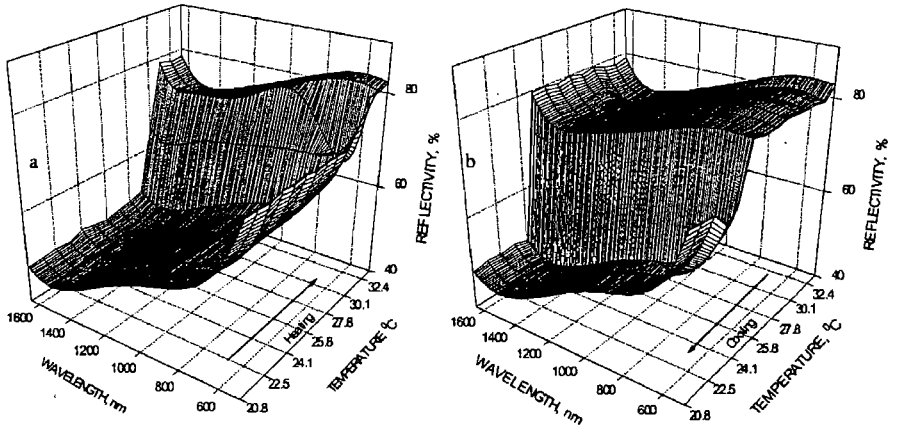


Fig. 1 Reflectivity of a gallium-glass interface of unpolarized light as a function of temperature, near the melting point, illustrating a strong change of reflectivity, overcooling and a reflectivity hysteresis. A considerable reflectivity change is seen across visible and near infra-red parts of the spectrum. Graphs a) and b) show the reflectivity change with increase and decrease of the temperature.

Therefore the gallium nonlinearity promises to be exceptionally broadband, allowing cross-wavelength optical switching with the control and signal wavelengths to be virtually anywhere in the visible and near-infrared parts of the spectrum down to at least 1.7μm. The broadband properties of the liquefying gallium mirror nonlinearity have been recently demonstrated when two fiber laser, operating at wavelengths of 1550 and 1030nm respectively have been Q-switched using the same type of gallium mirror [3]. Here we demonstrate that gallium nonlinearity may be used for a cross-wavelength intensity modulation.

The cross-wavelength characteristics of gallium nonlinearity response of liquefying gallium were characterized in pump-probe experiments using the optical switch set-up shown in Fig.2. The fiberised gallium mirror was formed by immersing a freshly cleaved end of a single-mode silica optical fiber into a small bead of initially molten gallium of 5N purity. The sample temperature was controlled by a miniature Peltier heat pump to a precision of 0.01°C at temperatures around the melting point of gallium (30°C). The control source A was an amplified, directly modulated DFB

#11936 - $15.00 US
Received July 20, 1999; Revised September 22, 1999
(C) 1999 OSA

diode laser operating at $\lambda = 1.550\mu m$ (1 MHZ linewidth.). The probe source B was a continuous-wave diode laser operating at $\lambda = 1.3\mu m$. The pump and probe beams were coupled onto and off the gallium mirror using a wavelength division multiplexer WDM. The fibre mode-field diameter was ~12 μm. The peak power of the pump pulses incident on the mirror could be varied between 0 and 90mW, while the power of the continuous wave probe beam was 60 μW at the mirror surface. The probe beam was detected at the switch output with a 125 MHz 3 dB bandwidth InGaAs detector.

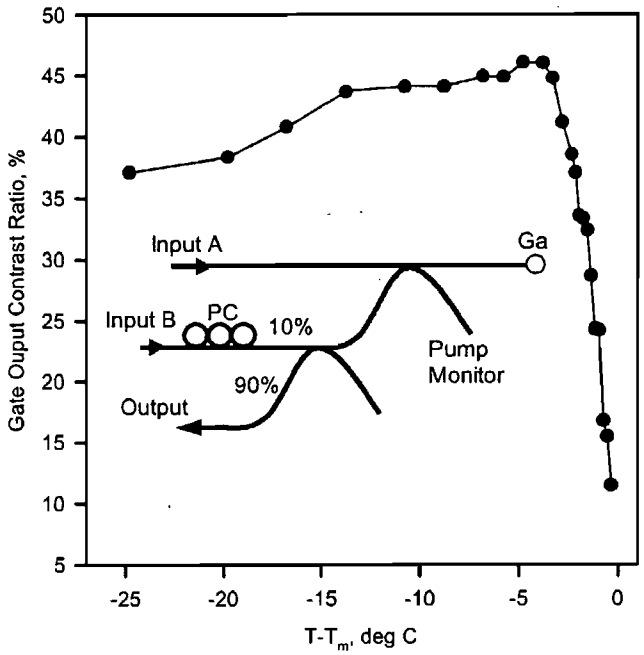


Fig. 2The performance of the cross-wavelength all optical gate. The gate's output contrast ratio is presented as function of the gallium bead temperature, T, $T_m = 30°C$. The inset shows a schematic of the fiberized gate. Input A is the control channel, Input B is the signal channel and PC is a polarization controller.

We investigated the dynamic properties of the mirror at temperatures in the vicinity of the melting point of gallium (~30°C) using control pulses of 100ns duration and 10kHz repetition rate. The control pulse at $\lambda = 1.55$ μm induces the mirror reflectivity increase, this leads to a corresponding increase of the output signal at $\lambda = 1.3\mu m$. After the control beam excitation is withdrawn, the induced reflectivity change rapidly returns to its original level (see inset on Fig.3). We observed that the reflectivity recovery time depends on the gallium bead temperature and increases with the temperature approaching the melting point of bulk gallium (see fig.3).

#11936 - $15.00 US
(C) 1999 OSA
Received July 20, 1999; Revised September 22, 1999

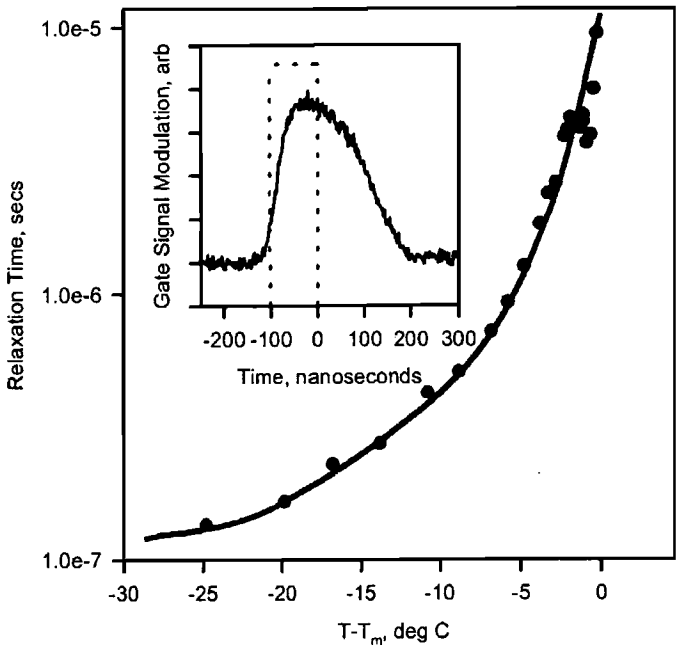


Fig. 3 Gate switch-off time, $\tau$, as a function of temperature, T. A typical gate response function with a 100ns control pulse (dashed line) is presented in the inset for $T-T_m = -25°C$.

As the temperature T is increased towards the melting point $T_m$ the induced nonlinear response rises steadily up to a level of ~40% as shown in Fig.2. Here percentage of the probe beam output intensity increase is presented. The pulse response on the control beam stimulation within this temperature region is highly stable and reproducible. At higher temperatures, just about 4°C below the bulk melting point, the induced reflectivity falls rapidly. The induced modulation becomes undetectable once the metal melts. On subsequent recooling the gate performance is fully restored. In Fig.4 we plot the intensity dependence of the induced change in reflected probe power for a number of temperatures in the proximity of the melting point. Once again the gallium bead was in the solid phase. We observed up to ~40% changes in the reflected probe intensity induced by the control beam powers of only a few tens of mW.

#11936 - $15.00 US
(C) 1999 OSA
Received July 20, 1999; Revised September 22, 1999

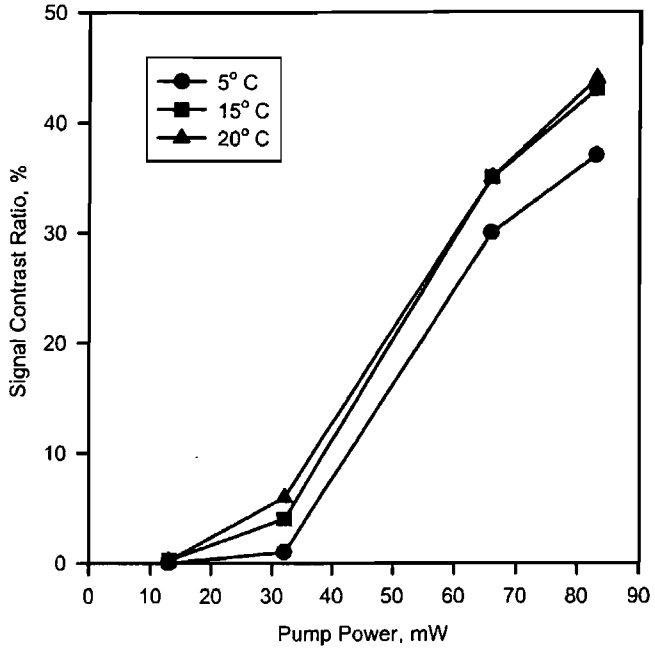


Fig. 4 The signal contrast ratio as a function of the control beam peak power for various temperatures.

The huge optical nonlinearity in gallium relies on the coexistence of the molecular and metallic properties of α-Ga. α-Ga is a structure which is built up from polyhedral fragments which can be described as a 'molecular metallic crystal' where some of the bonds are strong covalent bonds, with the rest being weaker metallic-type bonding [3,4]. Gallium is also one of only a few metals showing the surface melting effect at normal conditions [5]. The following working model of the light-induced structural phase transition corroborates well with our experimental data: light stimulates a bonding-antibonding transition in α-Ga and the covalent bonding of the crystalline structure becomes unstable provoking a phase transition from α-Ga to a metastable phase with essentially free electron characteristics. As the system is very close to surface melting we interpret our results as the silica interface assisting the creation of a metastable layer. The layer thickness critically depends on the interface temperature and propagates with a high velocity appropriate to non-equilibrium epitaxial growth. The layer thickness also increases with the level of light excitation because the energy difference between α-Ga and the metastable phase reduces; reflectivity of the interface increases with layer thickness. The effect saturates and rolls-off as the thickness reaches the optical skin depth. When the excitation is withdrawn, the metastable layer re-crystallizes back to the α-Ga phase. The crystallization front moves towards the gallium/silica interface. The recovery time increases as gallium approaches the melting point as the velocity of the thermodynamic epitaxial growth decreses as $T_m$-T.

In conclusion, we have demonstrated that a nonlinear mirror formed at the gallium-silica interface allows for sub-microsecond cross-wavelength switching with up to 40% [40%] modulation in reflected light intensity. This has been observed in a compact, fiberized switch. We consider this nonlinearity to offer tremendous potential for the development of a wide range of truly practical nonlinear optical devices compatible with existing waveguide technology.

#11936 - $15.00 US
Received July 20, 1999; Revised September 22, 1999
(C) 1999 OSA

**Acknowledgements**

The authors are grateful to Goodfellow Cambridge Ltd for the free supply of high-quality gallium samples and the Royal Society and the EPSRC for the financial support.

#11936 - $15.00 US
Received July 20, 1999; Revised September 22, 1999
(C) 1999 OSA

# Femtosecond cubic optical nonlinearity of thin nickel films

**P. J. Bennett, V. Albanis, Yu. P. Svirko, and N. I. Zheludev**

*Department of Physics and Astronomy, University of Southampton, Southampton SO17 1BJ, UK*

Received July 23, 1999

Transient pump–probe measurements of circular anisotropy in nickel films induced by 38-fs optical pulses show an instantaneous response that is related to the optical orientation of the spins of free electrons. Measurements in a sample of variable thickness, performed in both transmission and reflection, revealed that the surface significantly influences the degenerate cubic optical nonlinearity of the nickel films to a depth of approximately 4–5 nm into the bulk. © 1999 Optical Society of America

*OCIS codes:* 190.7110, 190.4710, 190.4350, 160.3900, 320.2250, 320.7110.

It was recently established that the cubic optical nonlinearity of metals associated with the optical orientation of spins is one of several mechanisms[1–6] that play a very important role in the femtosecond optical response of bulk metals,[7–9] in ferromagnetics in particular.[10–13] The study of spin-related nonlinearity is of fundamental interest and practical importance, in particular for optical data storage. Here we report the results of a study of thin, semitransparent films of nickel of various thicknesses, using femtosecond time-resolved polarimetry. For what is believed to be the first time, we have combined transmission and reflection measurements and studied glass and air interfaces of nickel. We find that the ultrafast component of light-induced circular dichroism is insensitive to the optical anisotropy due to spontaneous magnetization of the film.

We identify the importance of the surface contribution to the film nonlinearity and also observe that not only the magnitude of the nonlinearity in nickel but also its sign can be different, depending on the nature of the interface. We also show that the nonlinearity is very fast and put an upper limit of ~40 fs on its relaxation time.

The nonlinearity of semitransparent nickel films of variable thickness was studied by use of an ultrafast polarization-sensitive pump–probe polarimeter with a Ti:sapphire laser with a central wavelength at $\lambda =$ 810 nm, an average power at the sample of ~50 mW, a pulse duration of ~38 fs, and a repetition rate of 82 MHz. A circularly polarized pump pulse induced circular birefringence and dichroism in the sample, which was then probed by a weaker linearly polarized pulse at the same wavelength. The probe propagated at a small angle to the pump, and both the probe and the pump were focused to a spot size of 130 $\mu m^2$. Using semitransparent nickel films deposited upon a glass substrate, we performed experiments in four different configurations, two reflective and two transmissive, from the air and glass substrate sides (see Figs. 1 and 2). In all cases the pump (dashed lines) was initially circularly polarized. The probe (solid lines) was initially linearly polarized, and its polarization azimuth was monitored after interaction with the sample. Our technique had an accuracy in measuring the pump-induced probe polarization-azimuth rotation of better than $10^{-6}$ rad and was based on continuous modulation of the probe polarization and the pump intensity.[14] Unlike other techniques in which the circular birefringence–dichroism is calculated from the data on reflectivity for different polarizations,[9] our technique is directly sensitive to the pump-induced circular birefringence–dichroism in the sample. This technique is practically insensitive to the background change of the sample reflectivity and the transmission. All these features make the technique particularly suitable for studying spin dynamics, as has been demonstrated in GaAs.[14]

Semitransparent nickel samples of variable thickness were deposited by electron-beam evaporation of 99.98% pure nickel onto a glass substrate in a vacuum with a growth rate of approximately 1.5 nm/min. The substrates were glass microscope slides supplied by Chance Propper, Ltd. Measurements of the reflectivity at the air–nickel interface as a function of the transmission of the films (see Fig. 2) gave good agreement with the values calculated for pure nickel [$n = 2.50 + i4.41$ (Ref. 17)], indicating high quality and purity of the films. Our measurement of the natural polarization rotation of the sample owing to magneto-optical Kerr and Faraday effects (on reflection and in transmission) as a function of the incident polarization orientation showed spontaneous magnetization in the plane of the film and a slow variation of the magnetization direction along the sample.

The pump-induced polarization-azimuth rotation appeared on the background of the natural rotation owing to transverse spontaneous magnetization of the nickel sample. However, all our experiments showed that the pump-induced component of the rotation does not depend on the magnitude and the sign of the linear underlying (natural) polarization rotation. Within the available range of pump intensities, i.e., up to 16 GW/cm$^2$, the rotation increased linearly with the pump intensity. We also observed that with the 38-fs pump and probe pulses the nonlinear response was almost instantaneous (inset of Fig. 1). The rotation direction was reversed with opposite handedness of the pump, but its magnitude was unaffected. This observation is consistent with a picture of the pump inducing transient circular birefringence, which is a perturbation to the linear birefringence–dichroism induced by transverse spontaneous magnetization. The pump-induced probe-azimuth rotation when the pump was circularly polarized was at least a factor of 30 larger than the probe-azimuth rotation with the

0146-9592/99/191373-03$15.00/0 © 1999 Optical Society of America

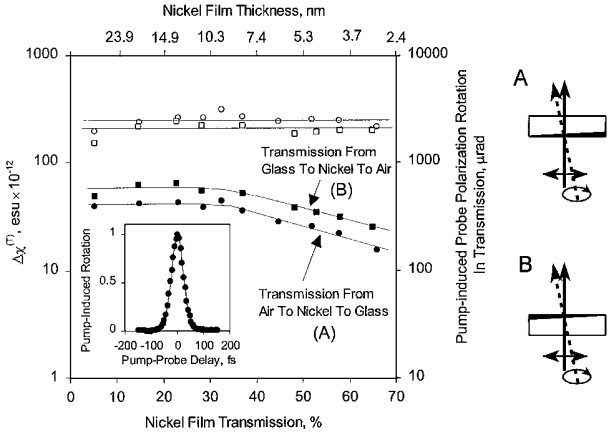


Fig. 1. Pump-induced probe polarization-azimuth rotation at zero pump–probe delay observed in transmission experiments for opposite directions of propagation (● and ■) and the corresponding values of the optical nonlinearity $\Delta\chi^{(T)}$ in nickel, calculated from Eq. (1) (○ and □). The inset shows the normalized pump-induced probe polarization azimuth rotation as a function of the pump–probe delay in transmission through the sample. In all cases the response was instantaneous within the time resolution available, with 38-fs optical pulses.

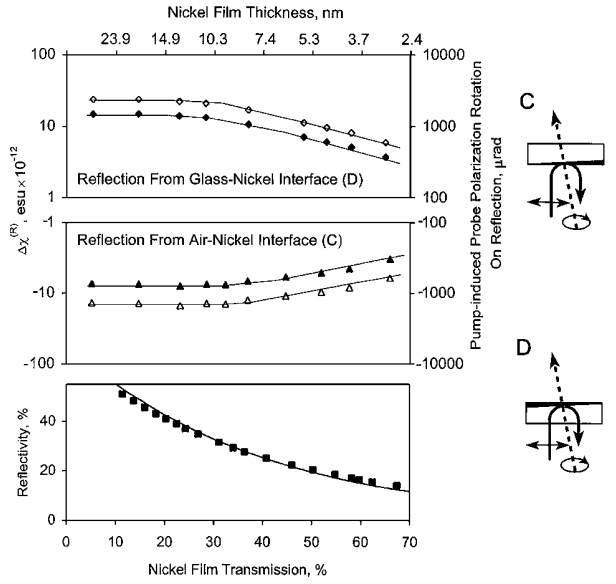


Fig. 2. Pump-induced probe polarization-azimuth rotation at zero pump–probe delay on reflection as a function of the transmission of the nickel film. Note that the direction of the rotation at the nickel–air interface (▲) is the opposite of that at the glass–air interface (◆). The left-hand scale shows the corresponding effective nonlinearity $\Delta\chi^{(R)}$, as calculated from Eq. (2) (△ and ◇). The bottom graph shows a plot of the reflectivity from the air–nickel interface (■). The solid curve is calculated from a numerical model for a refractive index of $n = 2.50 - i4.41$.[15]

pump linearly polarized at 45° to the probe. For the results reported below, the pump was always circularly polarized.

In transmission experiments we found that the sign of the pump-induced probe polarization is independent of the direction of propagation through the sample and depends only on the handedness of the pump pulse. For a given pump intensity, the rotation tends to increase with the sample thickness and is slightly higher for propagation from the glass substrate into the nickel film. Such a difference in rotation may be anticipated, as the reflectivity of the two interfaces, and therefore the intensities inside the nickel film, are different. Presuming that the film is homogeneous, we can calculate the nonlinearity of the nickel layer from the following formula[16]:

$$\Theta^T = \pm \frac{32\pi^3}{c\lambda \left| 1 + \frac{n}{n_0} \right|^2} \mathrm{Re}\left\{ \frac{\chi_{xxyy} - \chi_{xyyx}}{n} \right\} \int_0^L I_p(z)\mathrm{d}z \,. \tag{1}$$

Here $\Theta^T$ is the pump-induced probe polarization-azimuth rotation in transmission through a sample of length $L$ and $I_p(z)$ is the intensity of the pump wave in the sample. Equation (1) is valid when the optical response is instantaneous, as was observed in our experiments. Equation (1) also assumes a weak dependence of the nonlinear susceptibilities and the complex refractive index on frequency within the laser pulse spectrum, which is the case in metals. Equation (1) neglects multiple reflections, which is a reasonable assumption for a highly absorbing sample. This formula is suitable for propagation in both directions; however, if the light enters the nickel film from the glass side, $n_0 = 1.50$ should be assumed, but for the opposite direction one has to use refractive index $n_0 = 1$. The plus and minus signs refer to right- and left-hand circular polarizations of the pump, respectively. Here the nonlinearity has been introduced in standard fashion by use of the nonlinear constitutive equation, $P_i^{\mathrm{nl}}(\omega) = \chi_{ijkl}(\omega, \omega, \omega, -\omega)E_j(\omega)E_k(\omega)E_l^*(\omega)$. The coherent contribution to the nonlinear rotation, which depends on the mutual phase between the pump and the probe, was neglected in Eq. (1), as in our experiments the coherent component was suppressed by use of the technique described in Ref. 17.

The effective nonlinearity that was recovered from the transmission experiment is presented in Fig. 1, in which the following notation is used: $\Delta\chi^{(T)} = \mathrm{Re} \times [(\chi_{xxyy} - \chi_{xyyx})/n]$. One can see that the nonlinearity is practically independent of the film thickness, $\Delta\chi^{(T)} \sim 2 \times 10^{-10}$ esu. Neglecting multiple reflections and modeling the pump intensity as a decaying exponential across the film lead to an error of less than 15% in the estimate of the nonlinearity. A small difference between the values of the nonlinearities derived from the data for the opposite directions of preparations can be attributed to a surface contribution that we discuss below. Our transmission measurements suggest that the nonlinearity, $\Delta\chi^{(T)} = \mathrm{Re}[(\chi_{xxyy} - \chi_{xyyx})/n]$, in nickel can be approximated to be homogeneous within the range of thicknesses measured in our experiment, with the surface effects making only a small contribution.

The results of our measurements of the reflected light suggest a very different picture for the nonlinearity that is responsible for the reflective effects: $\Delta\chi^{(R)} = \mathrm{Im}((\chi_{xxyy} - \chi_{xyyx})/\{n[1 - (n/n_0)^2]\})$. For a

homogeneous nickel layer it would be expected that the induced rotation sign would be independent of which interface the light is reflected from. However, this expectation was not confirmed experimentally (see Fig. 2).

To our astonishment we observed the opposite sign of rotation when the sample was turned over and illuminated from the opposite side, for the same handedness of the pump polarization with the same experimental setup. We emphasize again that the pump-induced polarization rotation is independent of the spontaneous magnetization. If we again assume that the film was homogeneous and calculate its nonlinearity by use of a formula derived with this assumption,[16]

$$\Theta^R = \pm \frac{32\pi^2 I_p}{c n_0 \left| 1 + \frac{n}{n_0} \right|^2} \mathrm{Im}\left\{ \frac{\chi_{xxyy} - \chi_{xyyx}}{n\left[1 - \left(\frac{n}{n_0}\right)^2\right]} \right\}, \qquad (2)$$

we find that the nonlinearity on opposite sides of the film will have different signs (see Fig. 2). This result shows that in nickel films the nonlinearity, $\Delta\chi^{(R)} = \mathrm{Im}((\chi_{xxyy} - \chi_{xyyx})/\{n[1 - (n/n_0)^2]\})$, is very inhomogeneous and that the surface strongly affects the optical properties of the medium. It is possible to estimate the depths, $\xi_1$ and $\xi_2$, to which the two surfaces influence the optical response of the material from our measurements. As nonlinearities at different interfaces have different signs, if $\xi_1 \approx \xi_2 = \xi$, the film thickness at which the nonlinearity calculated from Eq. (2) starts to decrease is approximately $2\xi$, when the layers with opposite signs of nonlinearity start to overlap, giving $\xi \approx 4$–$5$ nm.

We believe that the bulk optical nonlinearity in nickel films has the same origin as the ultrafast component of the polarization-sensitive optical response that was recently observed in $CoPt_3$ alloy films.[9] The nonlinearity is related to the spin polarization of electrons excited with a circularly polarized pump. This nonlinearity was first discussed with relevance to metals in Ref. 7. Following the impulse of photoexcitation with a circularly polarized pump, an electron-spin distribution is created with finite net spin polarization, giving rise to circular birefringence–dichroism in the sample. The net spin polarization decays through electron–electron scattering processes. As the induced birefringence–dichroism is instantaneous within the pulse duration, this puts an upper limit on the spin relaxation time of ≈40 fs. As the electron-collision time in nickel is ~2 fs, our results show that the spin-flipping occurs on average at least every 20 collisions. The spin relaxation time can be compared with the electron-spin relaxation time that is due to exchange interaction and spin-orbit coupling, which was recently calculated to be a few femtoseconds for nickel.[18] The spin relaxation time, which governs the observed nonlinearity response time, should be clearly distinguished from the much longer electron-thermalization time, which was measured to be 280 ± 30 fs in nickel,[13] and also from the even-longer spin-lattice relaxation time, which is a few hundred picoseconds for nickel.[18,19]

The dramatic change of the nonlinearity at the interface from the bulk observed in our experiments, and in particular the change of the sign of the pump-induced rotation on reflection from the nickel–air and the nickel–glass interfaces, is not completely understood. It may be related to specific surface states created by the presence of the interface or to interface contamination–oxidation, or it may be related to the local field effects owing to surface roughness. It is also known that the spin relaxation processes at the interface are considerably different from those in the bulk.[20]

The authors thank B. D. Rainford and V. V. Shuvalov for their discussions of this work and Goodfellow Cambridge, Ltd., and NATO (grant CRGP960274) for their financial support. N. I. Zheludev's e-mail address is n.i.zheludev@soton.ac.uk.

## References

1. W. K. Burns and N. Bloembergen, Phys. Rev. B **4,** 3437 (1971).
2. G. L. Eesley, Phys. Rev. B **33,** 2144 (1986).
3. R. W. Schoenlien, W. Z. Lin, J. G. Fujimoto, and G. L. Eesley, Phys. Rev. Lett. **58,** 1680 (1987).
4. X. Y. Wang and M. C. Downer, Opt. Lett. **17,** 1450 (1992).
5. C. K. Sun, F. Vallee, L. H. Acioli, E. P. Ippen, and J. G. Fujimoto, Phys. Rev. B **50,** 15337 (1994).
6. A. Liebsch, Surf. Sci. **307/309,** 1007 (1994).
7. N. I. Zheludev, P. J. Bennett, H. Loh, S. V. Popov, I. R. Shatwell, Yu. P. Svirko, V. E. Gusev, V. F. Kamalov, and E. V. Slobodchikov, Opt. Lett. **20,** 1368 (1995).
8. S. Dhanjal, S. V. Popov, I. R. Shatwell, Yu. P. Svirko, N. I. Zheludev, and V. E. Gusev, Opt. Lett. **22,** 1879 (1997).
9. G. P. Ju, A. Vertikov, A. V. Nurmikko, C. Canady, G. Xiao, R. F. C. Farrow, and A. Cebollada, Phys. Rev. B **57,** R700 (1998).
10. R. P. Pan, H. D. Wei, and Y. R. Shen, Phys. Rev. B **39,** 1229 (1989).
11. T. Rasing, M. G. Koerkamp, B. Koopmans, and H. Vander Berg, J. Appl. Phys. **79,** 6181 (1996).
12. E. Beaurepaire, J. C. Merle, A. Daunois, and J. Y. Bigot, Phys. Rev. Lett. **76,** 4250 (1996).
13. J. Hohlfeld, E. Matthias, R. Knorren, and K. H. Benneman, Phys. Rev. Lett. **78,** 4861 (1997).
14. A. R. Bungay, S. V. Popov, I. R. Shatwell, and N. I. Zheludev, Phys. Lett. A **234,** 379 (1997).
15. E. D. Palik, ed., *Handbook of Optical Constants of Solids* (Academic, London, 1985), p. 323.
16. Yu. P. Svirko and N. I. Zheludev, *Polarization of Light in Nonlinear Optics* (Wiley, New York, 1998), Chap. 7.
17. S. V. Popov, N. I. Zheludev, and Yu. P. Svirko, Opt. Lett. **19,** 13 (1994).
18. W. Hubner and G. P. Zhang, Phys. Rev. B **58,** R5920 (1998).
19. A. Scholl, L. Baumgarten, R. Jacquemin, and W. Eberhardt, Phys. Rev. Lett. **79,** 5146 (1997).
20. V. F. Gantmaher and I. B. Levinson, *Scattering in Metals and Semiconductors* (Nauka, Moscow, 1984), Chap. 13.

# Light-induced specular-reflectivity suppression at a gallium/silica interface

**V. Albanis, R. T. Bratfalean, S. Dhanjal, and N. I. Zheludev**

*Department of Physics and Astronomy, University of Southampton, Southampton SO17 1BJ, UK*

**V. I. Emel'yanov**

*Department of Physics and International Laser Centre, Moscow State University, Vorobievy Gori, 119899 Moscow, Russia*

**P. Petropoulos and D. J. Richardson**

*Optoelectronics Research Centre, University of Southampton, Southampton SO17 1BJ, UK*

Received July 6, 2000

The reflectivity of a gallium/silica interface formed on an optical flat or at the tip of a cleaved optical fiber can be reduced in a reversible fashion when the interface is excited by a few milliwatts of laser power. This phenomenon occurs at temperatures just below gallium's melting point. We believe that the effect can be attributed to light-induced structuring at the interface. © 2000 Optical Society of America

*OCIS codes:* 190.4350, 190.4720.

Interfaces between elemental gallium and silica have recently attracted attention because of their unique nonlinear optical properties, which can be observed when gallium is on the verge of a structural phase transition. The nonlinearity manifests itself as a reversible light-induced reflectivity increase at temperatures several degrees below bulk gallium's melting point, $T_m = 29.6\,^{\circ}\mathrm{C}$. The potential applications of this nonlinearity are in nonlinear mirrors for control of light by light[1,2] and laser $Q$ switching in the infrared part of the spectrum.[3,4] In this Letter we report an additional light-induced effect that takes place within a narrow temperature interval, typically less than $1\,^{\circ}\mathrm{C}$, just below $T_m$. In this region the reversible light-induced reflectivity increase is replaced by an abrupt light-induced decrease in reflectivity, which is also reversible.

In our samples a gallium film of $\sim$1-$\mu$m thickness was deposited on the ceramic surface of a miniature Peltier heat pump by ultrafast pulsed laser deposition in a vacuum of $10^{-6}$ Torr.[5] The substrate temperature was $\sim -100\,^{\circ}\mathrm{C}$ during deposition. Substrate cooling was found to be essential to achieve the correct crystalline phase of gallium ($\alpha$ phase). After deposition, the gallium-covered surface of the Peltier element was covered with a silica glass, and the mirror was fused by heating of the sample to just above gallium's melting point. Samples prepared in this way have nonlinear optical properties similar to those reported in Ref. 1 for mirrors manufactured on the tip of an optical fiber. The Peltier heat pump was then used to control the gallium/silica interface temperature to a nominal precision of $0.02\,^{\circ}\mathrm{C}$. A cw argon-ion laser operating at 514 nm, with beam-direction stabilization, was used to measure the reflectivity of the interface. The beam was focused onto the sample at normal incidence, to a spot of 12-$\mu$m diameter. Experiments were performed with both linearly and circularly polarized light. The typical temperature dependence of the gallium/silica interface reflectivity, under conditions in which the darkening effect takes place, is shown in Fig. 1. The starting point of the reflectivity–temperature curve, far below the melting point of gallium, corresponds to the reflectivity level of the interface between crystalline $\alpha$-gallium, the ground state of gallium at normal pressure, and silica. The value of the interface's reflectivity depends on the polarization state of the laser as a result of the anisotropy of the gallium film. The reflectivity increases with both light intensity and sample temperature, as reported in Ref. 1. Then, within a narrow temperature interval just below $T_m$, the darkening effect takes place, and the reflectivity decreases rapidly with increasing temperature. Figure 1 shows a typical reflectivity decrease of 25% at a pump power of 8 mW (7 kW/cm$^2$). The reflectivity decrease develops only for intensities exceeding a threshold of $\sim$500 W/cm$^2$, as can be seen from the inset of Fig. 1. When $T_m$ is reached, the reflectivity jumps to $\sim$87%, the reflectivity level of the molten gallium/silica interface. The temperature width of the darkened region increases from $\sim 10^{-2}\,^{\circ}\mathrm{C}$ at 500 W/cm$^2$ to $\sim 0.4\,^{\circ}\mathrm{C}$ at 7 kW/cm$^2$ (see the inset of Fig. 1). We studied the reproducibility of the effect with square-wave-modulated light at 200 Hz and found the process to be remarkably repeatable from pulse to pulse across the whole range of temperatures. The light-induced low-reflectivity state is a typical feature shown by most of the samples prepared by the technique described above. However, we failed to see the darkening effect in samples in which gallium was deposited by ultrafast pulsed laser deposition directly on both the cover glass of the sample and the ceramic surface of the Peltier heat pump. This clearly indicates that the interface conditions are important for observation of the effect.

0146-9592/00/211594-03$15.00/0 © 2000 Optical Society of America

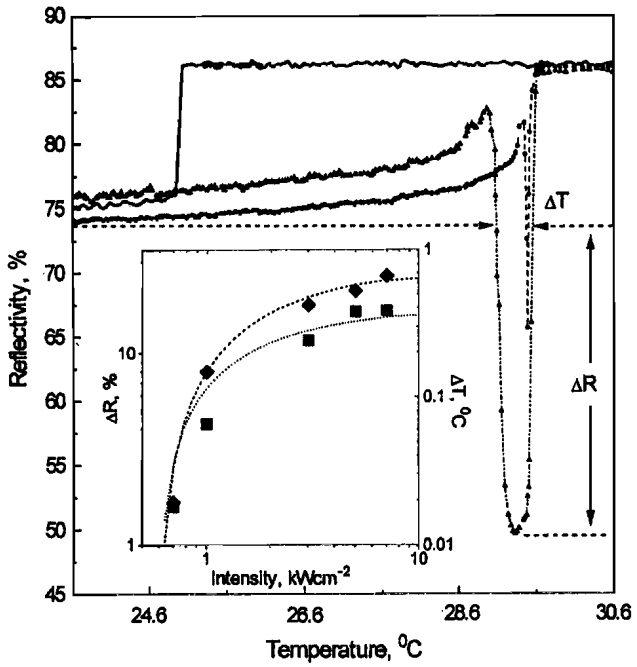


Fig. 1. Reflectivity–temperature curve of the gallium/silica interface, showing light-induced darkening at (▲) 7 kW/cm$^2$ and (●) 1 kW/cm$^2$; the solid curve shows the dependence of reflectivity on decreasing temperature. The inset shows (◆) the dependence of $\Delta R$, the magnitude of the reflectivity drop, and (■) $\Delta T$ the temperature width of the drop on light intensity.

We also saw a similar darkening effect with mirrors prepared by immersion of the tip of a single-mode optical fiber of 100-$\mu$m$^2$ mode area into a bead of molten gallium as described in Ref. 1. In this case the reflectivity of the interface was monitored with a 60-$\mu$W cw distributed-feedback diode laser at a wavelength of 1.550 $\mu$m. The interface was simultaneously stimulated by another, more powerful amplified external-cavity diode laser with power ranging from 0 to 8 mW, at a wavelength of 1.536 $\mu$m. The pump laser was modulated at a frequency of 500 Hz. A sequence of oscilloscope frames showing the intensity of the reflected probe beam in the time domain for different mirror temperatures is presented in Fig. 2. Frames 1 and 2, taken at $T$ = 15.0 °C and $T$ = 23 °C, respectively, show the previously reported regime of reversible light-induced reflectivity increase.[1] The effect is more pronounced at higher temperatures (compare frames 1 and 2). Note that in frames 1 and 2 the increase of reflectivity is in phase with the modulated pump intensity. Frame 3, taken at 28.1 °C shows the first sign of the darkening effect: A sharp spike appears immediately after the pump is switched on, which is followed by a rapid but relatively small decrease of reflectivity from the peak level achieved by the spike to a new, lower level. Frame 4, at $T$ = 28.5 °C, shows the dynamics even more profoundly. Frame 5, taken at $T$ = 28.9 °C, shows the fully developed darkening effect. Note that in frame 5 reflectivity decreases in the presence of the pump. Frame 6 shows that, above the melting temperature of Ga, the light-induced modulation has disappeared. It can be seen from Fig. 2 that the low-reflectivity level is fully developed in approximately a few hundred microseconds (~200 $\mu$s in frame 5) and recovers to the initial level within a few microseconds.

In our opinion the specular-reflectivity suppression in the narrow temperature interval below the melting point is likely to result from light-induced structuring of gallium at the interface with silica. This correlates with the fact that rigid interfaces prepared directly on the cover silica glass by pulsed laser deposition do not show the effect, whereas looser interfaces do. There are several potential candidate mechanisms that could be responsible for the effect, as described below; however, as yet we are unable to present quantifiable evidence for the prevalence of any of them.

The formation of a surface grating consisting of alternating strips of molten and solid silicon was reported to occur during laser melting of silicon films.[6] Such a grating results from a light-induced self-organization process. The grating is imposed by the interference pattern of the incident and the scattered surface waves, and its period is equal to the optical wavelength. Such a grating leads to an increase in the film's absorption.[7] A similar light-induced grating may be formed in gallium, thus reducing the reflectivity of the interface. Such an interpretation has difficulties, however, as the darkening effect in our experiments was also observed with circularly polarized light at strictly normal incidence to the sample. If the gallium layer at the interface were truly isotropic in the interface plane, coherent grating formation would be forbidden.[6,7] It is not quite clear to what

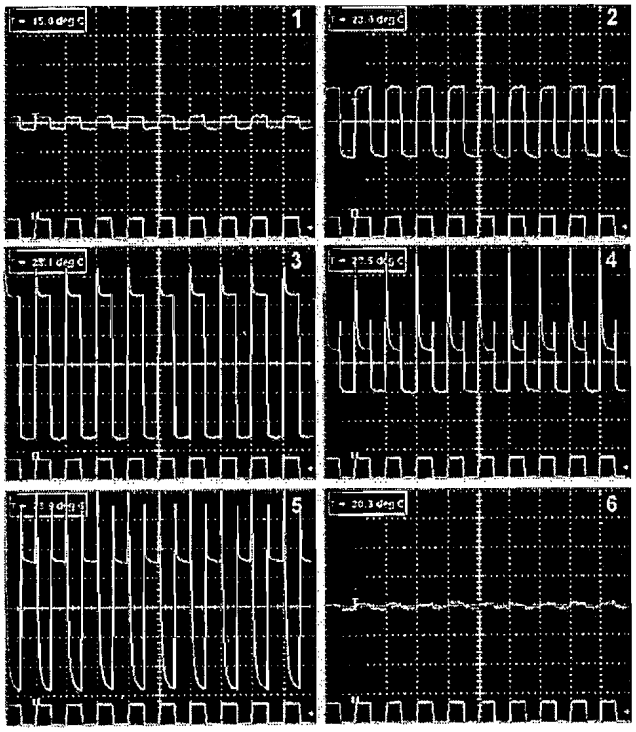


Fig. 2. Reflectivity of the fibrerized gallium interface at 1.550 $\mu$m modulated by the presence of pump light at 1.536 $\mu$m. In all frames the top oscilloscope trace shows the reflected probe intensity (arbitrary units, AC coupling mode, time base 2 ms/division), and the bottom trace shows the pump intensity (not on the same scale as the top trace).

extent the pronounced anisotropy of the gallium film is sufficient to overcome this restriction. Another mechanism of the reported darkening effect could be a light-induced roughening of the gallium–glass interface. Roughening of solids near the melting point is known to appear even in the absence of any light excitation.[8,9] The possible mechanisms underpinning such light-induced roughening are now being investigated, and we are considering not only relief formation but also clustering of defects and nanoscale phase separation on the surface. If a nanoscale quasi-periodic disturbance of the surface layer occurs, its effective dielectric permeability will have a resonance that depends on the bulk plasma frequency of the metal and on the shape and characteristic size of the nanoscale modulation.[9,10] If the conditions are correct, this may lead to a decrease in reflectivity.[11,12] Another possible mechanism is the formation of a stratified planar structure. Such a structure could result from the formation of a quasi-liquid layer, separated from the $\alpha$-gallium bulk by an $\alpha$-gallium layer containing metallic inclusions. It has been shown that, for a particular dielectric coefficient of the layers, the reflectivity of such a three-layer structure can be greatly reduced.[13] Finally, intense light scattering could be responsible for the specular-reflectivity decrease. Such scattering is known to occur when the dielectric parameters of the material show pronounced spatial–temporal fluctuations, with a characteristic correlation length equal to the wavelength. Therefore this mechanism relies on the hypothesis that such fluctuations at a gallium/silica interface may take place near the melting point and are somehow stimulated by light.

In conclusion, we have reported a reversible, dynamically light-induced decrease in the reflectivity of a gallium/silica interface that occurs within a narrow temperature interval just below gallium's melting point. The magnitude of the reflectivity drop and its temperature width increase with incident light power. Possible applications of this darkening effect in power limiting are being investigated.

The support of the Engineering and Physical Science Research Council (UK), the Royal Society (London), and Goodfellow Cambridge, Ltd., is acknowledged. The authors thank V. A. Fedotov and K. F. MacDonald for discussions and A. V. Rode for deposition of the high-quality gallium samples at the ultrafast pulsed laser deposition facility of the Australian National University. V. Albanis's e-mail address is va@phys.soton.ac.uk.

## References

1. P. J. Bennet, S. Dhanjal, P. Petropoulos, D. J. Richardson, N. I. Zheludev, and V. I. Emel'yanov, Appl. Phys. Lett. **73,** 1787 (1998).
2. V. Albanis, S. Dhanjal, N. I. Zheludev, P. Petropoulos, and D. J. Richardson, Opt. Express **5,** 157 (1999), http://epubs.osa.org/opticsexpress.
3. P. Petropoulos, H. L. Offerhaus, D. J. Richardson, S. Dhanjal, and N. I. Zheludev, Appl. Phys. Lett. **74,** 3619 (1999).
4. N. J. C. Libatique, J. D. Tafoya, and R. K. Jain, in *Conference on Lasers and Electro-Optics* (Optical Society of America, Washington, D.C., 2000), paper CMP2.
5. E. G. Gamaly, A. V. Rode, and B. Luther-Davies, J. Appl. Phys. **85,** 4213 (1999); A. V. Rode, B. Luther-Davies, and E. G. Gamaly, J. Appl. Phys. **85,** 4222 (1999).
6. J. S. Preston, H. M. van Driel, and J. E. Sipe, Phys. Rev. B **40,** 3942 (1989).
7. J. S. Preston, J. E. Sipe, H. M. van Driel, and J. Luscombe, Phys. Rev. B **40,** 3931 (1989).
8. E. A. Jagla, S. Prestipino, and E. Tossatti, Phys. Rev. Lett. **83,** 2753 (1999).
9. V. I. Emel'yanov, Laser Phys. **8,** 937 (1998).
10. J. R. Wait, *Electromagnetics and Plasmas*, 2nd ed. (Pergamon, Oxford, 1970).
11. J. G. Bergman, D. S. Chemla, P. F. Liao, A. M. Glass, A. Pinchuk, R. M. Hart, and D. H. Olson, Opt. Lett. **6,** 33 (1981).
12. M. J. Regan, P. S. Pershan, O. M. Magnussen, B. M. Ocko, M. Deutsche, and L. E. Berman, Phys. Rev. B **54,** 9730 (1996).
13. F. Abeles, in *Optical Properties of Metallic Films*, M. H. Francombe and R. W. Hoffman, eds., Vol. 6 of Physics of Thin Films: Advances in Research and Development (Academic, New York, 1971), pp. 171–190.

ELSEVIER

Journal of Luminescence 87–89 (2000) 646–648

JOURNAL OF LUMINESCENCE

www.elsevier.com/locate/jlumin

# The light-induced structural phase transition in confining gallium and its photonic applications

V. Albanis[a], S. Dhanjal[a], K. MacDonald[a,*], P. Petropoulos[b], H.L. Offerhaus[b], D.J. Richardson[b], A. Rode[c], N.I. Zheludev[a]

[a]*Department of Physics and Astronomy, University of Southampton, Southampton, Hampshire SO17 1BJ, UK*
[b]*Optoelectronics Research Centre, University of Southampton, Southampton, Hampshire SO17 1BJ, UK*
[c]*Laser Physics Centre, Australian National University, Canberra ACT 0200, Australia*

**Abstract**

We report on a study of the dynamics of a recently discovered light-induced, surface-assisted, structural phase transition from a common orthorhombic phase of α-gallium to a highly reflective phase that occurs at temperatures just below the metal's bulk melting point (30°C). It is fully reversible with dynamics occurring on a nanosecond/microsecond time scale and can be stimulated by very low-intensity radiation, typically $\sim 10^{-5}$ W/μm$^2$. The two gallium phases involved have significantly different optical properties and this difference gives rise to a gigantic optical nonlinearity, $\chi^{(3)} \sim 1$ esu, that offers tremendous new opportunities for controlling light with light. The microscopic model of the effect is discussed. © 2000 Elsevier Science B.V. All rights reserved.

*Keywords:* Optical nonlinearity; Phase transition; Gallium

Recently, we have found that low intensity ( ~ 5 kW/cm$^2$) optical excitation of a gallium/glass interface can induce a considerable change in its reflectivity at temperatures just below gallium's melting point, ~30°C. This effect has allowed the demonstration of a resonator-less all-optical switch operating at milliwatt power levels [1] and has also been used to achieve Q-switching of erbium and ytterbium fibre lasers [2]. We believe that the large optical nonlinearity implied by this effect is due to an optically induced non-thermal transition between phases of gallium with significantly different optical properties. In this paper we describe a model, supported by experimental data, for the structural/electronic mechanisms responsible for this huge nonlinearity.

Fig. 1 shows how the reflectivity of a gallium/glass interface varies with temperature at a range of probe intensity levels. At low intensity, where there is no nonlinear effect, a significant and abrupt reflectivity change is seen at the melting and solidification points. Supercooling is clearly observed, resulting in a well-defined hysteresis curve. On heating, a gradual reflectivity increase can be seen just below the bulk melting point indicating the presence of surface melting at the interface (gallium is one of the few metals that show such an effect [3]). At higher intensities, the hysteresis curve is modified, making the melting transition far less abrupt. Considerable reflectivity changes ( >30%) can be induced by only a few milliwatts of laser power and are fully reversible. We studied the dynamics of the transition in pump–probe experiments (inducing a reflectivity change with pump pulses of varying peak power and duration whilst monitoring the reflectivity with a low-power probe beam). The results of these studies are presented in Figs. 2 and 3.

We believe that the interface reflectivity changes because the pump light induces a structural phase transition, converting α-gallium (the normal crystalline form at room temperature and ambient pressure) to a more metallic, more reflective phase. This new phase may be liquid gallium, which is highly reflective, but it is not formed by thermally induced melting of α-gallium (the energy absorbed in the light–matter interaction

* Corresponding author. Fax: + 44-1703-593-910.
*E-mail address:* kfm@phys.soton.ac.uk (K. MacDonald)

0022-2313/00/$ - see front matter © 2000 Elsevier Science B.V. All rights reserved.
PII: S0022-2313(99)00340-3

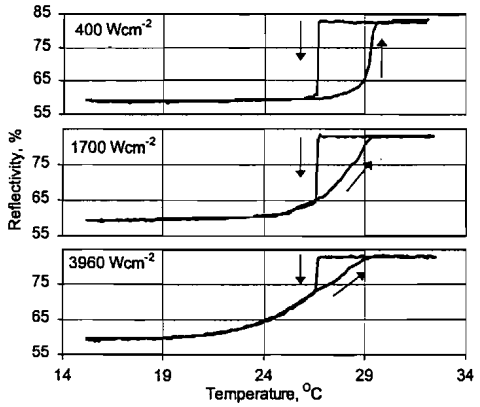


Fig. 1. Reflectivity (at 810 nm) of a gallium/glass interface, formed by ultrafast pulsed laser deposition, as a function of temperature at a selection of probe intensity levels.

volume is not enough to raise the interface's temperature to gallium's melting point). Thus, the mechanism responsible for α-gallium metallization must be one that confines the pump energy to the optical skin layer.

We propose that this mechanism involves a fast non-thermal light-induced transition from α-gallium to a phase which is only stable in the presence of light. On withdrawal of the excitation the new phase recrystallizes back to the α-phase. This process naturally restricts energy dissipation into the bulk, confining it to the optical skin layer ( ~25 nm). This metastable phase could be liquid, quasi-liquid or one of several metastable crystalline gallium phases [4–6]. The reversible transition is made possible by α-gallium's unique structure, in which molecular and metallic properties coexist: Some interatomic bonds are covalent, forming well-defined $Ga_2$ dimers (molecules), and the rest are metallic [5,7,8]. The molecular character of this structure allows for the assumption that absorption leads to highly localised excitation of the dimers due to the localisation of electron–hole pairs on the dimers and the local nature of the excitation itself. Light absorption thus excites a dimer from the bonding to the antibonding state, reducing the stability of the surrounding crystalline cell. α-gallium subsequently undergoes a transition to a new configuration, creating a microscopic inclusion of the new phase. The efficiency of this process is enhanced at the interface by the presence of seeds of the metallic phase [3,5].

The rapid increase in reflectivity which follows excitation can be explained by high velocity propagation, at ~1 m/s, of the metallic phase into the bulk by non-equilibrium epitaxial growth. Although this mechanism explains the experimental observations, we do not exclude the possibility that the reflectivity increase may be due to an increase in the size of new phase inclusions. Thermodynamical considerations show that the final

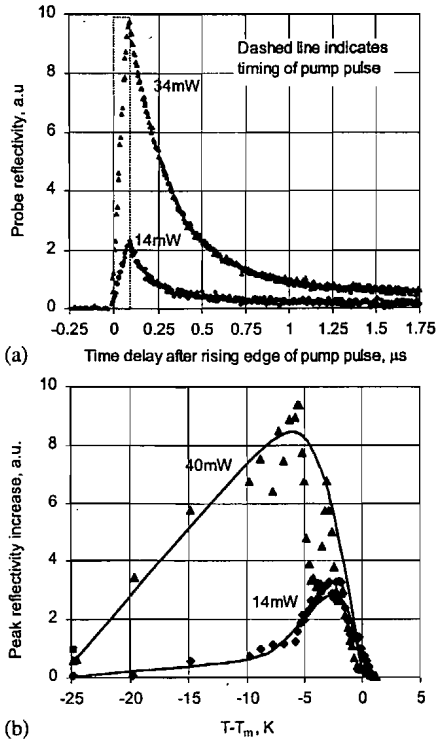


Fig. 2. Magnitude of the change induced in the reflectivity of a gallium/glass interface formed by immersing a cleaved optical-fibre tip in a bead of molten gallium. (a) As a function of time after excitation with 100 ns pump pulses of varying peak power (interface temperature = 24°C); (b) As a function of temperature, $T$, relative to the gallium's melting temperature, $T_m$, for different peak pump powers. Pump wavelength = 1536 nm, probe wavelength = 1550 nm.

(stationary) thickness, $d$, of the new-phase layer depends on $(T_m^* - T)$, where $T_m^*$ is the critical temperature of the transition between photoexcited α-gallium and the metallic phase, and on $L_{\alpha m}$, the specific energy difference between these phases. We consider that $L_{\alpha m}$ falls with increasing concentration of bonds broken by optical excitation and thus with increasing light intensity. A decrease in $L_{\alpha m}$ leads to an increase in $d$ and consequently in reflectivity. Our calculations show that a 25 nm layer of metastable phase on an α-gallium surface is sufficient to achieve nearly full metallic reflectivity. Furthermore, since $d$ also depends on $(T_m^* - T)$, the light-induced effect is expected to increase with temperature towards the melting point. This is exactly what has been observed (Fig. 2b). We believe that when the excitation is withdrawn, the metallic phase becomes metastable and recrystallizes back to the α-gallium phase via thermodynamical growth. Correspondingly, the reflectivity is restored to its initial value. The recovery time is critically increased on approaching $T_m^*$. This model predicts longer recovery times for larger induced reflectivity

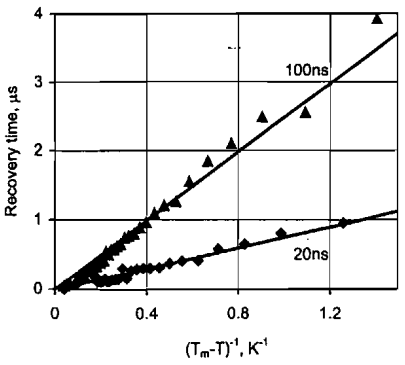


Fig. 3. Variation with temperature, $T$, relative to the gallium's melting temperature, $T_m$, of the time taken for the reflectivity of a gallium/glass interface to recover following excitation with pump pulses of different durations at a peak pump power of 70 mW. Interface formed by immersing a cleaved optical-fibre tip in a bead of molten gallium, pump wavelength = 1536 nm, probe wavelength = 1550 nm.

changes, i.e. thicker metallized layers, at a fixed temperature, and a slowing of the response at fixed optical excitation strength as the temperature is increased towards α- gallium's melting point. All of these features have been seen in our experiments, in particular, the recovery time increases as $\sim 1/(T_m - T)$, and its dependence on pulse duration is in excellent agreement with the model (Fig. 3). We can thus conclude that $T_m^*$ is in fact α-gallium's melting temperature $T_m$. This is not, however, enough to conclude that the metastable phase is a liquid. Indeed, it has been suggested [7] that α-gallium melting is in fact a continuous transition through several of the crystalline phases that are energetically very close to each other and therefore, the metastable phase could be one of these.

The light-induced transition in gallium is different from those observed in semiconductors such as Si and GaAs (see Ref. [9] for a review). To achieve non-thermal effects in these materials high-intensity femtosecond optical excitation is needed. Importantly, in silicon and GaAs the result of optical excitation is highly delocalised and the phase transition occurs through plasma-induced instability in the acoustic phonon modes, typically on a sub-picosecond time scale. In gallium, localization of the excitation leads to local transformation of the structure. This allows us to discuss the transition in terms of the much slower nucleation and epitaxial growth mechanisms. A similar approach has been used to describe laser-induced amorphization of semiconductors [10].

In conclusion, the cubic optical nonlinearity associated with the transition is huge and it is of considerable interest for applications requiring light-by-light control at low power levels, and in particular for photonic switching devices. For light intensities that vary on a time scale slower than the nonlinearity's response time, the nonlinearity can be presented in terms of the third-order optical susceptibility, $\chi^{(3)}$. The magnitude of this susceptibility can be estimated from the difference between the dielectric coefficient of α-gallium, $\varepsilon_\alpha$, and that of metastable gallium, $\varepsilon_m$ (assumed to be close to that of liquid gallium), as $\chi^{(3)} \sim |\varepsilon_\alpha - \varepsilon_m|/(4\pi E^2) \sim 1$ esu (equivalent to $\sim 10^{-8}$ m$^3$/V$^2$ in SI), where $|\varepsilon_\alpha - \varepsilon_m| \sim 180$ and $E$ is the electric field in gallium (calculated in esu) that corresponds to an incident light intensity of $2 \times 10^{-4}$ W/μm$^2$. This value of $\chi^{(3)}$ should be compared to that of $10^{-14}$ esu for silica glass.

We would like to acknowledge the support of The Royal Society, NATO, The Engineering and Physical Sciences Research Council and Goodfellow Cambridge, Ltd.

## References

[1] P.J. Bennett, S. Dhanjal, P. Petropoulos, D.J. Richardson, N.I. Zheludev, V.I. Emel'yanov, Appl. Phys. Lett. 73 (1998) 1787.
[2] S. Dhanjal, P. Petropoulos, D.J. Richardson, H.L. Offerhaus, N.I. Zheludev, Appl. Phys. Lett. 74 (1999) 3619.
[3] R. Trittibach, Ch. Grutter, J.H. Bilgram, Phys. Rev. B 50 (1994) 2529.
[4] J. Wolny, S. Niziol, W. Luzny, L. Pytlik, J. Soltys, Solid State Commun. 58 (1986) 573.
[5] X.G. Gong, G.L. Chiarotti, M. Parrinello, E. Tosatti, Phys. Rev. B 43 (1991) 14277.
[6] L. Bosio, J. Chem. Phys. 68 (1978) 1221.
[7] H.G. Von Schnering, R. Nesper, Acta Chem. Scand. 45 (1991) 870.
[8] O. Züger, U. Dürig, Phys. Rev. B 46 (1992) 7319.
[9] Y. Segal, E.N. Glezer, L. Huang, E. Mazur, Annu. Rev. Mater. Sci. 25 (1995) 223.
[10] S. Roorda, W.C. Sinke, Appl. Surf. Sci. 36 (1989) 588.

# Nanosecond dynamics of a gallium mirror's light-induced reflectivity change

V. Albanis, S. Dhanjal, V. A. Fedotov, K. F. MacDonald, and N. I. Zheludev
*Department of Physics and Astronomy, University of Southampton, Highfield, Southampton SO17 1BJ, United Kingdom*

P. Petropoulos and D. J. Richardson
*Optoelectronics Research Centre, University of Southampton, Highfield, Southampton SO17 1BJ, United Kingdom*

V. I. Emel'yanov
*Department of Physics and International Laser Centre, Moscow State University, Moscow, Russia*
(Received 2 October 2000; published 4 April 2001)

Transient pump-probe optical reflectivity measurements of the nano- to microsecond dynamics of a fully reversible, light-induced, surface-assisted metallization of gallium interfaced with silica are reported. The metallization leads to a considerable increase in the interface's reflectivity when solid $\alpha$-gallium is on the verge of melting. The reflectivity change was found to be a cumulative effect that grows with light intensity and pulse duration. The reflectivity relaxes back to that of $\alpha$-gallium when the excitation is withdrawn in a time that increases critically at gallium's melting point. It is shown that thermal processes cannot account for the effect and so a mechanism based on a nonthermal light-induced structural phase transition is proposed.

DOI: 10.1103/PhysRevB.63.165207 PACS number(s): 78.66.−w, 42.65.−k

The search for materials with large optical nonlinearities or that show a marked response to low-power optical excitation, as required for applications such as all-optical switching, has concentrated on media whose optical electrons exhibit a highly anharmonic response; most notably semiconductors, which exploit free excitonic and near-band-gap effects, and organic materials with weakly bound electrons. Here we report on a study of a novel type of reversible optical response associated with a surface-assisted, light-induced transition between structural phases with significantly different optical properties. One can illustrate this type of reversible response to optical stimulation by considering an ice cube at a temperature just below the bulk melting point. A skin of water develops on the ice because the energy of a water/air interface is lower than that of one between ice and air. This is known as premelting. The delicate balance between water and ice may be shifted very easily, for example by heating with light, thus inducing a change in the water skin depth. Water and ice have similar optical properties but if they were different, such an excitation would lead to a change in the sample's reflectivity and transmission. Recently we found that gallium confined at an interface with silica exhibits this type of response via light-assisted surface metallization.[1] This transformation engages only a few atomic layers but leads to a very considerable change in optical properties. In this paper we report on the transient dynamic characteristics of the response, measured with nanosecond time resolution at various excitation intensities and interface temperatures, and we propose a microscopic mechanism for the observed behavior.

We investigated gallium/silica interfaces formed by inserting a freshly cleaved single-mode optical fiber, with a mode radius of $r_0 = 4\ \mu$m, into an initially molten bead (~1 mm diameter) of 6$N$ purity gallium (see the inset to Fig. 1). The gallium was then frozen to form a mirror at the end of the fiber. The bead's temperature was controlled to a nominal precision of 0.01 °C. We studied the interface's response using pump-probe techniques: pump light, at 1536 nm, was used to modify the interface's reflectivity whilst it was being continuously measured with a much weaker probe beam, at 1550 nm. The pump and probe were generated by distributed-feedback laser diodes with the pump radiation subsequently amplified by an erbium-doped fiber amplifier and modulated with an acousto-optic modulator. The overall frequency bandwidth of the probe detection system was 125 MHz. Figure 1 shows the dependence of the interface's reflectivity on temperature around gallium's melting point in both the "ground" (no pump beam present) and "excited" regimes. In the absence of pump light a significant and abrupt reflectivity change is seen at the melting and solidifi-

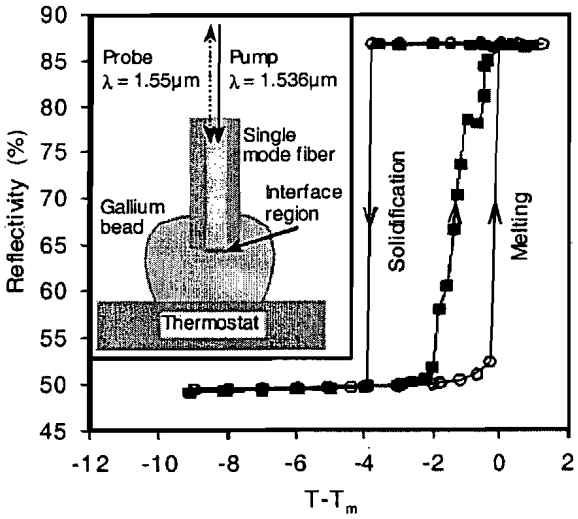


FIG. 1. Interface reflectivity as a function of temperature $T$ relative to gallium's melting point $T_m$ as measured by the probe beam in the absence of a pump beam (○) and in the presence of a 5-mW cw pump beam (■). The inset shows a schematic of the gallium/silica interface.

 ©2001 The American Physical Society

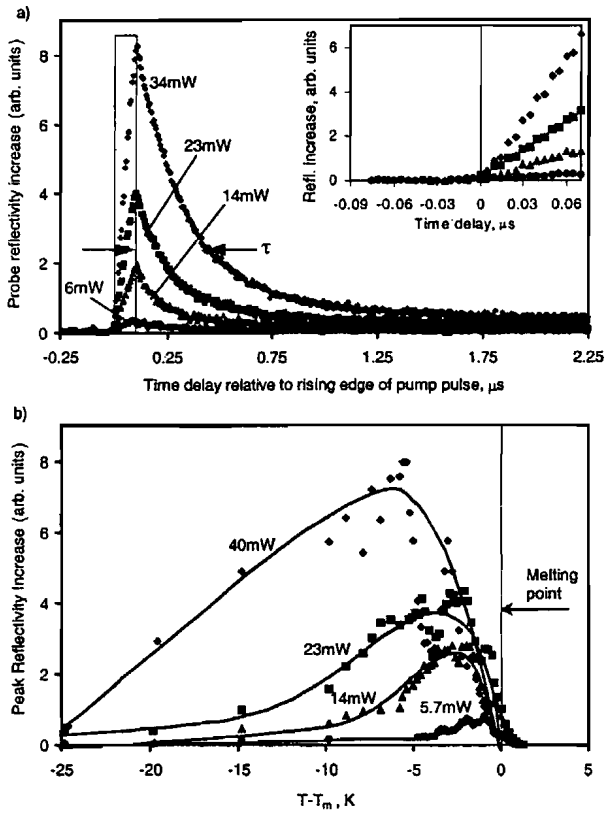


FIG. 2. (a) Dynamics of the reflectivity change after excitation with 100-ns pump pulses (dashed line) of varying peak power, at a temperature $T=24\,^{\circ}\mathrm{C}$. The inset shows dynamics near the rising edge of the pump pulse with an enlarged time scale. (b) Amplitude of the induced reflectivity change as a function of temperature $T$ relative to gallium's melting temperature $T_m$ for a range of peak pump powers.

cation points. Supercooling is clearly seen, resulting in a well-defined hysteresis curve. On heating, a small reflectivity increase can be seen just below the bulk melting point indicating the presence of premelting at the interface. Application of a cw pump beam modifies the hysteresis curve, making the melting transition far less abrupt. Considerable reflectivity changes (>30%) were induced by only a few milliwatts of laser power and were fully reversible. We studied the reflectivity change's dynamics by initiating it with nanosecond pump pulses of varying peak power and duration. These transient measurements show the reflectivity's fast response to optical excitation. Recent measurements performed with a femtosecond laser reveal that the intrinsic response time can be just a few picoseconds.[19] [see Fig. 2(a)]. Importantly, the reflectivity starts to increase *immediately* after commencement of the pump pulse [see the inset to Fig. 2(a)]. For the range of pump pulse parameters available in our experiment the effect accumulates with time and increases with laser power. The peak response for various excitation levels is presented as a function of temperature in Fig. 2(b). These data show that the effect is much more pronounced at temperatures just below the melting point of gallium and disappears completely above the melting point. Immediately after termination of the pump pulse the reflectivity level begins to recover to the initial level. The effect is fully repeatable and *perfectly reproducible* for at least $10^5$ pulses. The recovery time is relatively slow (ns to $\mu$s) and, importantly, temperature dependent. Figure 3 presents induced reflectivity change recovery time as a function of temperature. This graph shows the remarkably accurate proportionality of the recovery time $\tau$ to $(T_m-T)^{-1}$, indicating a "critical" enhancement of the effect: the closer the sample temperature is to the melting point, the longer the relaxation time. For a given temperature the relaxation time steadily increases with pump pulse energy density (see the inset to Fig. 3).

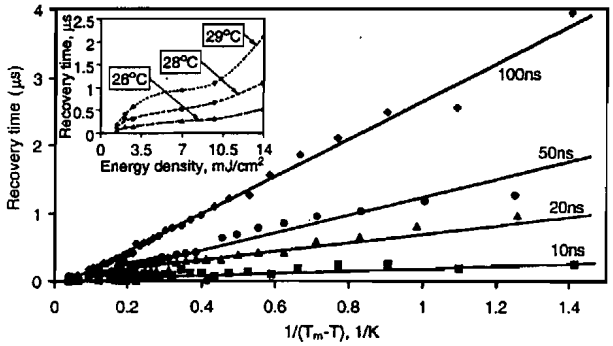


FIG. 3. Induced reflectivity change recovery time $\tau$ as a function of temperature $T$ relative to gallium's melting temperature $T_m$ for different pump pulse durations at a peak pump power $P=70$ mW. Inset: induced reflectivity change recovery time $\tau$ as a function of energy density for different temperatures of the gallium drop.

The laser-induced reflectivity change can be explained by conversion of $\alpha$-gallium (the normal crystalline form at room temperature and pressure) to a new, more metallic, more reflective phase. This new phase could be molten (liquid) gallium or a highly reflective crystalline phase. We begin by assuming that such a conversion is the result of laser-induced thermal melting. To evaluate the temperature change due to laser heating we solved the three-dimensional heat propagation problem in the time domain using a method based on Green's function.[2] Our heat propagation model described the experimental conditions very closely—accurately accounting for the geometry of the experiment and the materials' thermal characteristics. The incident radiation is absorbed within the optical skin depth, $\alpha^{-1}$, which in gallium is only ~38 nm at a wavelength of 1.55 $\mu$m. The reflectivity of the $\alpha$-gallium/silica interface was taken to be 60%. $\alpha$-gallium manifests considerable anisotropy in its thermal conductivity. It was established recently that gallium dimers in the liquid phase tend to be oriented perpendicular to an interface.[3] Therefore, we expect that after solidification this orientation would prevail near the interface. This expectation is supported by our measurements of interface reflectivity levels for the solid phase. In the direction perpendicular to the interface the thermal conductivity is $\lambda_c = 15.9\,\mathrm{W\,m^{-1}\,K^{-1}}$ and in the plane of the interface it is anisotropic with principal coefficients $\lambda_a = 41\,\mathrm{W\,m^{-1}\,K^{-1}}$ and $\lambda_b = 88\,\mathrm{W\,m^{-1}\,K^{-1}}$.[4] All of these parameters were used in our calculations. Using this model we were able to calculate,

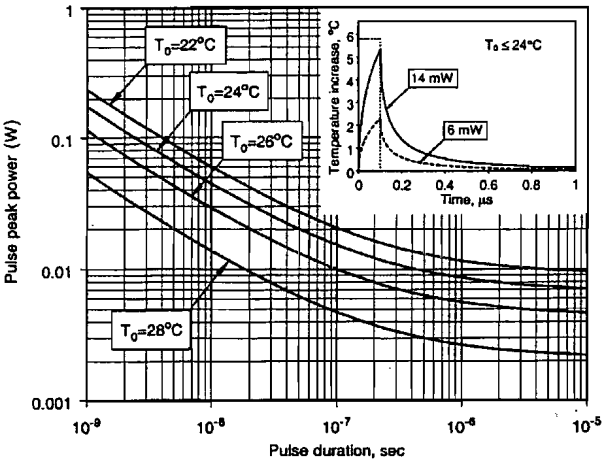


FIG. 4. Duration and peak power of the optical excitation pulse necessary to achieve gallium's melting temperature (29.8 °C) at the interface for different initial temperatures ($T_0$ = 22 °C,24 °C,26 °C,28 °C) of the gallium drop. Inset: dynamics of the interface temperature increase due to 100-ns excitation pulses of 14- and 6-mW peak power ($T_0 \leq 24.3$ °C).

for a given initial sample temperature, the optical power levels and laser pulse durations at which the melting temperature is reached (see Fig. 4). Since we neglected the thermal conductivity of the optical fiber, the values shown are upper estimates of the temperature increase. The assumption that thermal melting causes the reflectivity increase is clearly in conflict with our experimental observations (Figs. 2 and 3). For example, with an initial temperature of 24 °C we would have seen no reflectivity change at powers below 14 mW even with 100-ns pulses (the longest used in our experiments) and at higher power levels the reflectivity would only begin to change after a delay during which the interface is heated to the melting temperature and the latent heat of melting is accumulated. In contrast, we see reflectivity changes at intensities below 14 mW and we see in all cases that the change starts as soon as the pump pulse starts. Therefore, the laser-induced thermal melting mechanism does not explain the reflectivity behavior observed experimentally.

Let us now suppose that another hypothetical nonmelting mechanism exists wherein reflectivity depends on interface temperature (which changes due to laser heating) but does not involve a change in the phase of gallium. Reflectivity would then relax as temperature relaxes. According to our calculations, this would happen within approximately 60 ns following a 100-ns pulse (see the inset to Fig. 4). Importantly, this relaxation time would be *independent* of the thermostat temperature or laser power level. In contrast, our experiments show that the relaxation time is a strong function of the excitation level [see Fig. 2(a)] and background temperature (see Fig. 3). This leads us to conclude that a temperature-dependent mechanism that does not involve a change in the structural phase of gallium at the interface is also not possible. There must therefore be another mechanism behind the reflectivity increase, whereby $\alpha$-gallium is converted into a different phase.

Here we propose such a mechanism involving a nonthermal light-induced transition from $\alpha$-gallium to a phase that only becomes stable in the presence of light. This process naturally *restricts energy dissipation into the bulk*, confining it to the optical skin depth $\alpha^{-1}$. The light-matter interaction is thus confined within a volume $\pi r_0^2 \alpha^{-1} = 1.9 \times 10^{-18}\,\mathrm{m}^3$. The equilibrium energy difference between $\alpha$-gallium and the metastable metallic phases is of the order $8.3 \times 10^{-2}$ eV/atom ($1.3 \times 10^{-20}$ J/atom) (Ref. 5) and so to transform this volume, which contains $14.2 \times 10^{10}$ atoms, to the metallic phase, a total energy of 2 nJ is needed. Comparing this with the 5–10 nJ typically absorbed from the light pulse in our experiments confirms that the energy balance allows such a transition. The metastable phase could be quasi-liquid or amorphous gallium, or one of several "metallic" crystalline phases of the metal, which is known for its polymorphism.[6–11]

We believe that the light-induced transition is made possible by the unique structure of $\alpha$-gallium in which molecular and metallic properties coexist—some interatomic bonds are strong covalent bonds, forming well-defined $Ga_2$ dimers (molecules), and the rest are metallic.[5,7,12] Absorption results in highly localized excitation of the dimers from the bonding to the antibonding state, reducing the stability of the surrounding crystalline cell. $\alpha$-gallium subsequently undergoes a transition to a new configuration (crystalline or disordered), creating a microscopic inclusion of the new phase without achieving the melting temperature. The rapid increase in reflectivity, which follows excitation, is then a result of the increased density of the metallic phase in the skin layer. It is not quite clear yet whether, within the duration of the excitation pulse, the metallic phase inclusions form a well-defined metallic layer at the interface that grows during the pulse. If this is the case, the increase in the velocity of the $\alpha$-gallium/metallic-gallium interface upon approaching the melting point explains why the light-induced effect increases with temperature towards the melting point as shown in Fig. 2(b). It should be noted that this scenario of light-induced metallic film formation was recently found to be a very accurate model for the behavior of a gallium/silica interface subjected to cw excitation.[13]

When the excitation is withdrawn, the metallic phase becomes metastable and recrystallizes back to the $\alpha$ phase. Correspondingly, the reflectivity is restored to its initial value. The reflectivity relaxation time is a function of the growth velocity $v_r$ of the $\alpha$-gallium phase (i.e., the rate at which energy is released due to solidification) and the rate of thermal diffusion. Under the conditions used in our experiments, the former is dominant because the characteristic thermal diffusion time is shorter than the recrystallization time. The growth velocity depends on temperature: $v_r = g(1 - T/T_m)$, where $g$ is a function of the recrystallization mechanism.[14,15] The recovery time $\tau = d/v_r$ therefore increases critically on approaching $T_m$. One thus expects longer recovery times for larger induced reflectivity changes, i.e., thicker metallized layers, at a fixed temperature, and a slowing of the response at fixed optical excitation strength as the temperature is increased towards $\alpha$-gallium's melting point. All of these features have been seen in our experi-

ments, in particular, the recovery time increases as $\sim 1/(T_m - T)$ (see Fig. 3). Our data are not, however, sufficient to conclude that the metastable phase is liquid. Indeed, it has been suggested that $\alpha$-gallium melting is in fact a continuous transition through several of the crystalline phases that are energetically very close[5] and therefore, the metastable phase could be one of these.

The light-induced transition in gallium is different from those observed in semiconductors such as Si and GaAs (see Ref. 16 for a review) and recently in Al.[17] To achieve nonthermal effects in these materials high-intensity femtosecond optical excitation is needed. In crystalline silicon, for instance, all of the bonds are covalent and so its specific enthalpy of melting is 8–10 times higher than that of $\alpha$-gallium. Furthermore, the above-band-gap absorption depth in Si is 20–70 times greater than in gallium. Importantly, in silicon and GaAs the result of optical excitation is highly delocalized and the phase transition occurs through plasma-induced instability in the acoustic phonon modes, typically on a subpicosecond time scale. In gallium localization of the excitation is possibly an important factor, which could lead to local transformation of the structure. This allows us to discuss the transition in terms of the much slower nucleation and growth mechanisms.

In conclusion, the observed response of gallium to low power optical excitation is of considerable interest for applications requiring light-by-light control at low power levels, and in particular for photonic switching devices. The recent demonstration of gallium mirrors as effective $Q$-switching elements in fiber lasers[18] convincingly confirms this point.

We would like to acknowledge the support of The Royal Society, NATO, The Engineering and Physical Sciences Research Council, UK, and Goodfellow Cambridge, Ltd.

[1] P. J. Bennett, S. Dhanjal, P. Petropoulos, D. J. Richardson, N. I. Zheludev, and V. I. Emel'yanov, Appl. Phys. Lett. **73**, 1787 (1998).

[2] H. S. Carslaw and J. C. Jaeger, in *Conduction Of Heat In Solids* (Clarendon Press, Oxford, 1974).

[3] W. J. Huisman, J. F. Peters, M. J. Zwanenberg, S. A. De Vries, T. E. Derry, D. Abernathy, and J. F. Van Der Veen, Nature (London) **390**, 379 (1997).

[4] C. Y. Ho, R. W. Powell, and P. E. Liley, J. Phys. Chem. Ref. Data 1, 279 (1972).

[5] H. G. Von Schering and R. Nesper, Acta Chem. Scand. **45**, 870 (1991).

[6] J. Wolny, S. Niziol, W. Luzny, L. Pytlik, and J. Soltys, Solid State Commun. **58**, 573 (1986).

[7] X. G. Gong, G. L. Chiarotti, M. Parrinello, and E. Tosatti, Phys. Rev. B **43**, 14 277 (1991).

[8] L. Bosio, J. Chem. Phys. **68**, 1221 (1978).

[9] M. Bernasconi, G. L. Chiarotti, and E. Tosatti, Phys. Rev. B **52**, 9988 (1995).

[10] O. Hunderi and R. J. Ryberg, J. Phys. F: Met. Phys. **4**, 2096 (1974).

[11] A. Bizid, A. Defrain, and R. J. Bellissent, J. Phys. (Paris) **39**, 554 (1978).

[12] O. Züger and U. Dürig, Phys. Rev. B **46**, 7319 (1992).

[13] K. F. MacDonald, V. A. Fedotov, N. I. Zheludev, A. V. Rode, B. Luther-Davies, and V. I. Emel'yanov, J. Opt. Soc. Am. B **18**, 331 (2001).

[14] S. D. Peteves and R. Abbaschian, Metall. Trans. A **22**, 1259 (1991); **22**, 1271 (1991).

[15] V. T. Borisov and Yu. E. Matveev, Kristallogr. **14**, 895 (1969) [Sov. Phys. Crystallogr. **14**, 765 (1970)].

[16] Y. Siegal, E. N. Glezer, L. Huang, and E. Mazur, Annu. Rev. Mater. Sci. **25**, 223 (1995).

[17] C. Guo, G. Rodriguez, A. Lobad, and A. J. Taylor, Phys. Rev. Lett. **84**, 4493 (2000).

[18] P. Petropoulos, D. J. Richardson, S. Dhanjal, and N. I. Zheludev, Appl. Phys. Lett. **74**, 3619 (1999).

[19] A. V. Rode, M. Samoc, B. Luther-Davies, E. G. Gamaly, K. F. MacDonald, and N. I. Zheluder, Opt. Lett. **26**, 441 (2001).

Available online at www.sciencedirect.com
SCIENCE DIRECT®
Optics Communications 214 (2002) 271–276
OPTICS COMMUNICATIONS
www.elsevier.com/locate/optcom

# Light-induced reflectivity switching in gallium-on-silica films in the blue–green spectral region

V. Albanis*, V.A. Fedotov, N.I. Zheludev

*Department of Physics and Astronomy, University of Southampton, Southampton SO17 1BJ, UK*

Received 1 May 2002; received in revised form 25 September 2002; accepted 28 September 2002

**Abstract**

The dynamics of the light-induced, reflectivity switching at a silica–gallium interface prepared by ultrafast pulsed laser deposition, is studied for the first time in the blue–green spectral region. A considerable interface reflectivity increase is seen at fluencies of about 1 mJ/cm$^2$. The effect peaks at temperatures just below the gallium melting point (29.8 °C), while the reflectivity recovery times increase critically.
© 2002 Elsevier Science B.V. All rights reserved.

*PACS:* 42.65.–k; 78.20.–e; 78.66.–w

The search for materials with large optical nonlinearities, or ones that show a response to low-power optical excitation, as required for applications such as all-optical switching, has concentrated on media whose optical electrons exhibit a highly anharmonic response; most notably semiconductors, which exploit free excitonic and near-band-gap effects, and organic materials with weakly bound electrons. Recently, gallium confined at an interface with glass has attracted attention because of its enhanced nonlinear optical properties exhibited close to the melting temperature of gallium [1]. This nonlinear behaviour is broadband [2], and a number of applications, such as control of light-by-light [3] and q-switching of fibre lasers [4,5], have already been demonstrated. In this publication, we present an experimental study of the nonlinear optical response at a silica–gallium interface prepared by ultrafast pulsed laser deposition (UPLD) in the blue–green spectral region across the melting transition of gallium. Previous optical measurements at UPLD prepared interfaces were performed in the near-infrared at 810 nm using a quasi-cw [5] and mode-locked laser [7]. The optical response to pulse excitation (with pulse durations $\geqslant 10$ ns) was previously also studied using fiberized silica–gallium interfaces, i.e., interfaces made by dipping an optical fiber into molten gallium drop, at wavelengths of 1.5 μm [3] and 1.3/1.5 μm [8]. In this experimental study, we performed cw single beam reflectivity measurements in the wavelength range 488–514 nm

* Corresponding author. Present address: Optoelectronics Research Centre, University of Southampton, Southampton SO17 1BJ, UK. Fax: +44-23-8059-3142.
*E-mail address:* val@orc.soton.ac.uk (V. Albanis).

0030-4018/02/$ - see front matter © 2002 Elsevier Science B.V. All rights reserved.
PII: S0030-4018(02)02111-9

at different incident light intensities as a function of temperature. We also investigated the interface's reflectivity transient dynamics under pulsed excitation, in the nanosecond–microsecond range with respect to temperature, using a modulated pump at 514 nm and cw probe at 633 nm. Our results show that reflectivity can be modified by as much as 15%, by incident light of 3 kW/cm$^2$ intensity at a wavelength of 514 nm, close to the melting point of gallium, $T_m = 29.8$ °C. Under pulsed excitation, we observed two types of reflectivity response, depending on the silica–gallium interface properties. The mechanisms behind these phenomena were identified as a nonthermal and a predominantly thermal one.

Our measurements were performed on a silica–gallium interface (gallium mirror), produced by the UPLD method. A gallium film, of about 1–2 μm thickness, was deposited by gallium ablation under vacuum (~2 × 10$^{-6}$ Torr) directly on a silica substrate, which was cooled to about −100 °C during deposition, using a q-switched, mode-locked Nd:YAG laser at 1064 nm with 60 ps pulse duration. This process deposits amorphous gallium which, as a result of melting and subsequent solidification, is converted into the desired α-gallium phase. We have found this type of interface to be of exceptional structural stability, able to withstand numerous heating and cooling cycles, and exhibiting reproducible nonlinear optical properties. This stability can be attributed to the presence of a transitional layer, about 3 nm deep, at the interface between silica and gallium, formed by energetic gallium ions penetrating into the silica substrate during deposition [6].

We started with a single-beam experiment to examine the dependence of the mirror's linear reflectivity with respect to interface temperature, using light from an argon ion laser at wavelengths of 488, 496, 501 and 514 nm. The beam intensity was modulated at 200 Hz, and the light was focused at the gallium film, through the silica substrate, at near to normal incidence, to a spot of approximately 50 μm in diameter. The temperature of the gallium sample was controlled, in the range of 14–32 °C, by a thermoelectric heat pump (Peltier element) with a nominal accuracy of 0.1 °C. The optical properties of the gallium mirror are polarization sensitive, due to the crystallographic anisotropy of α-gallium [9]. To eliminate the dependence of the interface reflectivity on crystal orientation, the incident light was circularly polarised. In Fig. 1(a), the change of the UPLD silica–gallium interface reflectivity on melting, for low light intensity, is shown for the different wavelengths used. We compare our experimental data with values calculated using data for the optical constants of the solid and liquid phases. To calculate the reflectivity of the silica–gallium interface, at temperatures well below gallium's

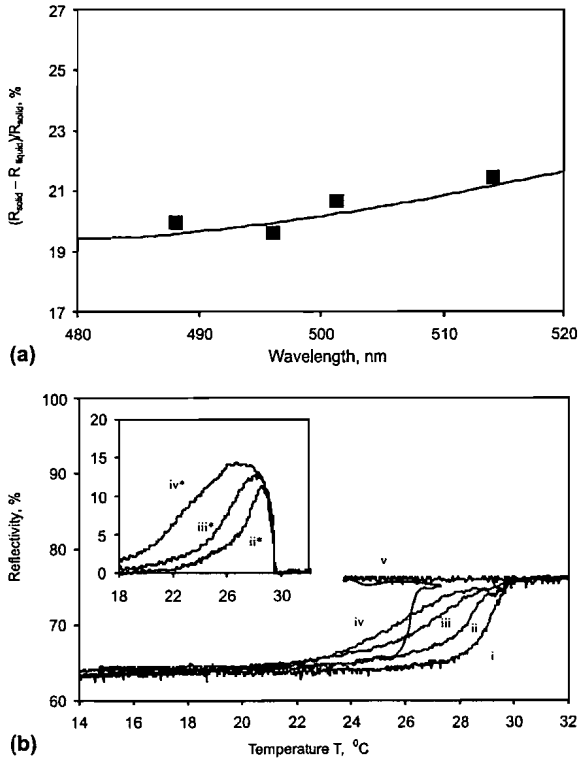


Fig. 1. (a) Reflectivity change at the silica–gallium interface on melting, as a function of wavelength. The solid line represents calculated value of the reflectivity change whereas the "■" is our experimental results. (b) Reflectivity of the silica–gallium interface as a function of sample temperature, for different light intensities. Curves i–iv correspond to silica–gallium interface reflectivity at incident light intensities of 100 W/cm$^2$, 500 W/cm$^2$, 1.5 kW/cm$^2$ and 3 kW/cm$^2$, curve v corresponds to decreasing temperature for 100 kW/cm$^2$ incident light intensity. In the inset, the magnitude of the light-induced reflectivity change is shown as the difference between reflectivity at higher intensity levels (curves ii–iv) and the lowest intensity one (curve i).

melting point, we used data for the anisotropic dielectric function of an α-gallium crystal from [10], and data from [11], to calculate the reflectivity of the interface formed by liquid gallium. In Fig. 1(a), the calculated reflectivity values account for the presence of a transient metallic layer, 3 nm thick. A good agreement between our experimental and calculated values, of the silica–gallium interface reflectivity change on melting, can be seen. Our results illustrate the broadband nature of the optical properties of the silica–gallium interface, and the potential for optical switching in the blue–green part of the spectrum.

Fig. 1(b) (curves i–iv) shows the interface reflectivity for $\lambda = 514$ nm with increasing temperature, and for various light intensities across the melting point of gallium, $T_m = 29.8$ °C. Solidification occurs at 24 °C, and the interface reflectivity exhibits a hysterisis with approximately 6 °C overcooling (curve v). Note that the peculiar behaviour observed with decreasing temperature (curve v), is due to the sudden increase in sample temperature, caused by the heat released during the solidification of the gallium film, which the thermal stabilisation circuitry is not able to cope immediately. In the inset of Fig. 1(b), the light-induced reflectivity change is shown for increasing temperature. It can be observed that the maximum change is achieved a few degrees below the melting point of gallium, $T_m$, while the effect disappears on melting.

One can possibly argue that the observed reflectivity behaviour is due to laser-induced melting of the thin gallium film at the interface. However, if this was the case, then the interface reflectivity curve would be shifted down the temperature axis, by an amount corresponding to the increase of temperature by the laser induced heating of the film. However, what we observed was a softening of the hysterisis curve instead of a shift. To address this question we modelled the temperature distribution and heat flow at the interface and calculated the rise of the local temperature, due to the presence of the laser beam. In our calculations we took into account the anisotropic character of the thermal conductivity of α-gallium at the interface, having values of $\lambda_c = 15.9$ $Wm^{-1}$ $K^{-1}$ perpendicular to the interface, and principal coefficients along the plane of the interface $\lambda_a = 41$ $Wm^{-1}$ $K^{-1}$ and $\lambda_b = 88$ $Wm^{-1}$ $K^{-1}$. We neglected convention and radiative losses from the sides of the sample. Our calculations show that the local rise in interface temperature is ~2 °C for an incident light intensity of 3 $kW/cm^2$ which can not explain the observed softening of the hysterisis curve across a much wider range of temperatures. Therefore, there should be another mechanism behind the increase in interface reflectivity, most likely of a nonthermal nature.

Indeed, recently such a nonthermal mechanism has been introduced in an attempt to explain the observed reflectivity behaviour of the silica–gallium interface under cw [6] and pulse laser excitation (for pulse durations $\geqslant 10$ ns) [8]. Our experimental observations in the case of the cw measurements of the interface reflectivity are clearly consistent with the nonthermal mechanism proposed in [6]. According to this mechanism, gallium undergoes a light-induced, nonthermal, surface-assisted phase transition when illuminated with light. This transition is made possible by the unique crystalline structure of α-gallium, comprising of metallic and molecular bonding, in which some of the bonds forming $Ga_2$ dimer units, and the rest being metallic. The presence of the covalent bonding results in an optical absorption band from ~310 to ~1820 nm. Our measurements were within this band, at 514 nm. Absorption of light leads to a highly localised excitation of the dimers, from the bonding to the antibonding state, reducing the stability of the surrounding crystalline cell, which subsequently undergoes a transition to a new phase of considerably different optical properties. The new phase is stable in the presence of light, and grows epitaxially as a layer at the interface between the silica substrate and α-gallium [12]. The increase in the interface's reflectivity is then a result of the increasing thickness of such a layer. The exact identity of this phase is not yet clear, but it is most likely to be one of the material's existing metastable phases, such as β-gallium, Ga(II) and Ga(III). These phases exhibit metallic characteristics, similar to those of the liquid state and are involved in the continuous transition from the solid crystalline α-phase to the liquid (α-gallium → β-gallium → Ga(II) → Ga(III) → liquid) [13].

The transient dynamics of the optical response were studied with a pump-probe technique, using a modulated pump at 514 nm with a peak power of 168 mW, and a 0.3 mW cw He–Ne laser, at 633 nm, as the probe source. An acousto-optical modulator, capable of producing 20 ns fronts, was used to alter the pump into pulses of duration, $\tau_p$, 150 ns, 400 ns and 1 μs, with a repetition rate of 100 Hz. Both the pump and probe beams were focused at the gallium film, through the silica substrate, at spot diameters of about 50 μm and 35 μm, respectively. The polarisation of the pump was circular. A digital oscilloscope was used to register and record the reflected probe signal, detected by a fast photodiode. The overall bandwidth of the detection system was 150 MHz.

The transient measurements, in the main frame of Fig. 2, illustrate the typical response of the silica–gallium UPLD interface's reflectivity. Our results show that reflectivity rises *immediately* after the start of the pump pulse (the dashed vertical line). In the range of pulses used in the measurements, the effect accumulates with time. In the inset of Fig. 2, the pump-induced, probe reflectivity change is shown with respect to the sample temperature, for the three pump pulse durations.

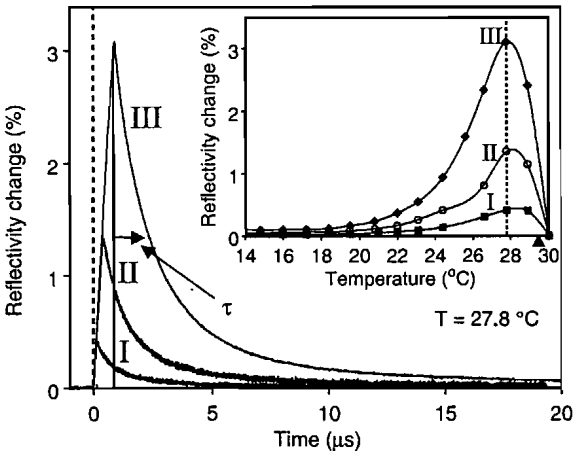


Fig. 2. The dynamics of the reflectivity change associated with the nonthermal effect plotted for three different pump pulse durations at $T = 27.8$ °C. The inset shows the magnitude of the reflectivity change. Curves I, II and III correspond to different pump pulse durations, 0.15, 0.40 and 1.00 μs, while $\tau$ indicates the recovery time.

From these data, the maximum light-induced change can be seen to occur just below the melting point, reaching a maximum at a temperature of 27.8 °C, before disappearing above melting. When the pump pulse ends, the interface reflectivity starts to recover back to its initial level, exhibiting recovery times that depend on sample temperature (Fig. 3). The rapid increase in the interface reflectivity, which follows excitation, is then a result of the increased density of the metallic phase in the skin layer. When the excitation is withdrawn the metallic phase becomes metastable and recrystallizes back to the α-phase. Correspondingly, the interface reflectivity recovers back to its initial level. If this was a temperature driven effect due to local laser heating involving no change in the α-gallium structure, reflectivity would relax as interface temperature relaxes and the recovery time would then be independent of the sample temperature. Within the duration of the excitation pulse the metallic phase inclusions form a well-defined metallic layer at the interface that grows during the pulse. The recovery time then depends on the velocity, $v_r$, with which the α-phase/metallic phase front moves towards the silica substrate, and the rate of thermal diffusion. In this case the recrystallization is the dominant factor, since the thermal diffusion time is much shorter than the recrystallisation time. The recrystallization velocity is a

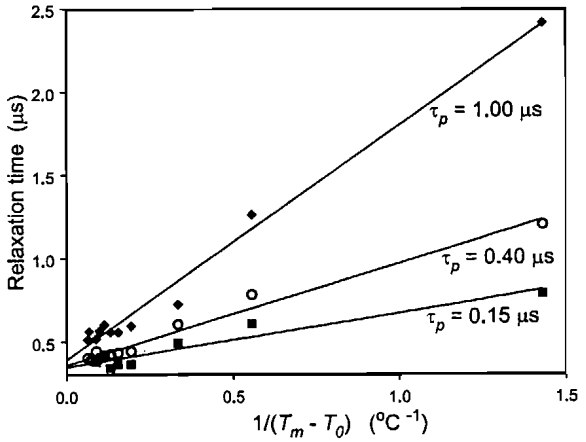


Fig. 3. The recovery time, $\tau$, of the pump-induced probe reflectivity change presented as a function of $1/(T_m - T)$, for three pump pulse durations.

function of the sample temperature: $v_r = g(1 - T/T_m)$, where $g$ is a function of the recrystallisation mechanism and $T_m$ is the bulk melting temperature [8]. From the transient reflectivity measurements corresponding to the sample temperature of 27.8 °C, (Fig. 2) we found $v_r$ to be $4 \times 10^{-4}$ ms$^{-1}$. The recovery time $\tau = d/v_r$ (where $d$ is the thickness of the metallized layer) is expected to be longer for larger induced reflectivity changes, i.e., thicker metallized layers and increase critically on approaching $T_m$. All of these features have been observed in our experiment, in particular the recovery time increases as $\sim 1/(T_m - T)$, see Fig. 3.

The results presented in Figs. 1–3, represent a typical response of the silica–gallium interface. However, when scanning the surface of the sample it was also possible to locate areas that responded differently to optical excitation. Fig. 4 shows the dynamics of the reflectivity change in the area of different characteristics. The reflectivity recovery times exhibit a much longer component compared with the measurements presented in Fig. 2. The pump-induced, probe reflectivity change can be seen to disappear before $T_m$, and the maximum light-induced change occurs at a temperature of 25.6 °C, see the inset in Fig. 4. However, a number of features similar to the previous case can still be seen. Namely, the reflectivity starts to rise *immediately* after the arrival of the pump pulse (dashed line) and the effect accumulates with time. Fig. 5 shows a direct comparison of the transient dynamics of the reflectivity change, with $\tau_p = 1$ μs, for the two types of response. We consider the second type of interface reflectivity behaviour as due to a predominantly thermal effect, because of the poor thermal quality of the interface at some areas. As a result, the gallium film undergoes melting before the melting temperature is reached due to the heat accumulated locally, as indicated by the inset in Fig. 4. Nevertheless, the nonthermal mechanics described above, still play an important role. This is indicated by the immediate rise of the interface reflectivity after the arrival of the pump pulse. If the effect was a fully thermal one, then there would be a delay before the interface reflectivity starts to rise, equal to the time needed to bring the local temperature above the melting point. When the pump excitation is no longer present the interface reflectivity starts to recover. The reflectivity relaxation times can be seen to increase as temperature approaches the melting temperature, exhibiting, though, much longer recovery dynamics. The results presented in Figs. 4

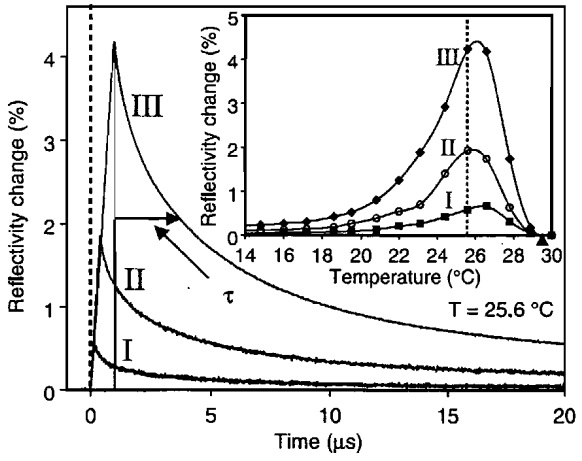


Fig. 4. The dynamics of the reflectivity change associated with the thermal effect plotted for three different pump pulse durations at $T = 25.6$ °C. The inset shows the magnitude of the reflectivity change. Curves I, II and III correspond to different pump pulse durations, 0.15, 0.40 and 1.00 μs, while τ indicates the recovery time.

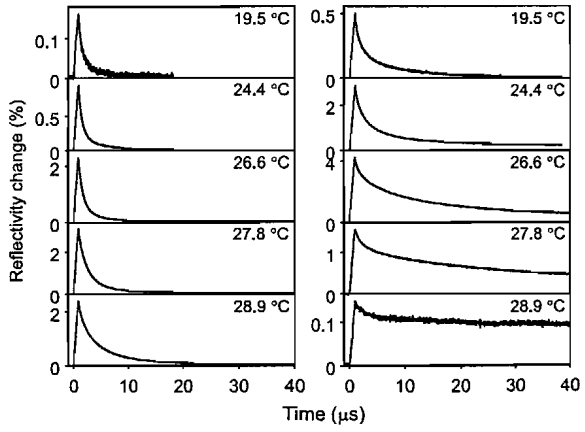


Fig. 5. Direct comparison of the transient dynamics of the pump-induced probe reflectivity change, showing the nonthermal (left) and thermal effect (right). Presented as a function of the sample temperature $T$, for pump pulse duration $\tau_p = 1.00$ μs. Note the increasing difference in the reflectivity change dynamics with respect to increasing temperature.

and 5 suggest that in these areas the growth velocity is no longer the dominant factor in the recovery of interface reflectivity. Under these conditions, both the recrystallization and thermal diffusion are important for the recovery of reflectivity. Indeed, due to the poor thermal quality of the interface at these points, the heat released on solidification is trapped in the gallium film. This significantly decelerates recrystallization and therefore results in longer recovery times.

In conclusion, we studied the nonlinear optical properties of a silica–gallium interface, prepared by UPLD, in the blue–green spectral region across the melting transition of gallium. We performed cw measurements of the optical properties, the results of which show a substantial reflectivity increase close to the melting temperature of gallium. We also performed transient measurements of the interface reflectivity under pulsed excitation. Two types of reflectivity response were observed, a nonthermal and a predominantly thermal. In the case of the nonthermal response our results indicate that the magnitude and recovery time of the interface reflectivity increase critically with temperature approaching the melting point of gallium. The nonthermal response can be accounted by a light-induced metallization of $\alpha$-gallium at the interface with silica. The thermal response is explained by laser-induced melting.

## Acknowledgements

We would like to thank A.V. Rode and B. Luther-Davies for manufacturing the UPLD silica–gallium interfaces in the facilities of the Laser Physics Centre, The Australian National University, Canberra Australia. In addition, the Liverhum Trust and EPSRC are acknowledged for financial support.

## References

[1] N.I. Zheludev, Contemporary Physics 43 (2002) 365.
[2] K.F. MacDonald, V.A. Fedotov, N.I. Zheludev, B.V. Zhdanov, R.J. Knize, Appl. Phys. Lett. 79 (2001) 2375.
[3] P.J. Bennett et al., App. Phys. Lett. 73 (1998) 1787.
[4] P. Petropoulos, H.L. Offerhaus, D.J. Richardson, S. Dhanjal, N.I. Zheludev, App. Phys. Lett. 74 (1999) 3619.
[5] N.J.C. Libatique, J.D. Tafoya, S.H. Feng, D.J. Mirell, R.J. Kain, in: Advanced Solid State Lasers, vol. 34, Opt. Soc. Am., Washington DC, 2000, p. 417.
[6] K.F. MacDonald, V.A. Fedotov, R.W. Eason, N.I. Zheludev, A.V. Rode, B. Luther-Davies, V.I. Eme'yanov, J. Opt. Soc. Am. 18 (2001) 331.
[7] A.V. Rode, M. Samoc, B. Luther-Davies, E.G. Garnaly, K.F. MacDonald, N.I. Zheludev, Opt. Lett. 26 (2001) 441.
[8] V. Albanis, S. Dhanjal, V.A. Fedotov, K.F. MacDonald, N.I. Zheludev, P. Petropoulos, D.J. Richardson, V.I. Emel'yanov, Phys. Rev. B. 63 (2001) 165207.
[9] W. Huisman et al., Nature 370 (1997) 379.
[10] R. Kofman, P. Cheyssac, J. Richard, Phys. Rev. B. 16 (1977) 5216.
[11] R.Sh. Teshev, A.A. Shebzukhov, Opt. Spectr. 55 (1998) 693.
[12] P. Petropoulos, H.S. Kim, D.J. Richardson, V.A. Fedotov, N.I. Zheludev, Phys. Rev. B. 64 (2001) 193312.
[13] F.J. Bermejo, P.R. Fernandez, M. Alvarez, B. Roessli, H.E. Fischer, J. Bossy, Phys. Rev. E. 56 (1997) 3358.